FIELD SIMULATION OF WASTE IMPOUNDMENT SEEPAGE IN THE VADOSE ZONE: MULTIPLE-TRACER TRANSPORT EXPERIMENT IN A STRATIFIED, HETEROGENEOUS, UNSATURATED FIELD SOIL

by

David P. Grabka

Submitted in Partial Fulfillment of
the Requirements for the Degree of
Master of Science in Hydrology

New Mexico Institute of Mining and Technology
Socorro, New Mexico

February, 1991

ABSTRACT

A multi-tracer field experiment was conducted west of the New Mexico Tech campus for the purpose of simulating migration of contaminants from a lined impoundment through heterogeneous, stratified soil. Water was applied through a drip irrigation system at a flux rate of approximately 10^{-4} cm/sec over a 10-m by 10-m area.

The water application system was split into four adjacent sections to isolate the water being applied into each section. Four fluoro-benzoates and bromide were used as tracers. A different fluoro-benzoate was injected into each section and bromide was added to all sections for one day. For 34 days soil water samples were taken at roughly eight hour intervals from a network of 72 soil water samplers located at various depths beneath the drip irrigation system and outside the system. Concentrations of tracers in the soil water samples were determined by high performance liquid chromatography.

For each sampler, relative concentration versus time data were used to optimize the one-dimensional advection-dispersion equation parameters: velocity, dispersion coefficient, and pulse duration. The temporal moments of the relative concentration versus time data of each sampler were determined, and a velocity and dispersivity calculated from the moments. Fractile diagrams were constructed of the parameters from each method. A log-normal distribution best fit velocity, dispersion coefficient, and dispersivity, while a normal distribution was adequate for pulse duration, mass recovered, and average volume of water pulled from samplers.

Lateral movement of fluoro-benzoates to adjacent sections was observed. Tracer migration appeared to have a northward component. Tracers were also detected in some soil water samplers outside the water application area to the east. Little solute movement was seen in the other directions.

Three methods were employed to aerially average concentrations for a particular depth for discrete times. The average flux-weighted concentration method predicted the fastest movement of tracer, while using average resident concentrations predicted lower solute velocities and greater tailing. Averaging the transport parameters from samplers at a given depth and inputting them back into the one-dimensional advection-dispersion equation yielded results intermediate of the other two averaging methods.

Jury's transfer function model (1982) was applied to average resident concentration data to ascertain whether the transfer function can predict solute distributions at depths other than the calibration depth. It was believed the model did not function well because of the great degree of heterogeneity at the site. The transfer function and the one-dimensional advection-dispersion were utilized to predict solute loading on the water table. The transfer function predicted solute loading much sooner.

TABLE OF CONTENTS

APPENDICES

LIST OF FIGURES

LIST OF FIGURES---(continued)

LIST OF FIGURES---(continued)

Figure Page

LIST OF TABLES

ACKNOWLEDGEMENTS

Much thanks is due to my advisor, Rob Bowman, and to Dan Stephens, who introduced me to this project. Their guidance and suggestions for the past three years are much appreciated. Also, thank you to the other faculty of New Mexico Tech who gave me the knowledge to tackle this project.

This project has been funded by the U.S. Bureau of Mines Generic Waste and Recovery Center. It provided funding for me as well as numerous other graduate and undergraduate students. We have spent numerous hours analyzing almost every aspect of the field site. Special thanks to Kevin Flanigan and Rolf Schmidt-Peterson for their unflagging devotion to "the site" and their willingness to sometimes take me seriously.

Also, much gratitude is owed to the bartenders and regulars at the Capitol Bar for putting up with me. They never quite let me go off the deep end, as I am apt to do.

Finally, special thanks must go Robert Liddle and Joe Gibbens, the people I could act natural around and who never completely discarded any idea of mine as nonsense. They are sorely missed.

I. INTRODUCTION

As society becomes more aware of the fragility of our environment, concern has grown over the disposal of toxic wastes and the widespread use of various chemicals such as herbicides and pesticides. The movement of chemicals through the unsaturated zone to groundwater is of primary importance to a number of hydrologists and environmental specialists. As the public becomes more and more aware of the dangers this pollution poses to its health, there will be mounting pressure on scientists and engineers to find and clean up contaminated areas.

The large volume of industrial wastes needing disposal, and the dependence of farmers on fertilizers, herbicides and pesticides, has created a situation where soil and groundwater contamination is a definite reality. The leakage of gasoline and industrial solvents from supposedly safe aboveground and underground storage tanks is of special concern to many people as these tanks are distributed all over this country. The safe disposal of nuclear wastes is another issue of great concern to society.

Many of the chemicals that move through the unsaturated zone and impact groundwater are left to degrade biologically or to dilute to concentrations below safety standards. Other chemicals are not degradable and are at concentrations well above public safety standards. Since water and solutes move slowly through both the saturated and unsaturated zones, the soil and groundwater may remain contaminated for very long

periods of time. Remediation of contaminated areas takes time and is very costly. Chemicals may enter the food chain or seep into surface waters, further threatening public health.

This paper deals with solute movement in a heterogeneous vadose (unsaturated) zone where there is a constant flux of water over a discrete area at or below the ground surface. This situation is seen in the real world in the application of chemicals over an agricultural plot where the constant flux of water corresponds to irrigation cycles; in waste impoundment seepage; and in the constant flow of gasoline or industrial solvents from leaking underground storage tanks.

Usually, the flow of water or solutes in these cases is considered one-dimensional, with flow directly downward to the water table. Recent experimental and theoretical research has suggested that heterogeneity and anisotropy cause three-dimesional fluid transport in the vadose zone. A field study by Crosby et al. (1968,1971) described significant lateral spreading of pollution away from its application point. They investigated the movement of chemical and bacterial pollutants from a 40-ft by 40-ft drain field and from a 150-ft by 150-ft feed lot, both underlain by glacial outwash deposits. Flanigan (1989) added a pulse of bromide across a 10-m x 10-m heterogeneous plot under constant water flux. Significant horizontal movement of solute away from the application area was seen. A laboratory study (Palmquist and Johnson, 1962) showed lateral movement of water at the interface of glass

beads of different sizes. Stephens and Heerman (1986) reported on an experiment utilizing a sand box with alternating coarse and fine sand layers. When water was applied at a point at the surface, significant lateral spreading of the fluid was seen. The advance of the wetting front was greatest in the finer material. Anisotropy has also been shown to create multi-dimensional flow. Mualem (1984) and Yeh et al. (1985) suggest that anisotropy increases with decreasing saturation.

In arid and semi-arid climates like that of New Mexico, the vadose zone can be many tens of meters deep. Therefore, lateral spreading of surface-applied water and chemicals due to heterogeneity and anisotropy in the vadose zone can be quite extensive. Previous models assumed that fluid flow was primarily downward. More recent models, e.g. UNSAT2 (Neumann and Davis, 1983) and FEMWATER (Yeh, 1987), incorporate multi-dimensional flow in their codes, but have not been rigorously validated by field studies.

Few field tracer tests have been done in unsaturated soils due to the large time involved and the extensive characterization of native soils under various degrees of saturation needed. Most of these tests have been done on the relatively uniform soils found in agricultural field plots. Biggar and Nielsen (1976) applied cloride and nitrate to a 150-ha agricultural field after steady state water content and flow conditions were achieved. They analyzed breakthrough

curves from soil suction probes at various depths in twenty randomly located 6.5-m-square plots within the field. In order to validate the transfer function model of Jury (1982), Jury et al. (1982) applied bromide in one centimeter of irrigation water to a 0.64-ha field of loamy sand and monitored the tracer movement driven by 93 cm of rainfall. Data from 96 suction samplers to a depth of 305 cm and from 36 soil cores to a depth of 360 cm were used to construct breakthrough curves of the tracer. Butters and Jury (1989) repeated the experiment at the site but instead of using rainfall, they used sprinkler irrigation to provide a constant flux of 0.05 cm/hour. Warrick et al. (1971) applied 7.5 cm of chloride solution to the surface of a 1-m^2 plot followed by 22.5 cm of solute-free water. Concentration versus time data, determined from soil water collected via porous cup samplers, were used to construct breakthrough curves for the chloride. Bowman and Rice (1986) conducted a field experiment on a 48.8 m x 128 m agricultural plot consisting of sandy loam. They sprayed the field with a solution containing the tracer pentafluorobenzoic acid and the moderately adsorbed herbicide bromacil. Destructive sample cores were taken to monitor the movement of the two solutes. Transport of the chemicals was faster than predicted, presumably due to preferential flow paths.

Currently, there are several theoretical transport models designed for unsaturated field soils. Biggar and Nielsen

(1976) suggested that the classical advection-dispersion equation will adequately describe solute transport under relatively uniform conditions. Dagan and Bresler (1979) and Bresler and Dagan (1981) considered the field to be composed of a collection of stream tubes whereby fluid flow was determined uniquely by the hydraulic properties (moisture content, saturated hydraulic conductivity, theta-psi curve, etc.) of the soil contained in the column. The transfer function model of Jury (1982) looked at the travel time distribution at a calibration depth and used a transfer function to predict the distribution of tracer at all other depths. Mantoglou and Gelhar (1987), Tang et al. (1982) and Gelhar and Axness (1983) applied stochastic convective transport theory of one or more dimensions to model chemical transport in saturated and unsaturated systems.

On the campus of New Mexico Institute of Mining and Technology, Socorro, New Mexico, a long term field experiment investigating unsaturated solute and fluid flow has been conducted since January, 1987. The experiment was designed to simulate the seepage of leachate from beneath a waste impoundment. Water was applied via buried drip irrigation lines covering a 10-m x 10-m area. The goals of the overall project were to: (1) investigate the vertical and lateral movement of solute and water induced by soil stratification, heterogeneity, and degree of saturation; and (2) validate analytical and numerical models predicting solute

and fluid flow through the unsaturated zone.

The experiments described in this paper will mainly cover transport of solutes in the vadose zone. The goal was to determine how non-reactive chemicals migrate through heterogeneous soils so as to better predict the transport of contaminants in similar systems. The specific objectives of this paper were to: (1) to conduct a field tracer experiment, (2) determine solute transport parameters from concentration versus time data, (3) look at distributions of these parameters, (4) compare parameters determined by the one-dimensional advection dispersion equation (1-D ADE) with those from moment analysis, (5) look at three methods of aerially averaging concentrations at a particular depth, (6) investigate horizontal movement of solute inside and outside the wetted region, (7) discuss in general the fitting of breakthrough curves, representing three-dimensional solute movement, with one dimensional models, and (8) apply a transfer function model to aerially averaged concentrations.

II. THEORETICAL

SOLUTE TRANSPORT PROCESSES

Solute transport through soils is controlled by several different processes - advection, mechanical dispersion, molecular diffusion, reactions between solute and the soil matrix, and biological reactions that can transform the chemical. The focus of this paper is on ideal, non-reactive tracers, so the last two processes will be ignored.

Advection deals with the bulk movement of fluid through the soil matrix. In the absence of mechanical dispersion and molecular diffusion, the general shape of a tracer pulse will not change with time or distance traveled.

Mechanical dispersion is the mixing of solute with advective flow. There are three components to mechanical dispersion. The first concerns variability of velocity on the microscopic or pore scale. Fluid in contact with the solid matrix will move slower than fluid centered in the pore due to frictional effects. The second component of mechanical dispersion is caused by differences between pore sizes, because differences in size, surface area, and roughness of pore channels will cause mixing of the chemical. The third mechanism concerns the tortuosity, branching and interfingering of channels where the solute is spread out over a larger cross-sectional area.

Molecular diffusion concerns the movement of a dissolved chemical down-gradient from high concentrations to lower concentrations. The process obeys Fick's law.

THE GENERAL THREE DIMENSIONAL STEADY-STATE UNSATURATED FLOW EQUATION

The general three-dimensional steady-state unsaturated flow equation is derived from the law of conservation of mass. The mass of solute per unit volume is θC, where θ is the volume of water contained in a unit volume of soil and C is the concentration of the solute in units of mass per unit volume of water. The solute is transported by advective and dispersive mechanisms. For flow entering the unit volume from the x-direction:

$$advective\ flux = \overline{v_x}\theta C \tag{2-1}$$

$$dispersive\ flux = D_x \frac{\partial(\theta C)}{\partial x} \tag{2-2}$$

where v_x is the seepage velocity equal to q_x/θ, q_x is the x-directional flux of water passing through a unit cross-sectional area of porous medium, θ is the moisture content and D_x is the dispersion coefficient. The dispersion coefficient is related to dispersivity α_x and the solute diffusion coefficient D^* by:

$$D_x = \alpha_x \overline{v_x} + D^* \tag{2-3}$$

The total mass of solute passing through a unit area perpendicular to the x-direction per unit time is:

$$F_x = \overline{v_x}\theta C - D_x \frac{\partial(\theta C)}{\partial x} \qquad (2\text{-}4)$$

The minus sign denotes that the solute moves down gradient towards lower concentration. For the other two directions:

$$F_y = \overline{v_y}\theta C - D_y \frac{\partial(\theta C)}{\partial y} \qquad (2\text{-}5)$$

$$F_z = \overline{v_z}\theta C - D_z \frac{\partial(\theta C)}{\partial z} \qquad (2\text{-}6)$$

The total amount entering any cubic element is:

$$F_x\, dy\, dz + F_y\, dx\, dz + F_z\, dx\, dy \qquad (2\text{-}7)$$

The total amount exiting the volume is:

$$(F_x + \frac{\partial F_x}{\partial x} dx)\, dy\, dz + (F_y + \frac{\partial F_y}{\partial y} dy)\, dx\, dz + (F_z + \frac{\partial F_z}{\partial z} dz)\, dx\, dy \qquad (2\text{-}8)$$

The partial derivative terms denote the spatial change of the solute mass in the specified direction. The difference between the mass entering and that leaving the representative volume is:

$$(\frac{\partial F_x}{\partial x} + \frac{\partial F_y}{\partial y} + \frac{\partial F_z}{\partial z})\, dx\, dy\, dz \qquad (2\text{-}9)$$

The rate of change of mass in the element is:

$$-\theta \frac{\partial C}{\partial t} dx\, dy\, dz \qquad (2\text{-}10)$$

The complete expression becomes:

$$\frac{\partial F_x}{\partial x} + \frac{\partial F_y}{\partial y} + \frac{\partial F_z}{\partial z} = -\theta \frac{\partial C}{\partial t} \qquad (2\text{-}11)$$

Substitution of expressions (2-4, 2-5, and 2-6) leaves:

$$\left[\frac{\partial}{\partial x}\left(D_x\frac{\partial(\theta C)}{\partial x} - \overline{v_x}\theta C\right) + \frac{\partial}{\partial y}\left(D_y\frac{\partial(\theta C)}{\partial y} - \overline{v_y}\theta C\right) + \frac{\partial}{\partial z}\left(D_z\frac{\partial(\theta C)}{\partial z} - \overline{v_z}\theta C\right)\right] = \theta\frac{\partial C}{\partial t} \qquad (2\text{-}12)$$

For a system which is heterogeneous, anisotropic but under steady state conditions, variables in the equation are functions of location but constant with time; thus

$D_x \neq D_y \neq D_z$ anisotropic

$D_x = D_x(x,y,z)$, $D_y = D_y(x,y,z)$, $D_z = D_z(x,y,z)$;

$v_x = v_x(x,y,z)$, $v_y = v_y(x,y,z)$, $v_z = v_z(x,y,z)$;

and $\theta = \theta(x,y,z)$ heterogeneous

Equation (2-12) is impractical to solve analytically, and is usually solved numerically, assuming functions can be determined for all the location dependent variables. Often, this is unrealistic, so simpler models are usually used.

A simpler model, and the one that is most often used, for water and solute movement, is a one-dimensional approach. For one-dimensional steady-state flow through a soil column, the Darcy velocity q is constant. If it is also assumed that the

dispersion coefficient is constant with depth, equation 2-12 is simplified to:

$$\theta \frac{\partial C}{\partial t} = \frac{\partial}{\partial z}\left[D_z \frac{\partial (\theta C)}{\partial z}\right] - \frac{\partial [v_z \theta C]}{\partial z} \qquad (2\text{-}13)$$

METHODS OF DETERMINING TRANSPORT PARAMETERS

A number of methods can be used to determine transport parameters from concentration versus time data. One method is to optimize the solute transport parameters v, D, and duration of solute addition t_o of the one-dimension homogeneous, isotropic transport equation to the actual concentration versus time data by means of non-linear least squares. A second method involves taking the zeroeth, first and second moments of the actual concentration versus time data by means of the trapezoid rule.

ONE-DIMENSIONAL ADVECTION-DISPERSION EQUATION

Concentration versus time data can be evaluated using the computer program CXTFIT of Parker and van Genuchten (1984). The program determines transport parameters v, D, and t_o for non-reactive solute movement during steady fluid flow in a one-dimensional homogeneous system. Moisture content is considered constant with depth. With constant θ, eq. 2-13 becomes:

$$\frac{\partial C}{\partial t} = D\frac{\partial^2 C}{\partial z^2} - v\frac{\partial C}{\partial z} \qquad (2\text{-}14)$$

In determining transport parameters, there are two most often used ways of considering concentration data that are in the literature. Concentrations of solute may be considered the volume-averaged resident concentration in the liquid phase or the flux-averaged concentration representing the "mass of solute per unit volume passing through a given cross-section during an elementary time interval" (Kreft and Zuber, 1978).

The initial and boundary conditions for a pulse type addition of non-reactive tracer are:

$$C(z,0) = 0 \qquad (2\text{-}15)$$

$$\frac{\partial C}{\partial z}(\infty,t) = 0 \qquad (2\text{-}16)$$

$$C(0,t) = \begin{bmatrix} C_0 & 0<t\leq t_0 \\ 0 & t>t_0 \end{bmatrix} \qquad (2\text{-}17)$$

An analytical solution (van Genuchten and Alves, 1982) to the equation is:

$$C(z,t) = \begin{bmatrix} C_0A(z,t) & 0<t\leq t_0 \\ C_0A(z,t) - C_0A(z,t-t_0) & t>t_0 \end{bmatrix} \qquad (2\text{-}18)$$

where:

$$A(z,t) = \frac{1}{2}erfc\left[\frac{z-vt}{2\sqrt{Dt}}\right] + \frac{1}{2}\exp\left(\frac{vz}{D}\right)erfc\left[\frac{z+vt}{2\sqrt{Dt}}\right] \quad (2\text{-}19)$$

Actual solute concentration versus time data is used to optimize: (1) time duration which the tracer was applied, t_o; (2) seepage velocity in the vertical direction, v_z; and (3) the dispersion coefficient, D.

The method used was non-linear least squares where the goal is to minimize the residual sum of the squares, R_s.

$$R_s = \sum_{i-1}^{n} [C_e(z,t_i) - C(z,t_i)]^2 \quad (2\text{-}20)$$

where n = the number of observed data points,

$C_e(z,t_i)$ = the observed concentration at sampler depth z and time t_i, and

$C(z,t_i)$ = the calculated data points at distance z and time t_i.

METHOD OF MOMENTS

A second method that can be used to determine transport parameters is moment analysis. The zeroeth, first and second moments of the concentration versus time data sets are

calculated using:

$$T_N = \int_0^\infty t^N C(t)\,dt \approx \sum_{k-1}^{M} \left[\frac{t_k + t_{k+1}}{2}\right]^N \left[\frac{C_k + C_{k+1}}{2}\right] [t_{k+1} - t_k] \qquad (2\text{-}21)$$

where N is the moment being determined.

The zeroeth moment (T_o) corresponds to the area under the concentration versus time curve, i.e. mass of solute seen. Division by the zeroeth moment of the first and second moment normalizes the curve. T_1/T_o corresponds to the time at which half the mass of solute or contaminant has been recovered, or center of mass, N_1. T_2/T_o corresponds to the spread of solute about its center of mass, N_2.

T_o corresponds directly to the mass recovery term t_o from the one-dimensional advection-dispersion equation (1-D ADE) discussed earlier. The normalized first moment can be converted into a velocity v by

$$v = \frac{z}{N_1 - .5 t_0} \qquad (2\text{-}22)$$

where z is the depth where the concentration versus time data was taken and t_o is the duration of tracer addition. According to Butters and Jury (1989), a dispersivity α can be calculated with the first and second normalized moments:

$$\alpha = \frac{z}{2}\left[\frac{N_2 - N_1^2}{N_1^2}\right] \qquad (2\text{-}23)$$

This assumes that the duration of the initial input of tracer is negligible compared with the travel time of the solute reaching the solute sampling location.

AERIALLY AVERAGING CONCENTRATION DATA

Hydrologists are often less interested in solute or contaminant movement past a particular point than they are of average contaminant movement across a cross-sectional area. In this paper three methods are discussed for the purpose of aerially averaging concentration: (1) average resident concentration (ARC); (2) flux weighted average concentration (AFWC); and (3) concentration determined from averaging transport parameters from fitted breakthrough curves (ATPC). Each method produces drastically different results.

An average resident concentration versus time curve for a particular depth z is calculated by:

$$ARC_z(t) = \frac{1}{k}\sum_{i-1}^{k} C_i(t) \qquad (2\text{-}24)$$

where i is the number of the particular sampler at depth z and $C_i(t)$ is the concentration found in sampler i at time t. By solving for $ARC_z(t)$ at a number of different times, an ARC breakthrough curve can be defined. To this, the 1-D ADE or moment analysis can be applied so as to calculate solute transport parameters for flux across the horizontal plane at depth z.

An average flux-weighted concentration (AFWC) versus time curve at depth z is calculated by:

$$AFWC_z(t) = \frac{\sum_{i-1}^{k} v_i \theta_z C_i(t)}{\sum_{i-1}^{k} v_i \theta_z} \qquad (2\text{-}25)$$

where v_i is the velocity calculated from the 1-D ADE for sampler i and θ is the average moisture content at depth z.

A breakthrough curve for a particular depth determined from averaging fitted transport parameters is calculated by finding the mean of the parameters v, D and t_o from the individual sampler breakthrough curves that are located at given depth. These mean values are then reentered into the 1-D ADE to generate the ATPC breakthrough curve.

TRANSFER FUNCTION MODEL

According to the transfer function model developed by

Jury (1982), the movement of solute through the vadose zone is governed by a travel-time probability density function, $f_L(t)$, such that $f_L(t)$ gives the probability that a solute entering the soil surface at z=0 will pass a calibration depth z=L in the time interval t to t+dt. The flux concentration at z=L is:

$$C(L,t) = \int_0^\infty C_{input}(t-t')\, f_L(t')\, dt' \qquad (2\text{-}26)$$

where C_{input} is the flux concentration imposed at z=0. For an arbitrary depth z, the travel-time density function at z can be related to the function at calibration depth L by:

$$f_z(t) = \left(\frac{L}{z}\right) f_L\left(\frac{tL}{z}\right) \qquad (2\text{-}27)$$

The probability density functions f_L and f_z are represented by a two-parameter log-normal function whose density is:

$$f_z(t) = [(2\pi)^{\frac{1}{2}}\sigma t]^{-1} \exp\left[\frac{\left(\ln(\frac{tL}{z}) - \mu\right)^2}{2\sigma^2}\right] \qquad (2\text{-}28)$$

where μ and σ are the log-normal mean and the square root of the log-normal variance, respectively. The input function for a square pulse is:

$$C_{input}(t-t') = \begin{bmatrix} C_0 & t-\Delta t < t' < t \\ 0 & t' < t-\Delta t \end{bmatrix} \qquad (2\text{-}29)$$

With this, equation 2-26 yields the solution:

$$C(z,t) = \frac{C_0}{2}\left[erf\left[\frac{\ln(\frac{tL}{z})-\mu}{\sqrt{2}\,\sigma}\right] - erf\left[\frac{\ln[(t-\Delta t)\frac{L}{z}]-\mu}{\sqrt{2}\,\sigma}\right]\right] \qquad (2\text{-}30)$$

According to transfer function theory, this equation will accurately describe concentration versus time breakthrough curves for any depth z, given the parameters μ and σ from calibration depth L, if the medium is vertically homogeneous.

The time moments T_N of the normalized log-normal travel time pdf $f_z(t)$ are calculated from the general equation:

$$T_N = \frac{\int_0^\infty t^N f_z(t)\,dt}{\frac{z^N}{L^N}\exp\left[N\mu + \frac{N^2\sigma^2}{2}\right]} \qquad (2\text{-}31)$$

From the first two moments,

$$\sigma^2 = \ln(T_2/T^2_1) \qquad (2\text{-}32)$$

$$\mu = \ln T_1 - \ln(z/L) - \sigma^2. \qquad (2\text{-}33)$$

Thus, from the first two normalized moments, lognormal distribution parameters can be calculated.

III. MATERIALS AND METHODS

SITE LOCATION AND GEOLOGY

A field site was established in a dry wash on the New Mexico Institute of Mining and Technology campus in Socorro. The site chosen lay in an arroyo bottom that was diked off to prevent runoff events. Figures 3-1 and 3-2 give the location of the field site in reference to the rest of New Mexico and to the campus. The soil is highly stratified and heterogeneous. Two distinct facies have been defined. The upper alluvial unit consists of interbedded silts, silty sands, sands, pebbles and distinct cobble layers. The lower facies consists of relatively uniform fluvial sands of ancestral Rio Grande origin. The water table lay approximately 24 meters below ground surface at the beginning of water application to the site. The site had never been irrigated prior to the experiment. Figures 3-3 and 3-4 are rough geologic cross-sections of the site in the north-south and east-west directions. A more complete description of the site characteristics and geology is provided in Parsons (1988).

The site chosen overlay a 30-m by 30-m square section of soil oriented roughly north-south. Water was applied to the site over a 10-m by 10-m square section centered within this plot. The coordinate system had the southwest corner of the plot labelled (0,0) and the northeast corner labelled (30,30). The first number represents the distance in meters north from

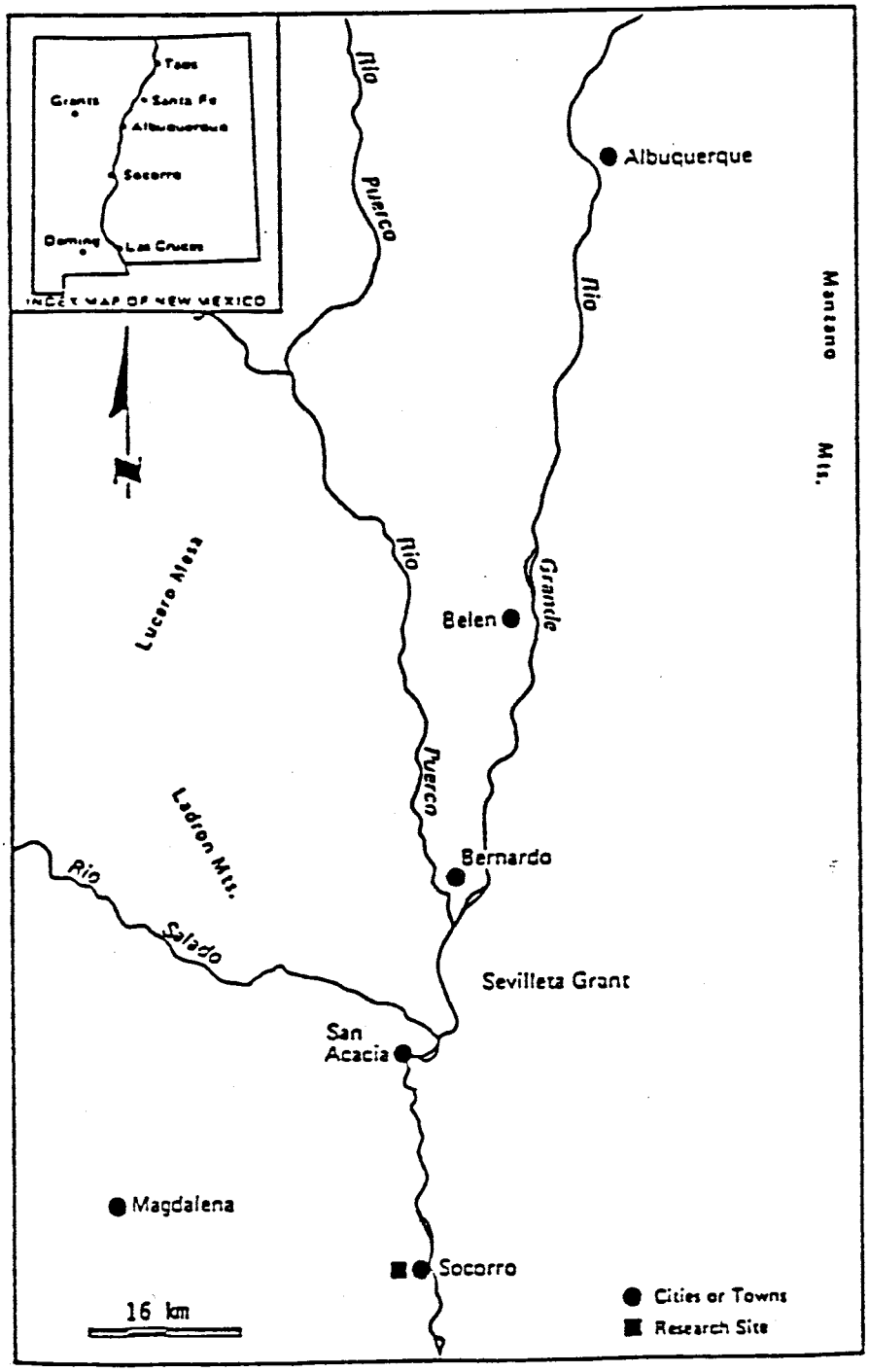

Figure 3-1. Index map (from Parsons, 1988).

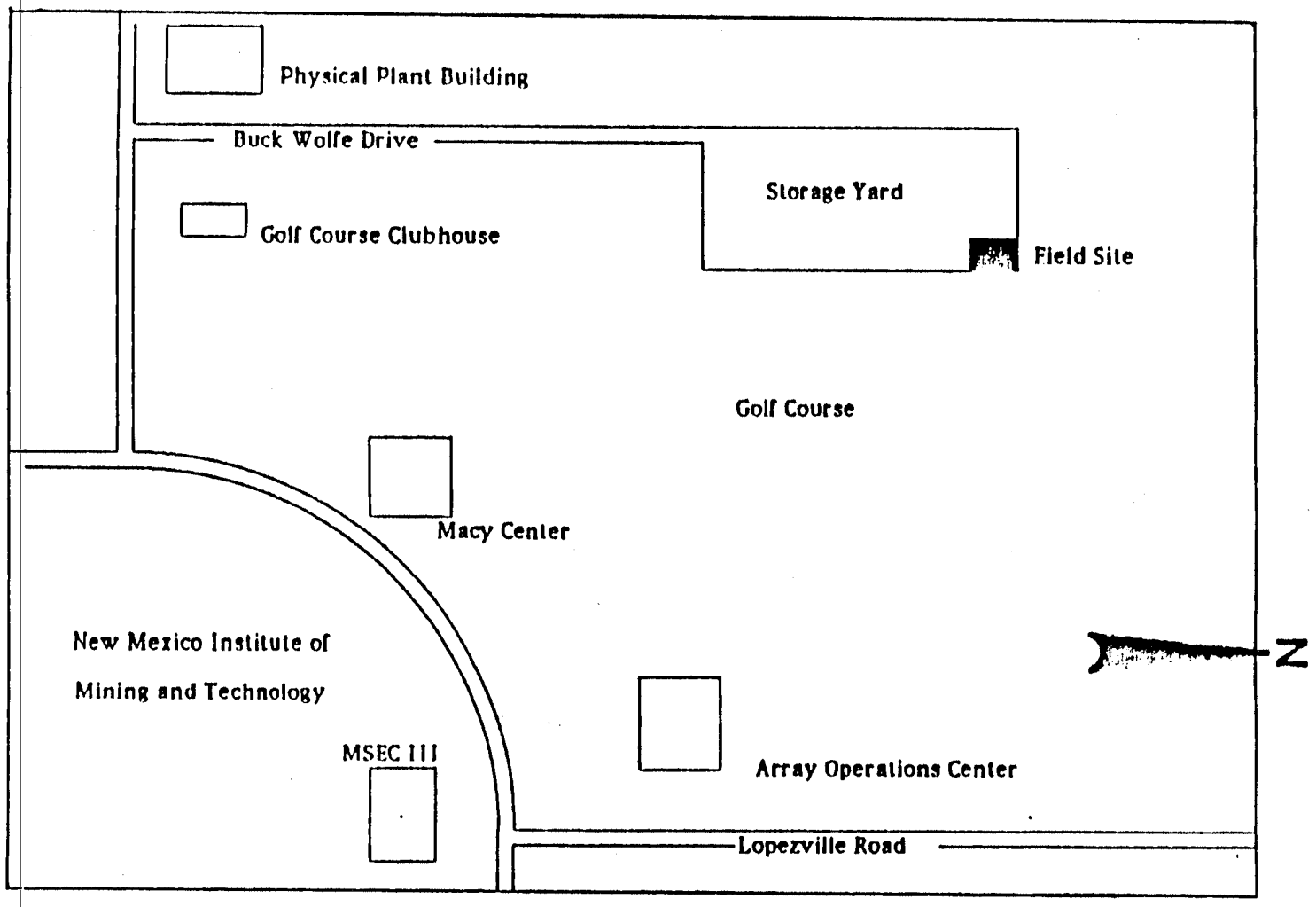

Figure 3-2. Site location map from Gibbens (1989). Not to scale.

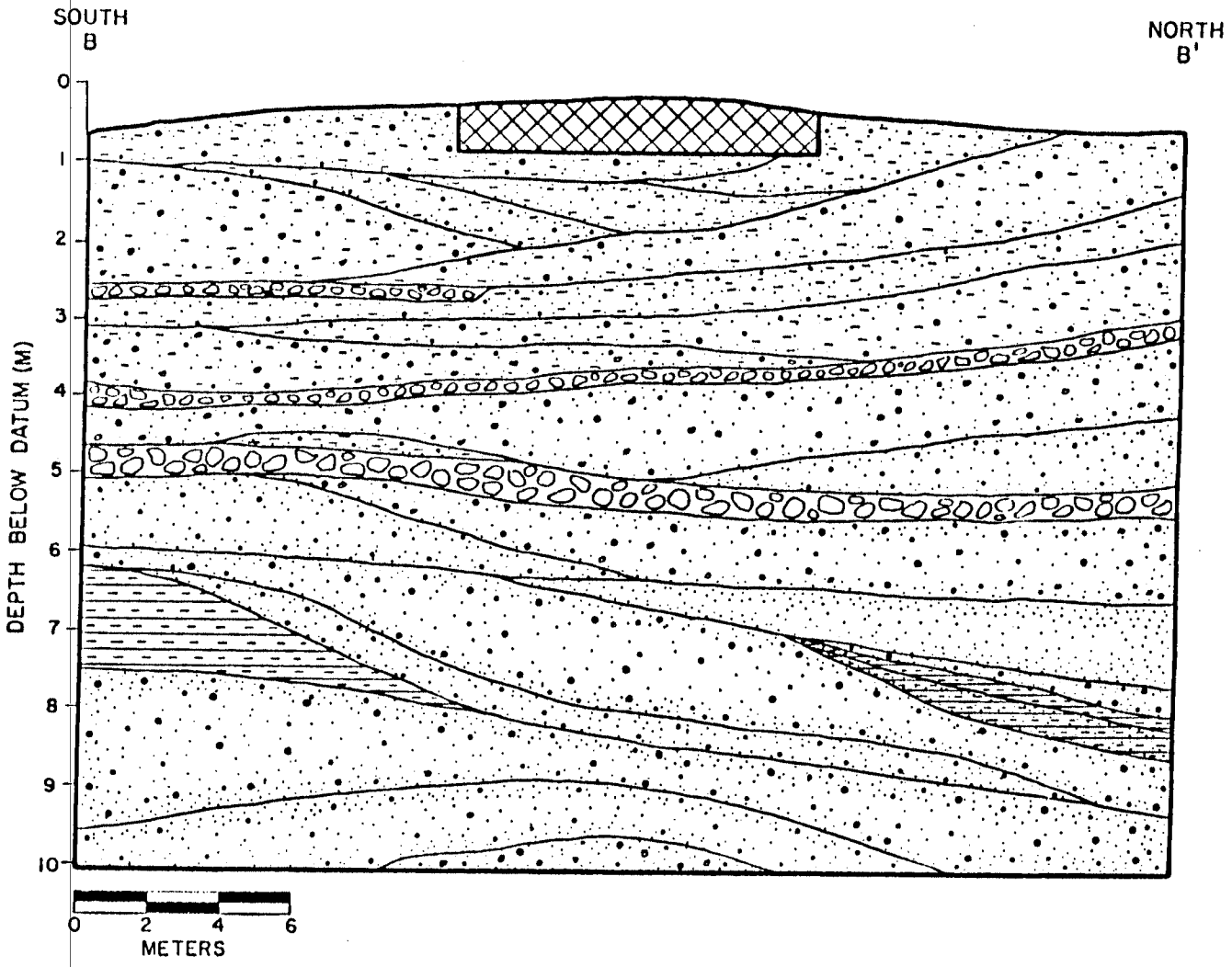

Figure 3-3. North-south geologic cross-section of field site (from Parsons, 1988).

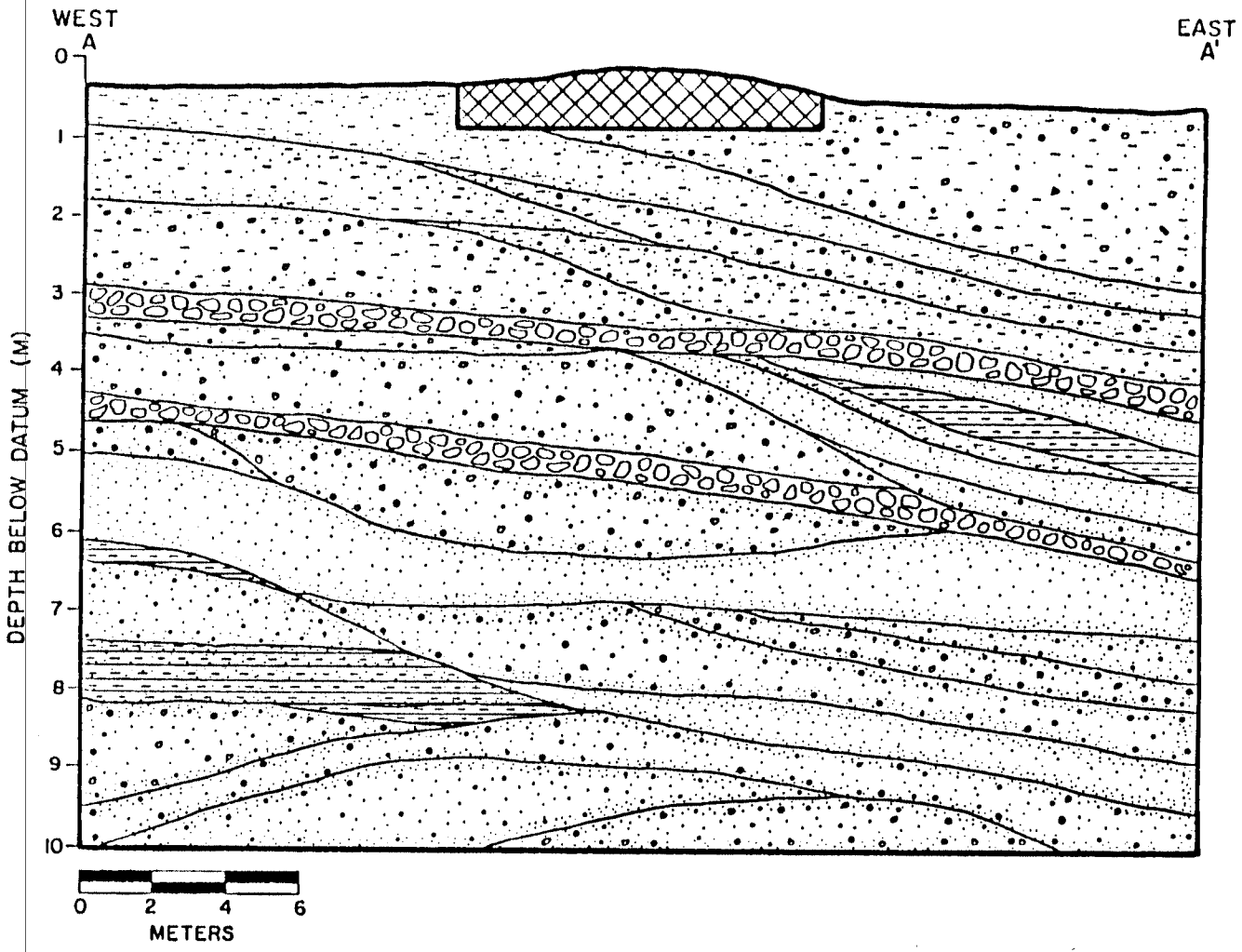

Figure 3-4. East-west geologic cross-section (from Parsons, 1988).

the southwest corner of the plot and the second number represents the distance east from this point.

WATER APPLICATION SYSTEM

A 30-m by 30-m area was cleared out and levelled. The water application system was constructed in the summer and fall of 1986. Details can be found in Mattson (1989). Alterations to the water application system were carried out in the spring of 1989.

The central 10-m by 10-m area was excavated to 60 cm below land surface. On this, 2 cm of sand were deposited as a base for the water application system. Twenty-one 10-m long polyethylene drip lines, with emitters spaced 50 cm apart, were laid down. The drip lines were placed 50 cm apart running east to west. This formed a 50 cm by 50 cm spaced grid of 441 drip emitters to evenly distribute water to the soil.

The drip lines were numbered 1 to 21 from south to north. The drip emitters were connected at their east and west ends to 3/4" PVC manifold headers, which ran north to south. The ends of the headers were capped. Originally, water was pumped into the eastern manifold header through two lines intersecting the header between drip lines 10 and 11. The northern line supplied the northern half of the emitter grid and the southern line supplied the southern half. The original

water application configuration is shown in figure 3-5.

The initial rate of water application was 10^{-5} cm/sec. Three studies were done with this configuration. Parsons (1989) applied a one-dimensional analytical model to observed moisture movement after water was initially applied. Mattson (1989) provided details on the water application design and construction, and applied a two-dimensional analytical model to the observed moisture movement. Flanigan (1989) described a bromide tracer experiment carried out at the site, applying different variations of the one-dimensional advection-dispersion equation to breakthrough of bromide seen in porous cup samplers. He also reported on unsaturated column studies using site material.

During the spring of 1989, alterations to the water application system were completed. The lines were grouped into four sections. Lines 1 through 5 composed section A; 6 - 10, section B; 11 - 16, section C; and 17 - 21, section D. Ball valves were installed on the east and western headers between lines 5 and 6, 10 and 11, and 16 and 17. The valves were closed in order to prevent any mixing of water between the sections.

Water entered the eastern manifold header sections via four 3/4" PVC pipe networks. The network divided a single water source into four roughly equal ones. Each network of pipe was instrumented with gate valves, totalizing flow meters, and a port whereby a tracer solution could be injected

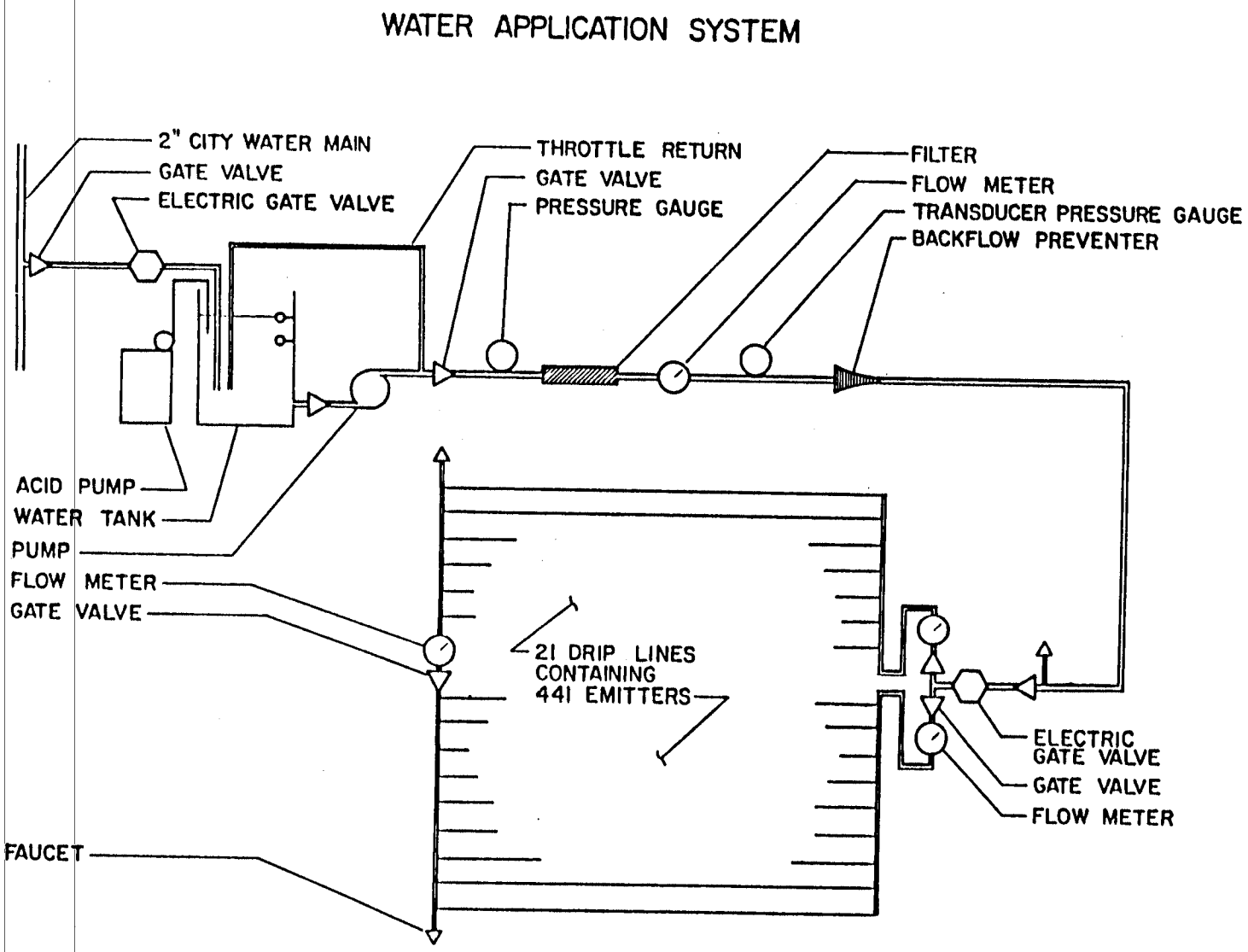

Figure 3-5. Schematic of initial water application system (from Parsons, 1988).

into the water stream. The gate valves allowed the adjustment of water flow to a particular section. Flow meters indicated the amount of water actually flowing into each section. The valves were adjusted to transmit 5/21 of the total water applied to the site to section A, 5/21 to section B, 6/21 to section C, and 5/21 to section D. Each emitter was then assumed to discharge an equal amount of water during any particular pump cycle. To allow sediment accumulating in the drip lines to be periodically flushed out, a faucet was attached to each section of the western header. The western manifold headers ensured that pressure was evenly distributed among the drip emitters of a section. The headers on both sides and the pipe network supplying water to the site were encased in wood lined trenches which prevented damage to the pipes and allowed access for maintenance. Figure 3-6 is a schematic of the altered water application system.

MOISTURE/PRESSURE HEAD INSTRUMENTATION

Prior to the construction of the water application system, tensiometers and neutron probe access tubes were installed at twenty-one stations in a symmetrical pattern across the site. Each station consisted of: a 5-cm diameter, 10-m long aluminum tube that served as an access tube for the neutron moisture probe; and two tensiometer nests, each consisting of 8 tensiometers emplaced at depths from 1 to 5

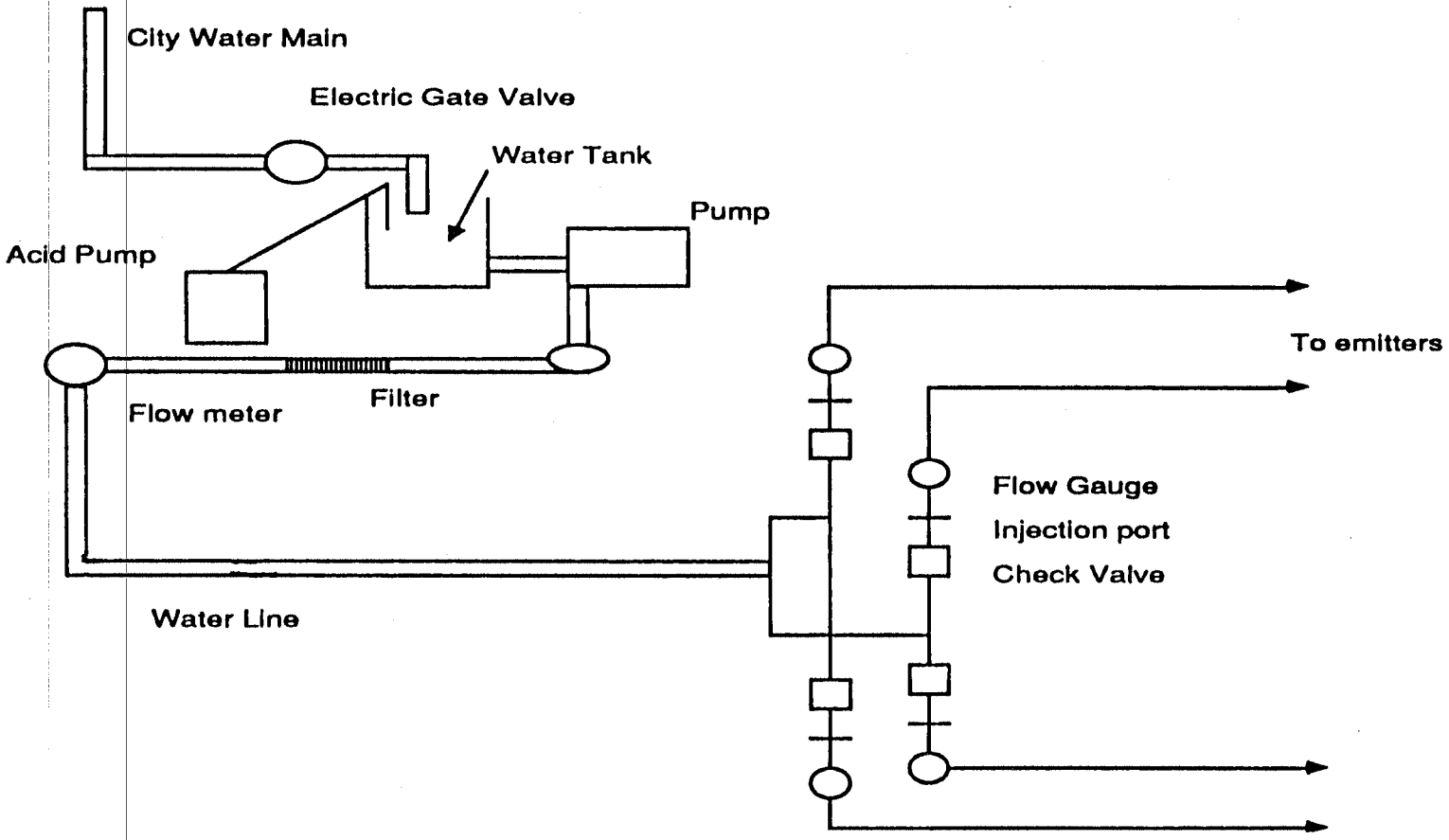

Figure 3-6. Schematic of water application system for use in tracer test (from Gibbens, 1989).

meters. The location of these instruments is shown on figure 3-7. Moisture measurements from the neutron probe and measurements of matric potential in the soil were collected daily after the flux to the water application system was increased. Data from these measurements provided evidence that water flow through the instrumented area reached steady-state before the tracers were applied. The instruments were read twice weekly during the tracer experiment till its completion.

MONITORING INSTRUMENTATION

Tracer transport through the soil was measured with soil water samplers, also called suction lysimeters. Samplers beneath the drip lines ranged from 33 cm to 320 cm in depth; samplers outside the wetted region ranged in depth from approximately 100 cm to 700 cm.

CONSTRUCTION

Soil water samplers consisted of a length of 2" diameter PVC pipe with a porous ceramic cup (No. 653X01-B2M2, SoilMoisture Equipment Corp., Santa Barbara, CA.) epoxied to one end. A black rubber stopper, with two 1/4" black polyethylene hoses passing through it, sealed the other end of the PVC pipe. One of the hoses reached the bottom of the ceramic cup for the purpose of removing all solution pulled inside the sampler. The other hose reached two to four inches

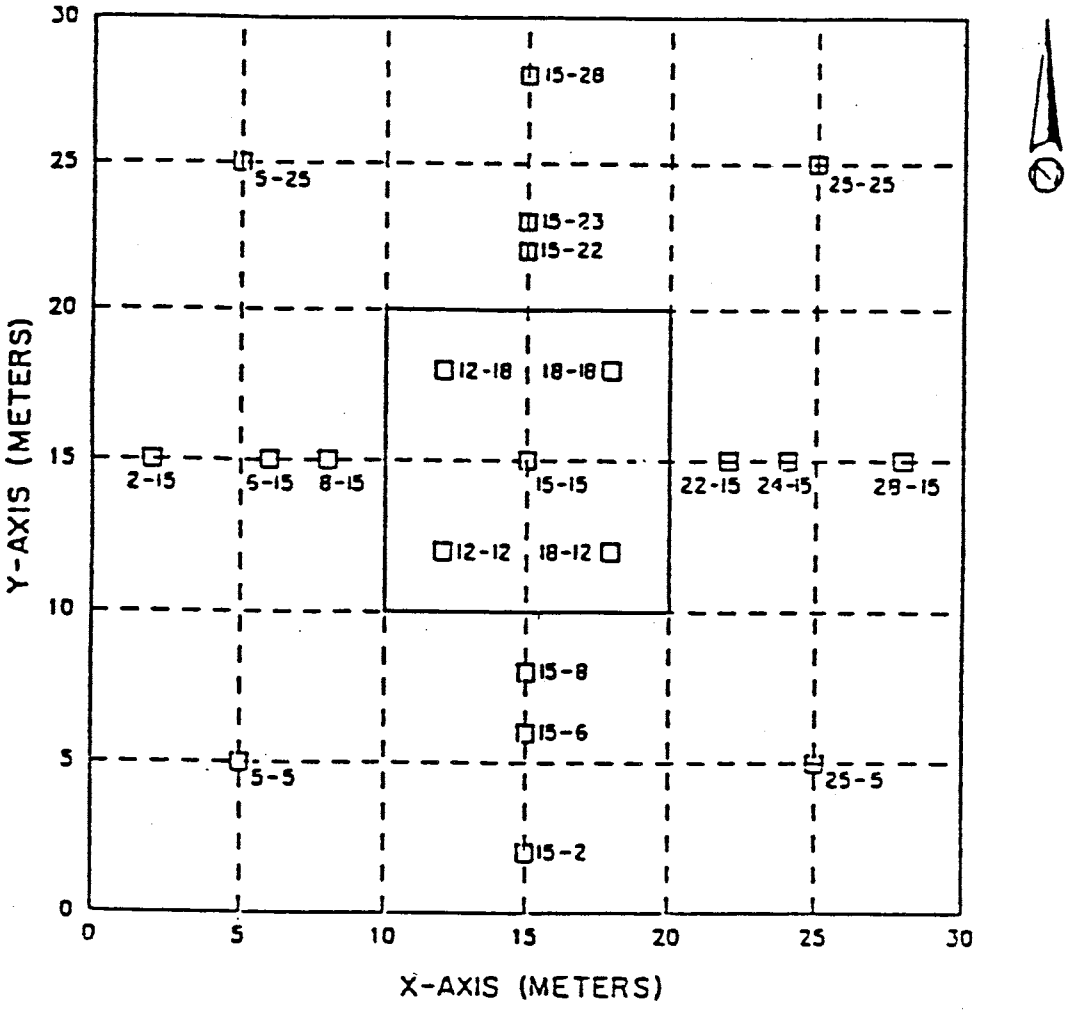

Figure 3-7. Diagram showing the location of instrument stations at the field site. Each square represents a neutron probe access tube and one or two tensiometer nests (from Parsons,1988).

into the sampler. The rubber stopper was glued to the other end of the PVC pipe with liberal amounts of epoxy. Figure 3-8 illustrates the way the soil water samplers were designed.

Prior to installing the soil water samplers at the site, the porous ceramic cups and PVC pipes were cleaned to remove any chemicals that might interfere with tracer analysis. This was accomplished by drawing approximately one liter of 6N hydrochloric acid followed by two liters of distilled, de-aired water through the sampler's porous cup under vacuum.

INSTALLATION OF SOIL WATER SAMPLERS

Table 3-1 presents a list of soil water samplers, their coordinates and their depths below drip lines. The number part of each sampler's name corresponds to the hole in which it was emplaced. When a letter follows the number, like a, b, c, or d, it refers to several samplers placed at different depths in one hole. Figure 3-9 shows the location of the sampler stations installed before a previous bromide tracer experiment (Flanigan,1989). Figure 3-10 and 3-11 plot the location of samplers installed for this experiment within and without the wetted region, respectively.

All samplers (except G24, H23, I22) within the wetted region were emplaced in holes dug with a 3" diameter hand auger. This digging method was employed because heavy machinery, such as a drill rig, could crush drip emitter lines and cause uneven water distribution across the site.

Soil water samplers G24, H23, and I22 had been placed in holes

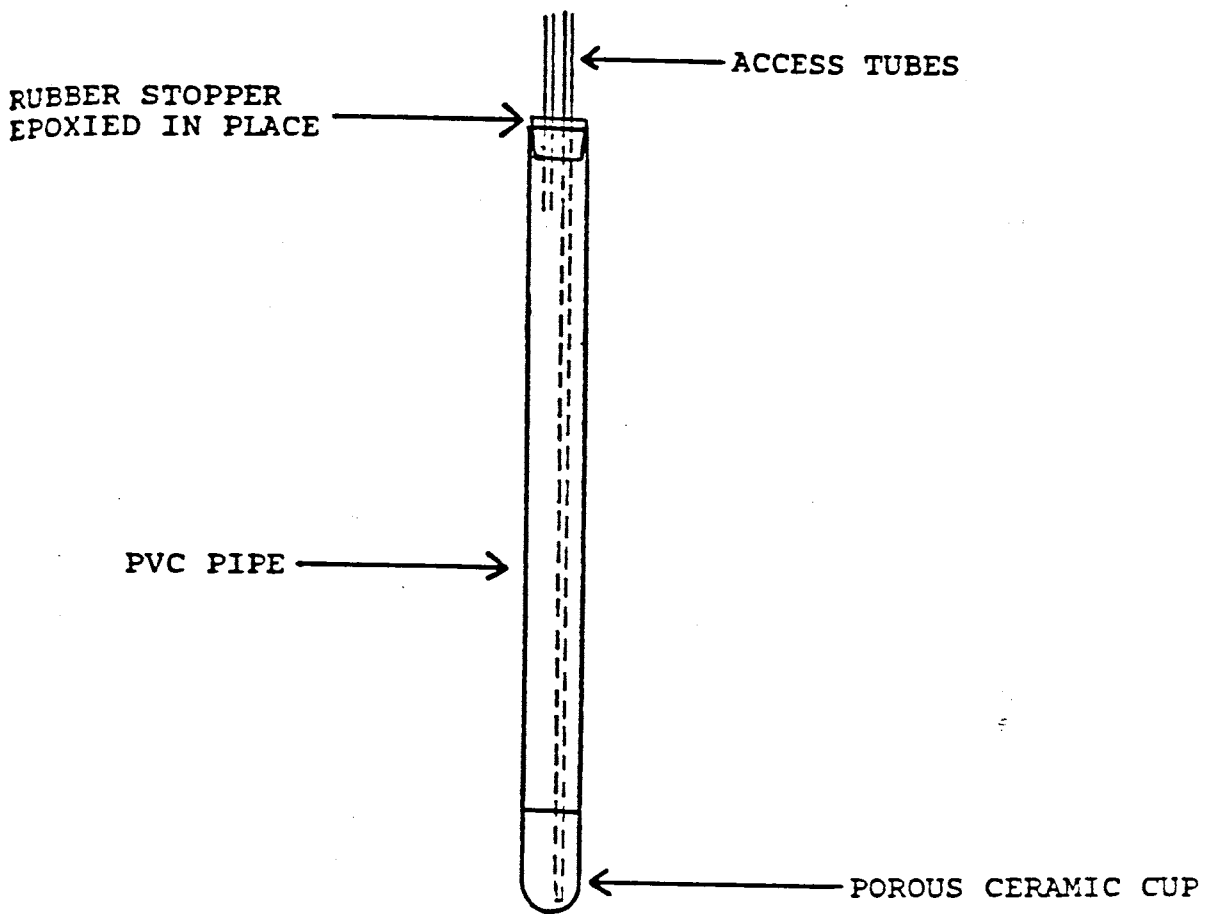

Figure 3-8. Soil water sampler (from Flanigan, 1989).

TABLE 3-1. X, Y, Z locations of soil water samplers.

SAMPLER	X(M)	Y(M)	Z(CM)
1a	11.25	11.25	100
1b	11.25	11.25	191
1c	11.25	11.25	265
2a	16.25	11.25	100
2c	16.25	11.25	239
3a	13.75	11.75	100
3c	13.75	11.75	242
4a	18.75	11.75	100
4c	18.75	11.75	145
5a	11.25	12.75	100
5c	11.25	12.75	208
6a	16.25	12.75	100
6c	16.25	12.75	225
7a	13.75	13.75	100
7c	13.75	13.75	204
8a	18.75	13.75	112
9a	11.25	14.25	100
9c	11.25	14.25	219
10a	16.25	14.25	100
11a	13.75	15.25	33
11b	13.75	15.25	99
11c	13.75	15.25	148

TABLE 3-1.(CONTINUED)

SAMPLER	X(M)	Y(M)	Z(CM)
11d	13.75	15.25	216
12a	18.75	15.25	100
12c	18.75	15.25	226
13a	11.25	16.25	100
13c	11.25	16.25	193
14a	16.25	16.25	100
14c	16.25	16.25	235
15a	13.75	17.25	100
15c	13.75	17.25	224
16a	18.75	17.25	100
16c	18.75	17.25	226
17a	11.25	18.25	100
17c	11.25	18.25	237
18a	16.25	18.25	100
18c	16.25	18.25	224
19a	13.75	19.25	100
19c	13.75	19.25	248
20a	18.75	19.25	100
20b	18.75	19.25	199
20c	18.75	19.25	288
D29	14.50	12.25	138
G24	15.50	17.25	107

TABLE 3-1. (CONTINUED)

SAMPLER	X(M)	Y(M)	Z(CM)
H23	15.00	17.25	244
I22	14.50	17.25	320
K25	14.00	15.25	158

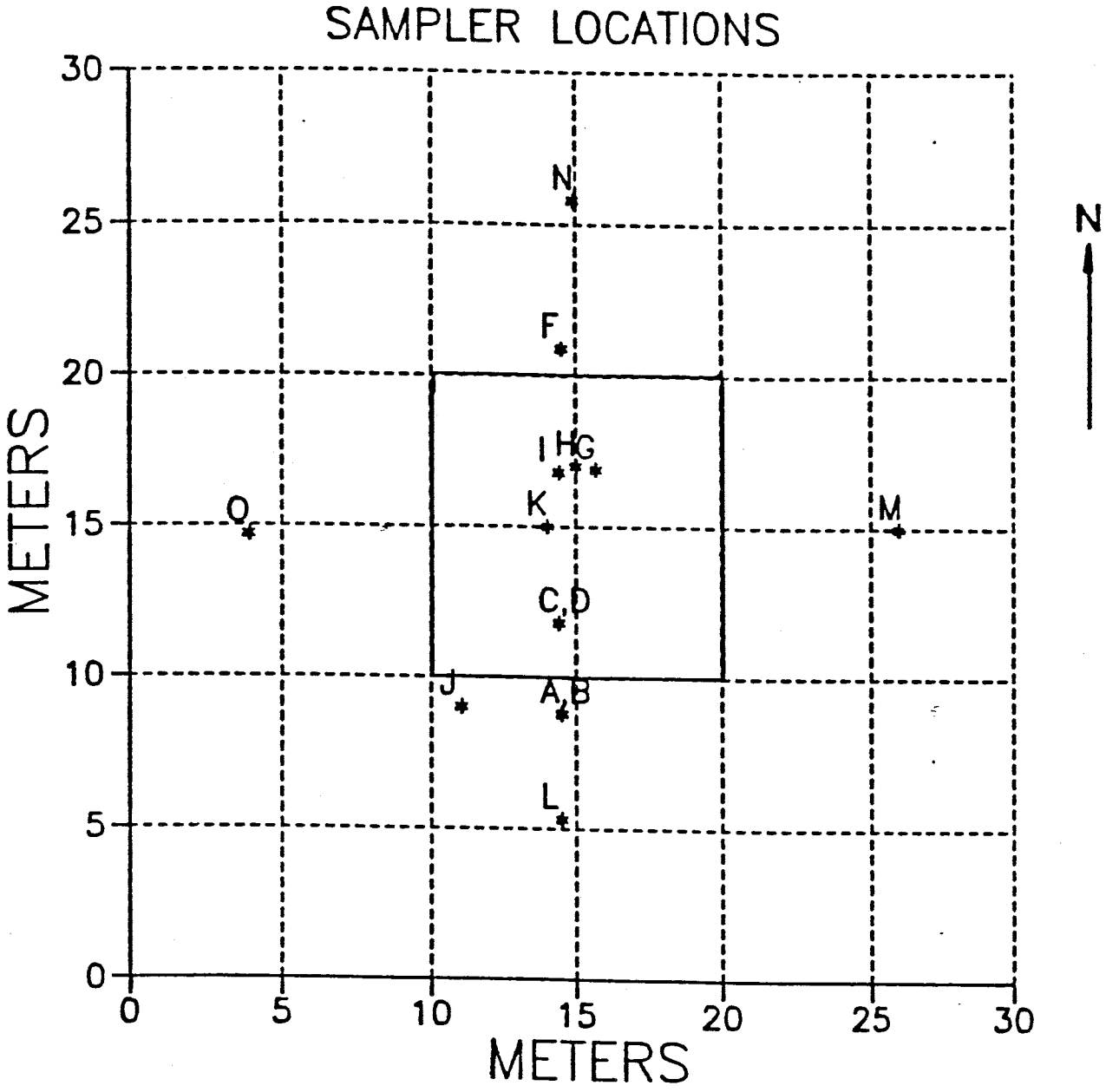

Figure 3-9. Locations of soil water samplers from the previous tracer experiment (from Flanigan, 1989).

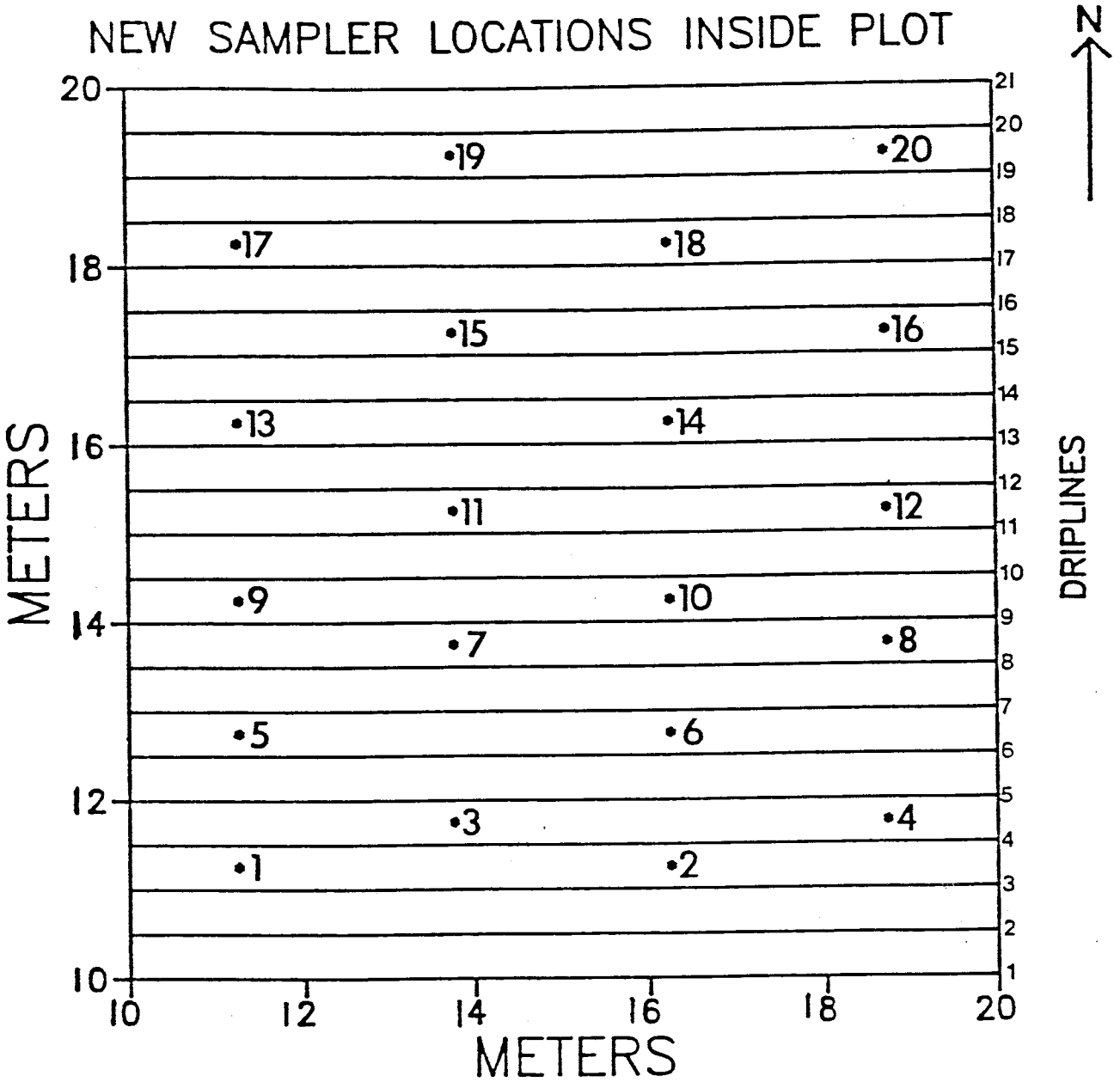

Figure 3-10. Location of sampler nests installed within drip lines for multiple tracer test.

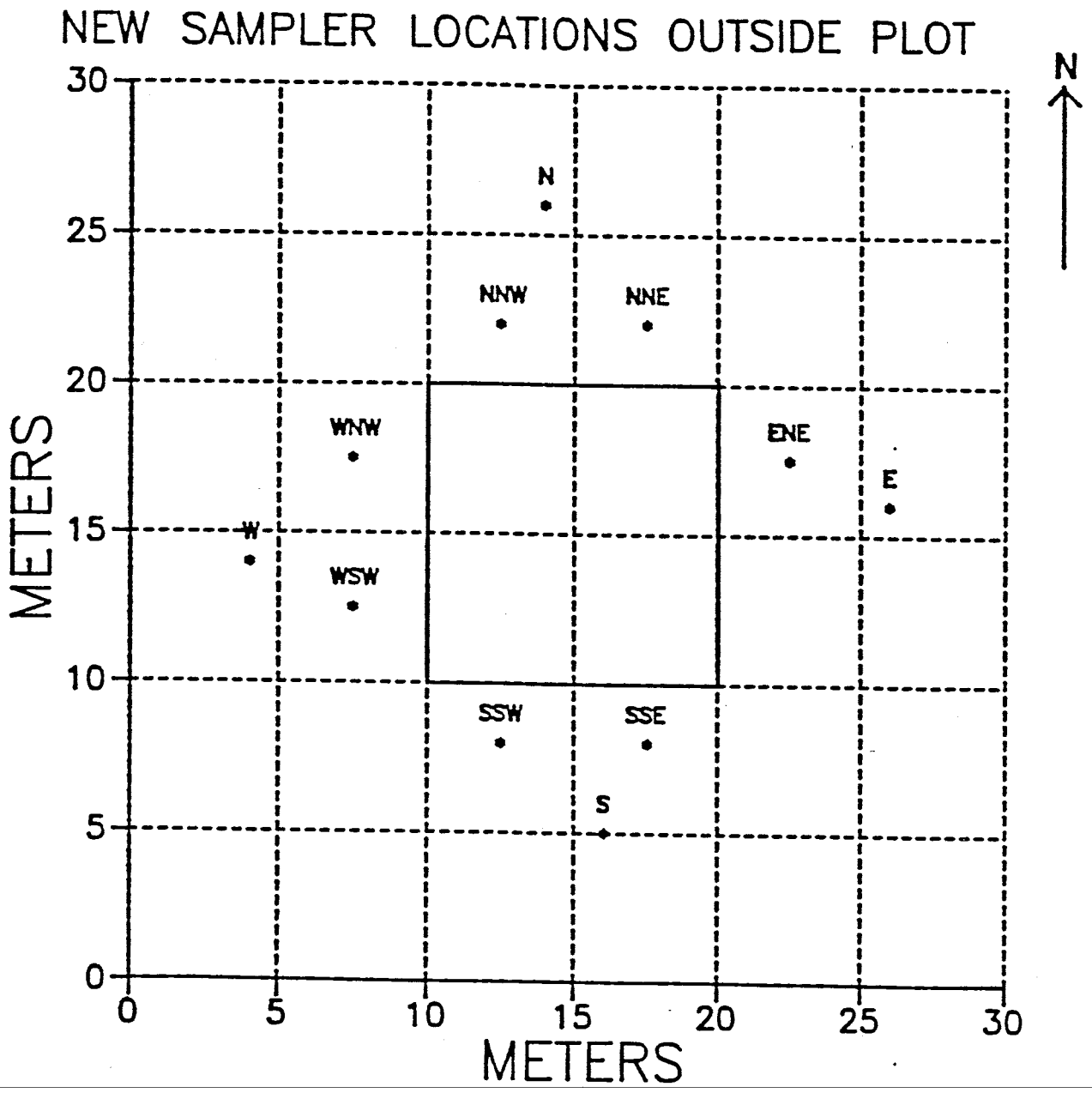

Figure 3-11. Location of sampler nests installed outside drip lines for multiple tracer test.

made by a rotary drill rig with an 8" diameter auger before the drip lines were laid down.

The samplers were installed as follows. The black 1/4" plastic hoses were inserted into a 7/8" O.D. 5/8" I.D. PVC pipe, with 5" of hose sticking out, for protection. Silica flour (200 mesh) was funneled to the bottom of the augered hole, the sampler lowered to the bottom and enough silica flour added to cover the ceramic porous cup. Several inches of native sandy soil, sieved through a #4 (6.3 mm) sieve, were added and tamped; then two inches of a 15 percent mixture of bentonite and sieved soil were added. The bentonite was expected to swell around the PVC pipe of the sampler and inhibit flow down the sides. Sieved sandy soil was added and tamped till the elevation of the next sampler, or until the level of the drip lines. Just below and above drip line elevation, 5 cm of bentonite/soil mixture were placed to prevent evaporation out or precipitation into the augered hole. Native material was used to fill the hole to ground surface.

Vinyl tubing was clamped onto the exposed ends of the black plastic hoses using hose clamps. Suction samplers placed outside of the wetted region were emplaced similarly, but holes were dug using a drill rig with a 20-cm auger. Names for these outside samplers correspond to points on a compass. For instance, SSW-C stands for a sampler placed at depth C in a hole drilled south-south west of the center of

the drip emitter grid. Samplers 11 a,b,c,d were installed without silica flour or bentonite seals except just above and below the drip lines. This was done to investigate how the installation of the porous cup samplers might influence tracer movement.

MULTI-TRACER TRANSPORT EXPERIMENT

In May, 1989, flow to the emitter system was increased tenfold to 1 x 10^{-4} centimeters per second. The water was applied using a positive displacement pump, controlled by an electronic timer and a control box. At fifteen minute intervals, water was pump out of a tank for approximately four minutes. A system of floats in the water tank ensured the volume of water fed to the drip lines during a pump cycle remained constant. Water was pumped from the tank until a bottom float activated a switch and turned off the pump. Shortly afterwards, an electronic timer, controlling a solenoid valve, would open the valve and let the tank refill until an upper float in the tank activated a switch and closed the valve. The timer then reactivated the pump fifteen minutes after the last water application cycle and repeated the cycle. To prevent carbonate from precipitating out of the tap water and clogging the drip emitters, a chemical feed pump was occasionally turned on. This pump delivered a small amount of 1:13 solution of muriatic acid (31.45%) to tap water

into the water tank (Flanigan,1989). This kept the pH of the water in the tank around 6.5.

On July 1, 1989, a multi-tracer field experiment was conducted at the site. The experiment consisted of injecting a different fluoro-organic acid tracer into each section of the water application system. Calcium bromide, potassium thiocyanate, and the herbicide bromacil were injected into all sections simultaneously with the fluoro-organic acids. The transport of the tracers was monitored using the soil moisture samplers.

TRACER APPLICATION

Four 50 liter reservoirs of concentrated tracer solution were prepared, each consisting of one of four different fluoro-benzoic acids, bromide, thiocyanate, and the herbicide bromacil. The fluoro-benzoate tracers used were *m*-(trifluoromethyl)benzoic acid (*m*-TFMBA), *o*-(trifluoromethyl)benzoic acid (*o*-TFMBA), 2,6-difluorobenzoic acid (2,6-DFBA) and pentafluorobenzoic acid (PFBA). The amount of tracer dissolved in each 50 liter reservoir is listed in table 3-2. Reservoir III had 20 percent more tracer since it supplied six, rather than five, driplines.

A multi-channel syringe pump (Soil Measurement Systems, Tucson, AZ) was used to inject concentrated tracer solution into the water stream flowing through the water application system, via four plastic syringes. The tracer application

TABLE 3-2. Masses of solutes added to 50 liter reservoirs.

	Fluorobenzoate				
Reservoir	Acronym	Mass Added	$CaBr_2$	KSCN	Bromacil
I.	PFBA	105	260	175	105
II.	2,6-DFBA	105	260	175	105
III.	*o*-TFMBA	125	310	210	125
IV.	*m*-TFMBA	105	260	175	105

masses in grams.

system was designed as follows. A 20-mL plastic luer lock syringe was connected to one end of a 5 cm long polyethylene tube, the other end of the tube connected to a "T" connection. Tubing ran from one end of the "T" to the tracer reservoir. The other end of the "T" had tubing running to a injection port, located between the gate valve and flow meter on the water application network previously described (see figure 3-6). High-flow uni-directional check valves were inserted into the lines running between the "T" and the reservoir and the "T" and the injection port. These check valves ensured that there was no backflow in the system. Hose clamps were placed on the tubing running from the solute reservoir to the "T". These clamps were pinched shut when the syringe pump was off. Otherwise, the head difference between the reservoir and the injection port would allow tracer to freely flow into the water application system.

An injection cycle consisted of two parts, a pull cycle and throw cycle. During the pull cycle, the stem of the syringe was pulled back, creating a suction that pulled reservoir solution into the syringe bore, while a check valve prevented water from being sucked from the water application system. During the throw cycle, the stem was pushed into the syringe bore, creating a positive pressure that forced reservoir solution into the injection port. Presumably, the tracer solution mixed thoroughly with the water flowing through the drip emitter system, smoothing out the pulsing

effect of the tracer injection cycle.

The tracer application system was attached to the water application system in late June of 1989. Each reservoir was hooked to a separate syringe, which in turn was connected to one of the four sections (figure 3-12). Reservoir I applied tracer to section A, reservoir II to section B, reservoir III to section C, and reservoir IV to section D. Tracer injection began at 7:00 am, July 1. The faucets on the western header were opened and mixed tracer solution and water allowed to fill the drip lines. The faucets were then closed and the experiment begun. The syringe pump was powered only when the water pump was activated. Tracer was applied for twenty-four hours, consuming approximately 28 liters of each reservoir. During the time tracer was being injected, drip line solution was sampled on three separate occasions. They were taken from the western header faucets one hour and 45 minutes, 14 hours and 45 minutes and 23 hours and 45 minutes after the start of tracer injection. These samples defined the initial tracer concentration entering each section of the site. After tracer application was discontinued, the faucets were opened and the lines flushed with tap water. To check for tracer still in the drip lines, water was sampled from the faucets during the next 3 pump cycles.

SAMPLE COLLECTION

Samples of soil water from interior samplers were taken with a portable vacuum/pressure pump three times a day at

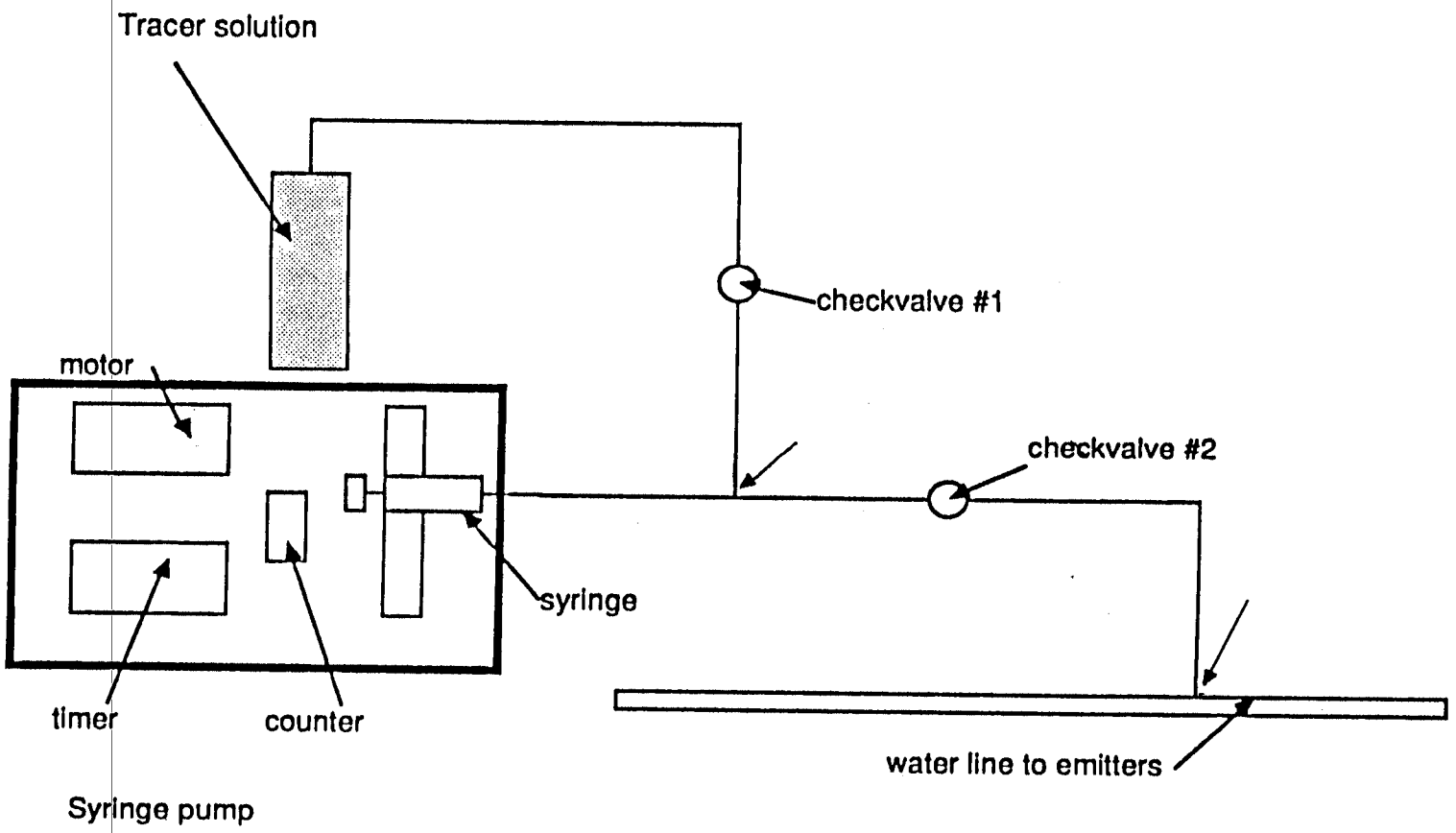

Figure 3-12. System for injecting tracer into water application system (from Gibbens, 1989).

approximately 0600, 1400, and 2200 military time for the first nine days after tracer injection was begun; then at steadily decreasing frequency through the remaining period the test was carried out. Extraction of soil water samples took place in two phases. The first phase consisted of putting a vacuum in the sampler and allowing soil water to be pulled into the instrument through the porous cup. This was accomplished by closing one of the lines to the sampler and pulling a vacuum on the other line of 15 to 25 centibars on interior samplers and 30 to 40 centibars on exterior samplers. The vacuum line was clamped shut and soil water allowed to enter the porous cup.

The second phase consisted of unclamping both lines and applying pressure to the line running to the top of the soil water sampler, thus forcing water out the other line. Almost all the water in the sampler was pumped out so that there would be no mixing between sampling runs. Samples were placed in 2-mL polyethylene sample bottles and the approximate volume of water extracted recorded. The volume of water extracted varied from no water to 500 ml.

DYE INJECTION AND TRENCHING

Immediately after the last soil water samples were taken, FD&C blue dye #1 was injected into the water flowing into the southern section of the site. This continued for five days.

days. Afterwards, dye was applied over the entire site for one day. This was done for the purpose of tracing actual fluid flow paths from the drip emitters through the soil and to test drip emitter uniformity.

Trenches were dug across the site to observe the dye and to better understand the degree of soil heterogeneity. This paper will discuss only one particular trench. This trench was excavated to determine whether there was any piping of flow down instrument nests in the area. The hole was approximately 3-m deep, 2.75-m long running east to west, and 1.3-m wide. Figure 3-13 gives the approximate location of the trench within the plot. The nests looked at were samplers 1a, 1b, 5a, 5c; neutron access tube 12-12 and tensiometer nest 12-12a.

ANALYSIS FOR TRACERS IN WATER SAMPLES

Water samples were analyzed for fluoro-benzoate, bromide, and thiocyanate using a model 501 HPLC pump, model 481 UV detector and model U6K injector (Millipore Corporation, Waters Chromatography Division, Milford, MA). The column used was a 25-cm x 4.5-mm I.D. Regis Rexchrom strong anion exchange column packed with 5μm solid phase (#728220, Regis Corporation, Morton Grove, IL). The mobile phase was .03M KH_2PO_4, pH 2.6, 20% CH_3CN v/v. Periodic adjustment of the mobile phase was necessary to enhance separation of the

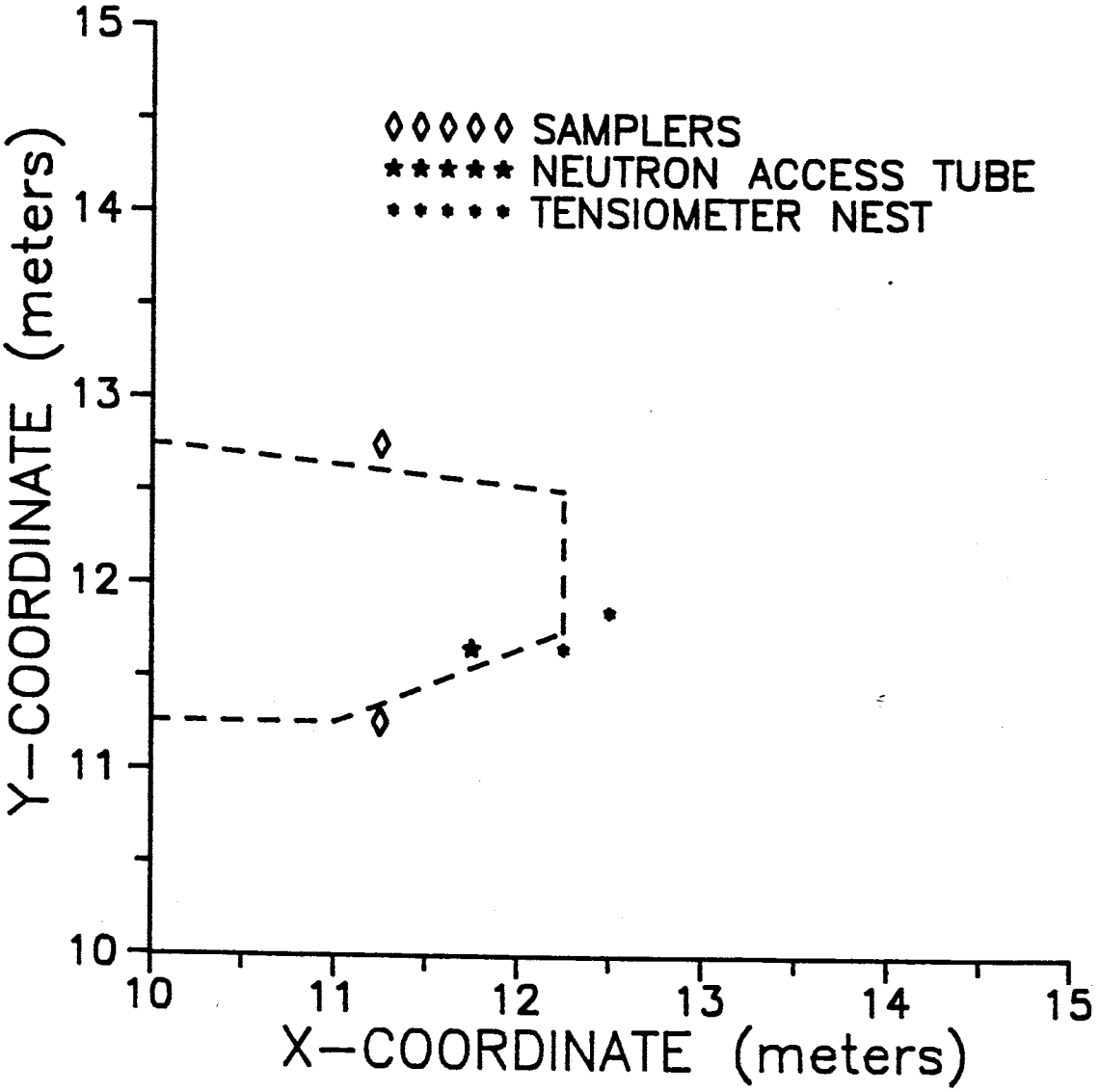

Figure 3-13. Trench location. Area inside dotted lines is location of trench (approximately 3 meters deep below ground surface).

tracers. Adjusting the concentration of KH_2PO_4 buffer sped up or slowed down the elution times for all the chemicals, while adjusting the pH permitted changing the elution times of the fluoro-benzoates relative to bromide and to each other. The mobile phase was pumped at 1 ml/min. The detection wavelength was 195 nm. High nitrate contamination at the site caused difficulties quantifying bromide in some samples. More information concerning the method for analyzing these tracers can be found in Bowman (1984). Figure 3-14 is a sample chromatogram showing an analysis of sampler 20b for bromide and *m*-TFMBA.

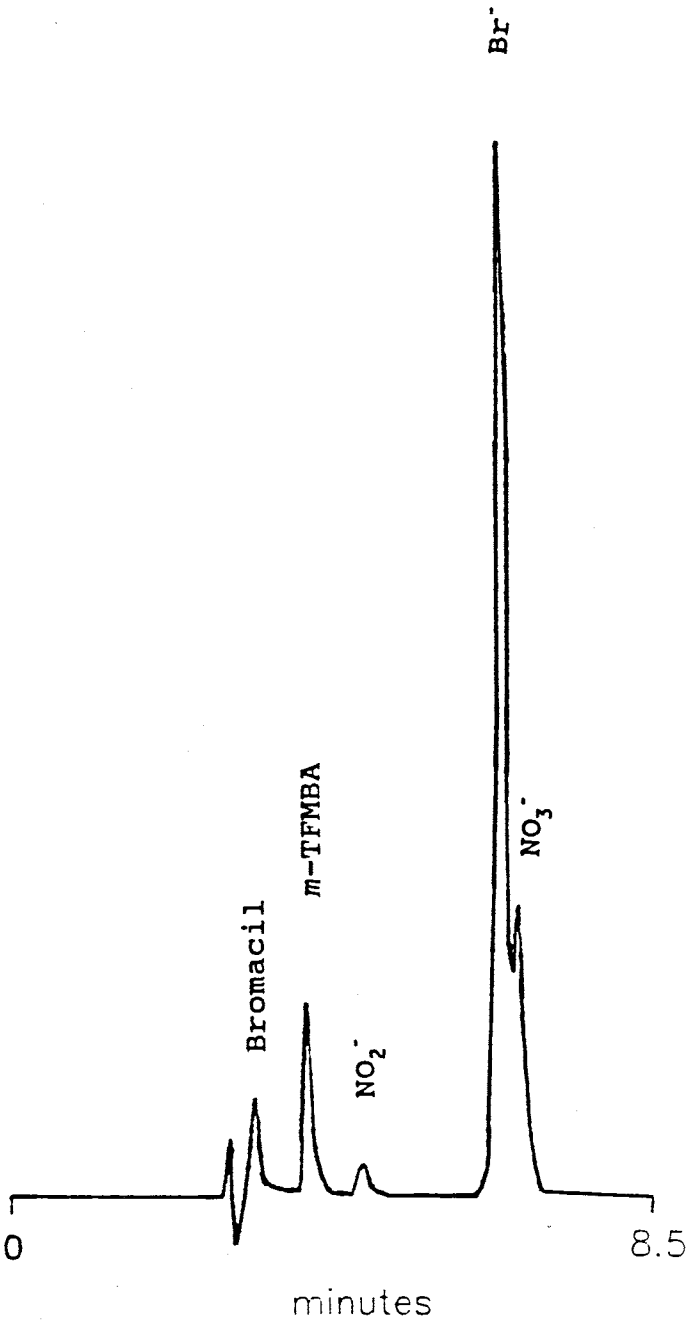

Figure 3-14. Sample chromatogram from sampler 20B. Sample was taken 7/6/90 at 14:00.

IV. RESULTS AND DISCUSSION

Concentration data from the water samples were used to construct breakthrough curves (BTC's) at each sampling location for each tracer. Tracer breakthrough curves were generated by plotting the concentration of tracer seen in a soil water sample versus the time at which that sample was drawn into the sampler. This time was considered to be two hours after vacuum was applied to the sampler. Because soil suction samplers were used to gather concentration versus time data, the way to look at the concentration is indeterminate. Flux concentrations have mostly been used in this situation, but it is most likely that a combination of the two types more clearly defines what occurs (Flanigan, 1989). For the purpose of determining transport parameters, flux concentrations will be assumed in this paper.

PROBLEMATIC SOLUTION SAMPLERS

Piping of dye down the instrumentation was seen only at sampler 1a. It was also noticed that the bentonite seal around the tube had pulled away from the PVC and that there were large voids in the silica flour around the porous cup. The silica flour around samplers 5a and 5c was intact and the bentonite seemed to make a good seal.

Breakthrough curves were plotted for sampler 1a and the two samplers directly beneath it. The BTC's of sampler 1a and 1b were distinctly different from most of the other BTC's that

were plotted. The tracer flowed very quickly to sampler 1a, less quickly by far to sampler 1b. The mass recovered from sampler 1b was also much less than that recovered from either sampler 1a or 1c. It is hypothesized that the quick movement of tracer to sampler 1a was due to piping down the side of the tube and that the diminished mass seen in sampler 1b was due to the direct extraction of the tracer directly above it. Figure 4-1 shows the breakthrough curves of bromide for samplers 1a, 1b, and 1c. For the reasons sited above, sampler 1a and 1b will not be used in modelling the tracer movement at the site.

The tracer breakthrough curve of sampler D29 also seemed to show extraordinarily fast tracer movement, faster even than sampler 1a. This sampler, used in a previous tracer experiment, had been pulled out once, because of clogging of the porous cup, and then replaced. The sampler tube extended above ground surface, so it was possible to observe the seal between the soil and the sampler. It appeared that the sampler was not in sound contact with the soil as the sampler could be wiggled in its hole. For these reasons, this sampler also was not used in modelling the tracer movement. Figure 4-2 shows the breakthrough curve for sampler D29.

Samplers 3a, 11b, and 20c would not hold a suction so that no soil water samples could be taken from them. Soil water samples were taken from samplers 2a and 6c, but no tracer was detected in either of them. This could be

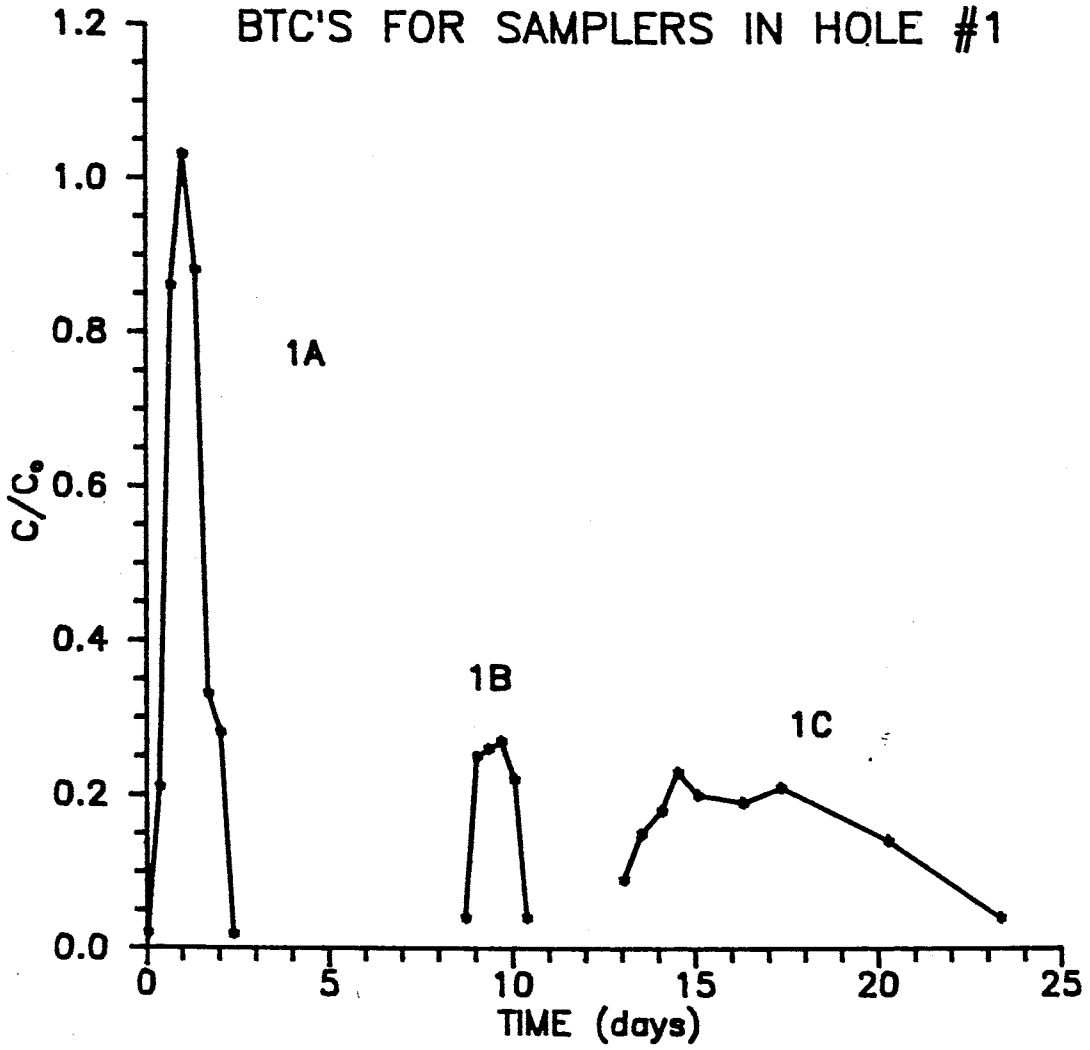

Figure 4-1. Bromide breakthrough curves for samplers 1a, 1b, and 1c.

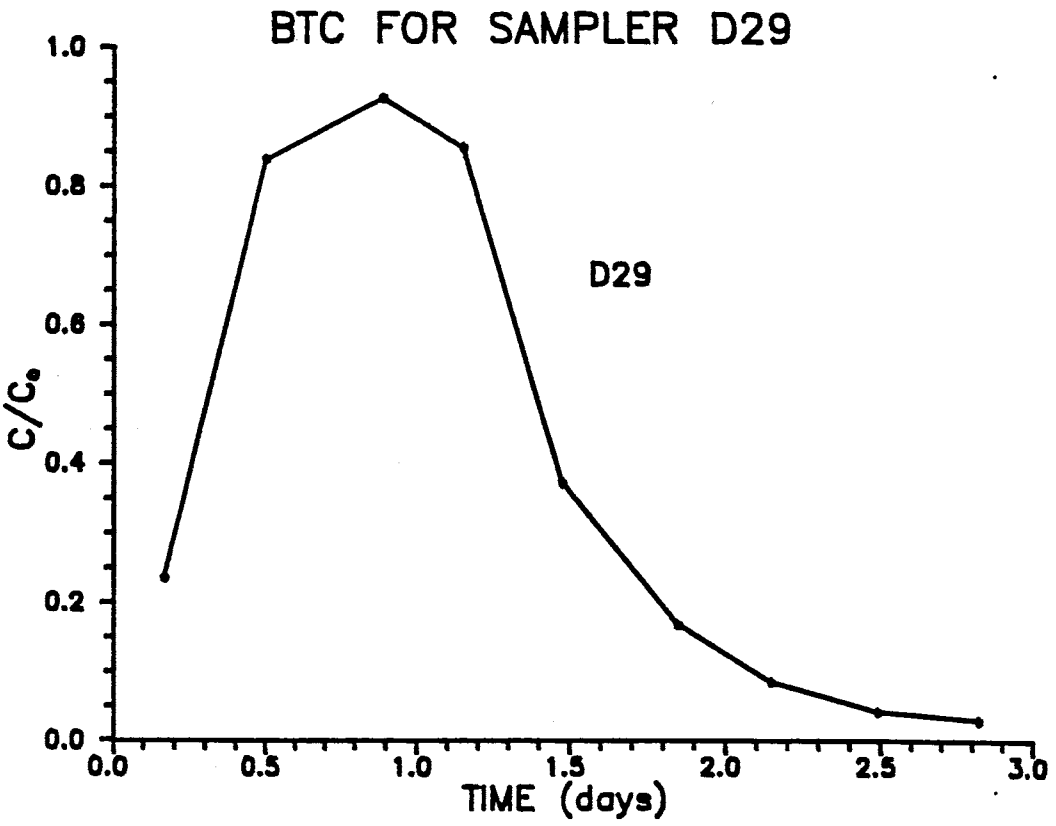

Figure 4-2. Bromide breakthrough curve for sampler D29.

explained by tracer movement around the sampler but not close enough to be pulled into it. It was also possible that much of the water pulled into the sampler was not removed during the extraction process. This could have happened if there were a hole in the extraction line well above the porous cup. The water that remained in the sampler would dilute the water that was pulled in the subsequent soil water extraction, possibly to the point of diluting it below detection limits. These samplers, like the ones mentioned above, have been disregarded for modelling purposes.

DETERMINATION OF TRANSPORT PARAMETERS FROM BREAKTHROUGH CURVES

Soil water samples were used to determine the movement of tracer through the unsaturated zone beneath the site. Relative concentrations were calculated by dividing the concentration of tracer in a particular sampler by the average concentration seen in three "standards," samples taken from the faucets during tracer application. The deviation of individual "standard" samples from the average concentration was no greater than 20 %. Plots of the standards compared with the average concentration, set equal to 1.0, are shown in figure 4-3 along with the residual concentration seen in the drip lines after the tracer application was stopped.

Two methods were used to determine hydrodynamic parameters

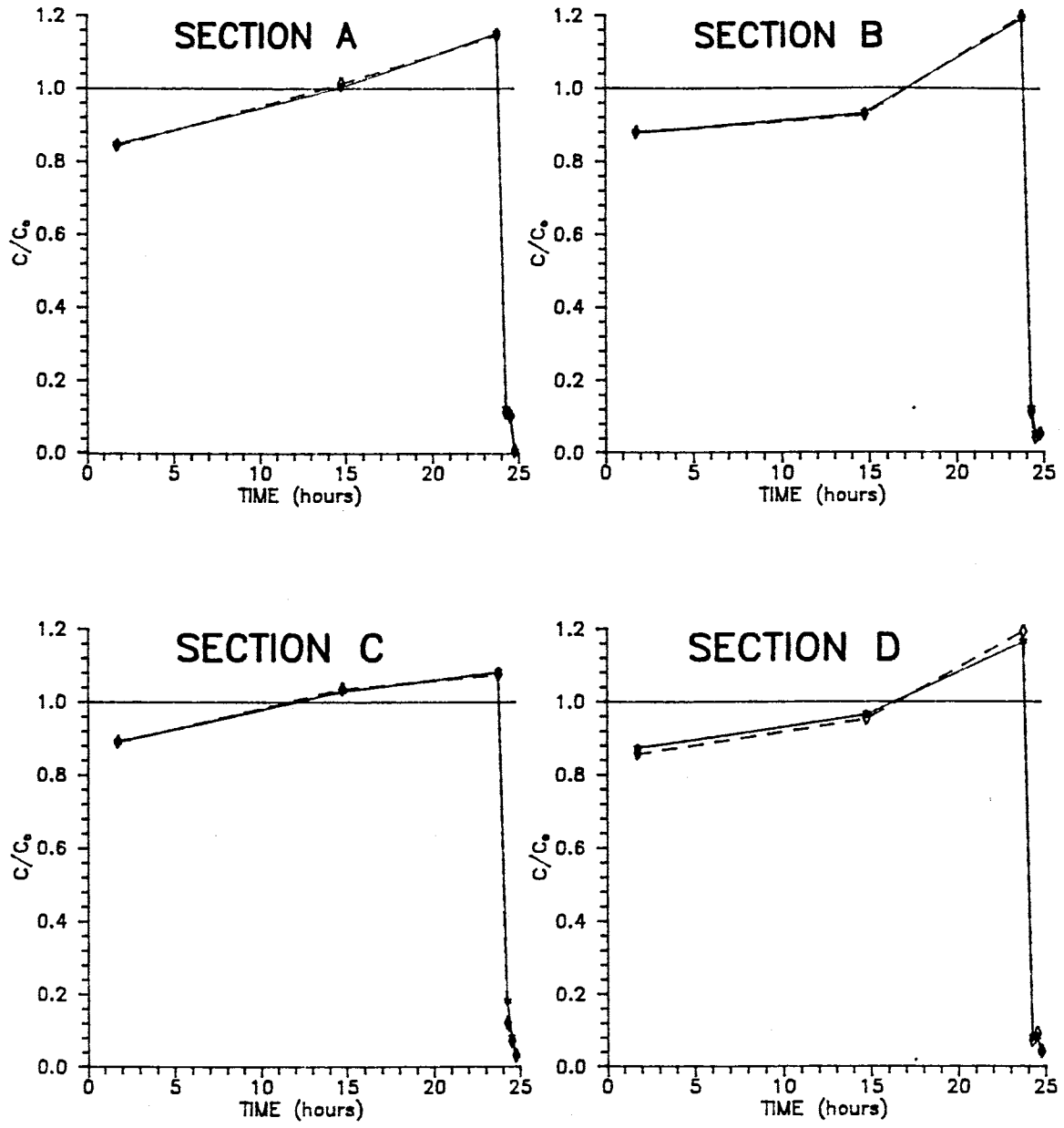

Figure 4-3. Tracer input concentrations in drip lines (during tracer application) for each section.

from the breakthrough curves. The first used was the program CXTFIT of Parker and van Genuchten (1984). This program uses a non-linear least squares method to fit the parameters velocity (v), dispersion coefficient (D), and mass recovered (t_o) to the one-dimensional advection dispersion equation. Mode 2 of the program, which assumes flux concentrations, was used. Flanigan (1989) suggested that flux concentrations more nearly represent the concentrations seen in porous cup sampling. The retardation factor was set equal to 1.0 as bromide and the fluoro-organic tracers are relatively non-reactive. The retardation factor is quite possibly not one, as anion exclusion of bromide was observed by Flanigan (1989) in repacked column studies of material from the site. Relative concentrations were input into the code. These concentrations were calculated by dividing sample concentrations by the average concentration seen in the lines during tracer injection. Table 4-1 lists the parameters and goodness of fit calculated for the solution samplers and figures in appendix A illustrate the fit of equation with the fitted parameters to the observed data.

The second method used was applying a moment analysis to the curves. There are two ways in which the concentration vs. time data was considered. The first was as a normal distribution, where the zeroeth moment is the mass recovered in a particular sampler; the first moment, divided by the zeroeth moment, is the time at which fifty percent of the

TABLE 4-1. 1-D ADE FITTED PARAMETERS FOR INDIVIDUAL SAMPLER BREAKTHROUGH CURVES.

SAMPLER	v(cm/day)	D(cm^2/day)	α(cm)	t_o(days)	R^2
1c	16.1	98.7	6.1	1.88	.87
2c	7.6	237.1	31.2	2.25	.93
3c	7.8	400.2	51.3	2.37	.86
4a	9.3	28.2	3.0	1.05	.68
4c	21.5	87.2	4.1	0.73	.86
5a	16.7	228.5	13.7	1.16	.96
5c	18.7	227.4	12.2	0.79	.92
6a	7.4	118.8	16.1	1.99	.93
7a	10.3	175.4	17.0	1.52	.90
7c	8.3	153.1	18.4	1.98	.97
8a	23.7	113.0	4.8	0.40	.94
9a	24.6	144.2	5.9	1.04	.99
9c	17.3	309.5	17.9	0.78	.90
10a	18.8	214.9	11.4	0.96	.98
11a	36.1	252.9	7.0	0.36	.88
11c	38.7	192.0	5.0	0.93	1.00
11d	22.5	192.9	8.6	0.72	.97
12a	4.9	148.3	30.3	2.56	.94
12c	12.9	652.4	50.6	1.52	.88
13a	15.0	197.7	13.2	1.23	
13c	27.2	189.1	7.0	0.89	.88
14a	49.1	383.6	7.8	1.12	.94
14c	36.1	412.7	11.4	0.85	.95

TABLE 4-1. (CONTINUED)

SAMPLER	v(cm/day)	D(cm^2/day)	α(cm)	t_o(days)	
15a	15.1	145.7	9.6	1.04	.87
15c	26.6	669.0	25.2	1.15	.74
16a	46.3	338.3	7.3	0.96	.98
16c	15.0	372.9	24.9	1.26	.83
17a	11.9	82.8	7.0	0.96	.79?
17c	21.9	244.3	11.2	1.20	.95
18a	8.2	28.8	3.5	0.76	.94
18c	11.0	169.2	15.4	1.48	.97
19a	8.5	30.1	3.5	0.45	.89
19c	12.8	182.4	14.3	1.51	.86
20a	30.7	247.1	8.0	1.35	.98
20b	45.0	880.6	19.6	1.40	.99
G24	93.3	627.8	6.7	1.07	1.00
H23	48.7	518.1	10.6	1.08	.90
I22	42.6	306.5	7.2	1.04	.98
K25	43.5	673.5	15.5	1.25	.93
AVERAGE	23.9	273.7	13.9	1.21	
STD. DEV.	17.3	198.5	11.1	0.51	

tracer seen has passed the sampler; and the second moment, also divided by the zeroeth moment, defines the spread of the tracer about the center of mass or first moment.

The second way to look at the data is as a log-normal distribution of travel times. This is most likely a better description of the curve as it not only confines the data, in that there can be no tracer appearing before it has been injected, but better represents the tailing seen in the BTC's.

It is not apparent to this observer whether, when applying a moment analysis to the raw data, it is more appropriate to use travel times from the time the tracer was first applied or to use travel times from the time at which half the tracer has been applied. For breakthrough curves showing very fast tracer movement, subtracting half a day from the time at which the tracer was seen leads to some negative times. This makes it impossible to determine the log-normal moments, as one cannot take the logarithm of a negative number. Table 4-2 lists the normal distribution moments calculated by trapezoid method described earlier (Eq. 2-13).

STATISTICS OF TRANSPORT PARAMETERS

Fractile diagrams of fitted transport parameters v, D, t_o, dispersivity (α) and the observed parameter volume pulled (Vp) are shown in figures 4-4 through 4-8. It is seen that a log-normal distribution of velocity, dispersion coefficient

TABLE 4-2. PARAMETERS DETERMINED BY MOMENT ANALYSIS

SAMPLER	0^{th} MOM []	1^{st} MOM [DAYS]	2^{nd} MOM [$DAYS^2$]
1c	2.20	14.70	245.6
2c	1.17	21.56	490.9
3c	2.14	29.40	1029.1
4a	0.90	10.92	122.8
4c	0.68	7.11	52.5
5a	1.21	7.01	58.9
5c	1.02	14.21	234.5
6a	1.93	13.43	214.1
7a	1.52	10.37	133.3
7c	2.01	25.79	767.2
8a	0.46	5.74	38.2
9a	1.07	4.79	25.9
9c	0.80	13.67	214.7
10a	1.06	6.37	50.3
11a	0.37	1.04	1.6
11c	0.96	4.31	20.0
11d	0.81	10.83	132.6
12a	1.26	11.18	137.3
12c	1.39	16.53	331.6
13a	1.72	10.96	164.2
13c	1.24	10.33	128.8
14a	1.56	4.50	31.6
14c	0.99	8.01	73.9

TABLE 4-2. (CONTINUED)

SAMPLER	0^{th} MOM	1^{st} MOM [DAYS]	2^{nd} MOM [$DAYS^2$]
15a	1.18	8.55	90.0
15c	1.39	11.15	160.5
16a	1.00	2.81	9.1
16c	1.39	17.64	372.9
17a	2.05	22.27	670.2
17c	1.82	19.67	574.5
18a	0.69	12.33	160.0
18c	1.51	20.32	472.4
19a	0.37	11.30	132.5
19c	1.62	21.86	534.2
20a	1.36	4.00	18.3
20b	1.40	5.09	29.6
G24	1.10	1.76	3.5
H23	1.08	5.34	30.4
I22	1.01	7.78	62.8
K25	1.29	4.56	24.4

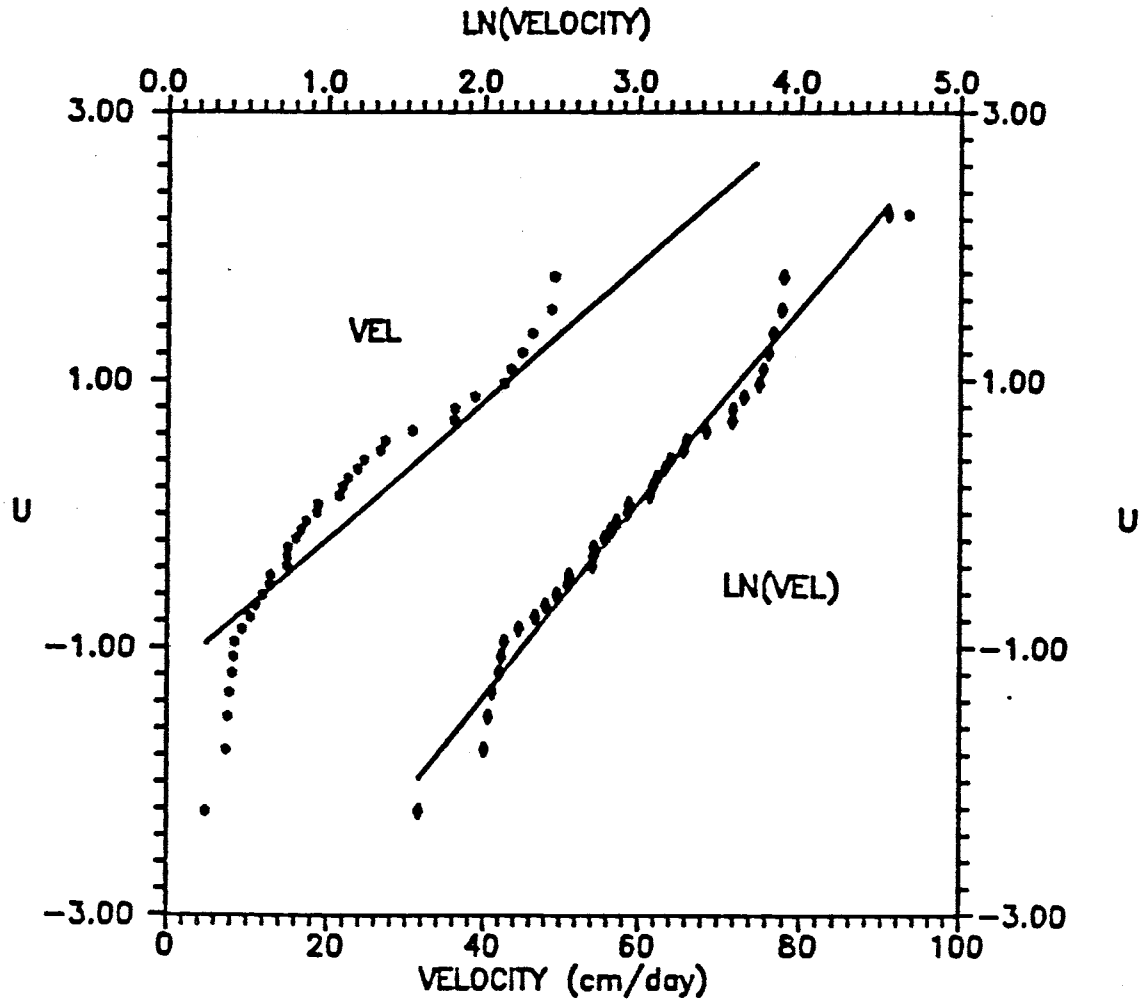

Figure 4-4. Fractile diagram of velocities determined from one dimensional advection dispersion equation.

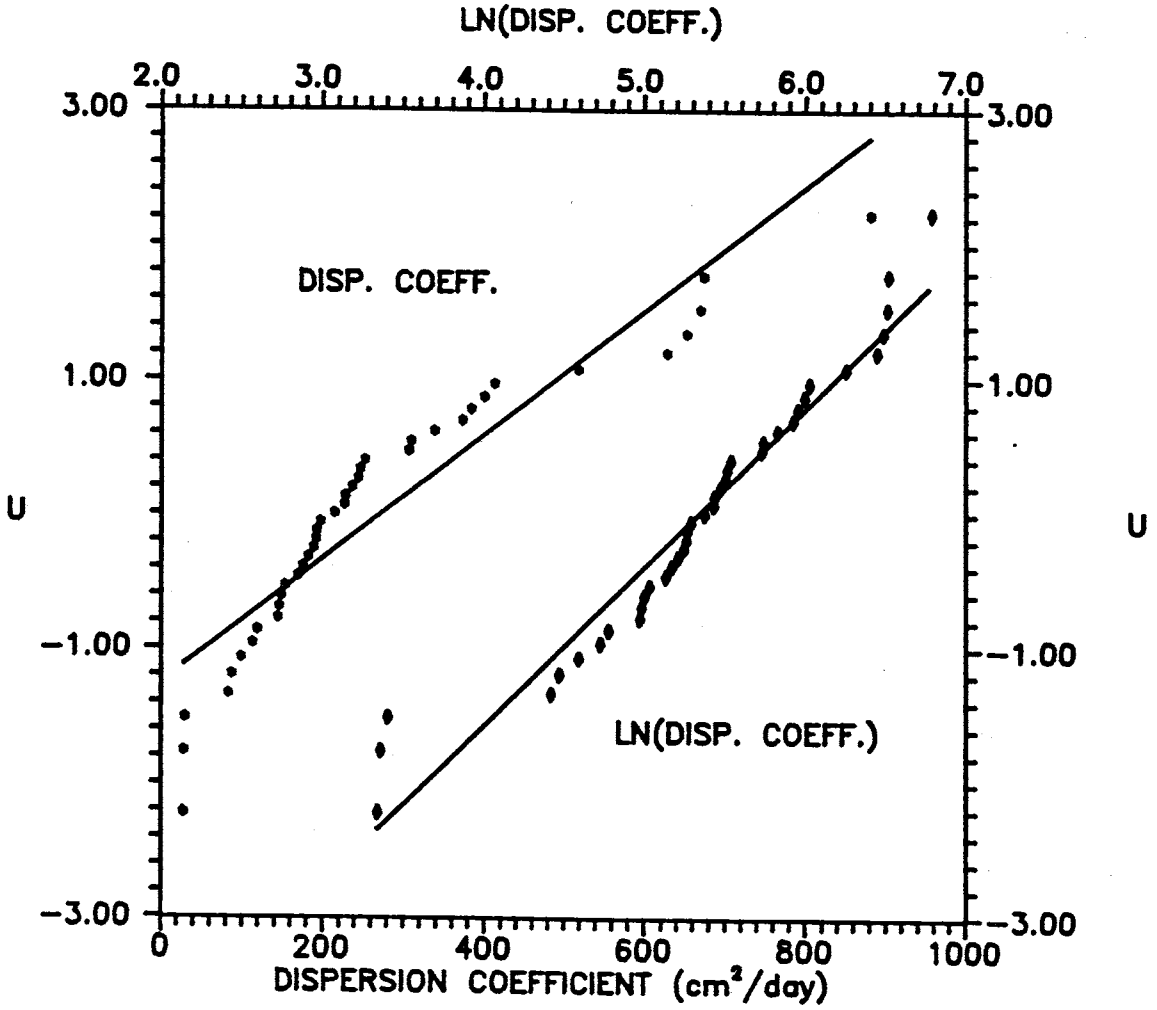

Figure 4-5. Fractile diagram of dispersion coefficient determined from 1-D ADE.

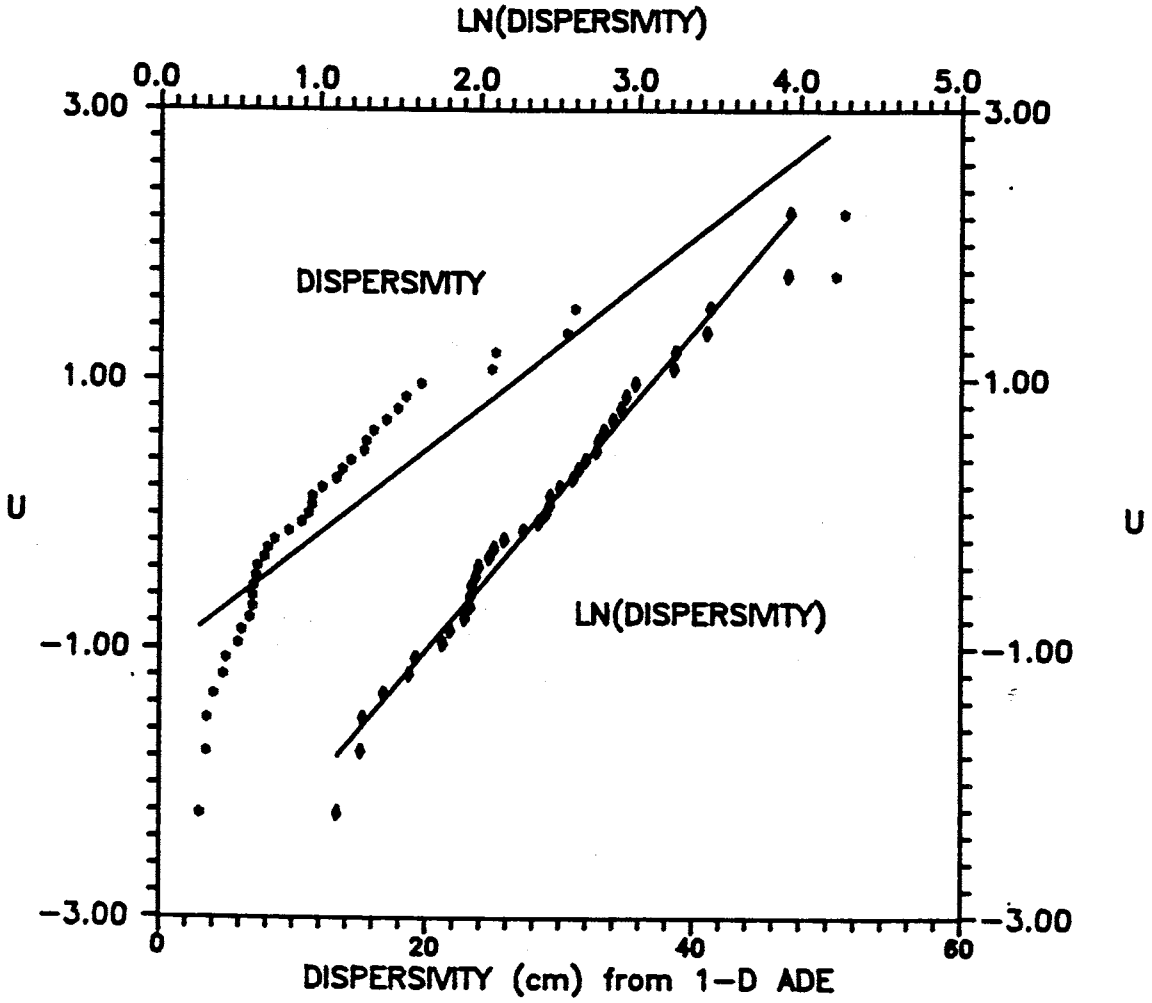

Figure 4-6. Fractile diagram of dispersivity determined from 1-D ADE.

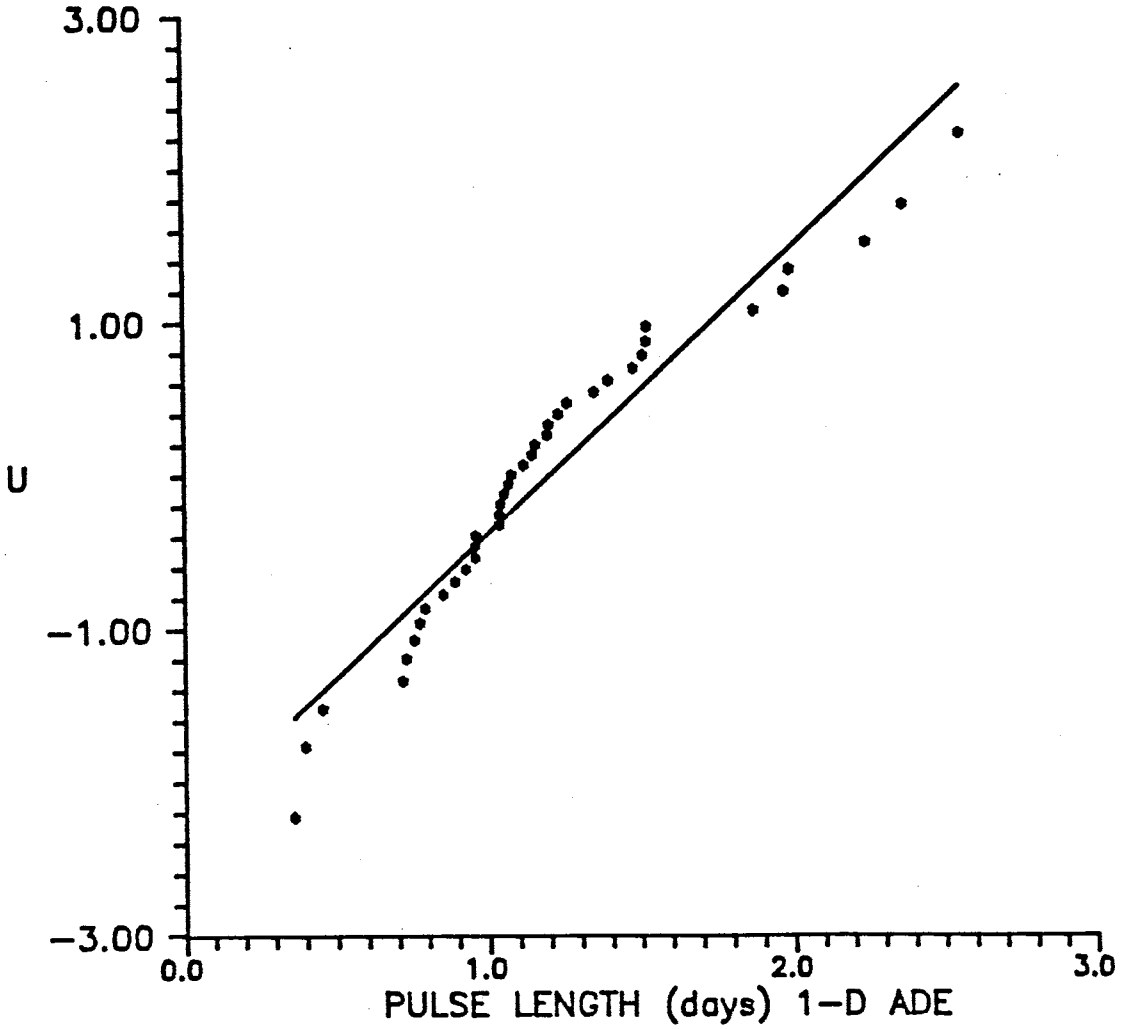

Figure 4-7. Fractile diagram of pulse duration determined from 1-D ADE.

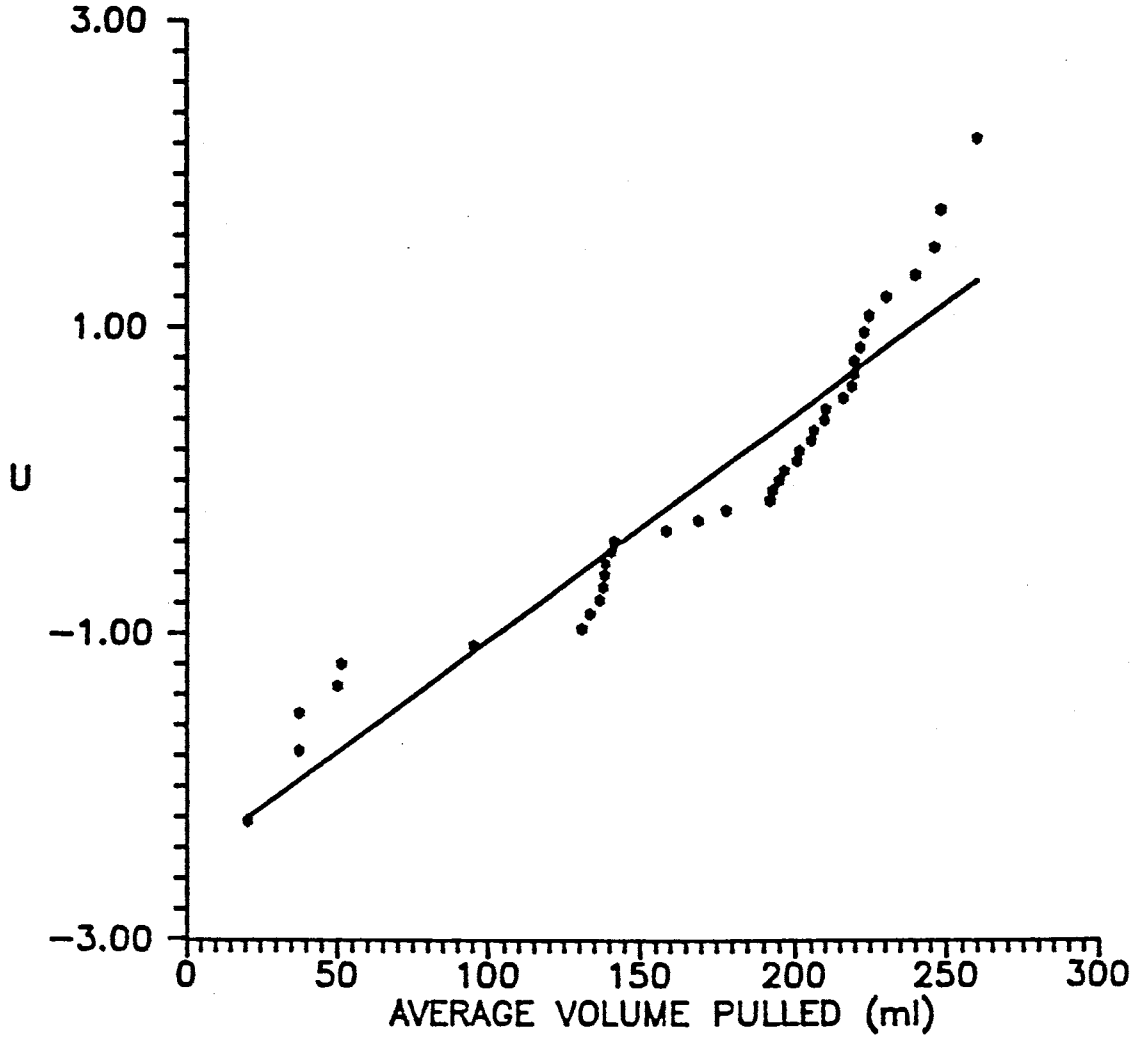

Figure 4-8. Fractile diagram of average volume pulled per sampler.

and dispersivity more clearly represents the fitted parameters while normal distributions characterize the mass recovered and volume pulled. Log-normal distributions of velocity, dispersion coefficient and dispersivity were seen in similar studies by Biggar and Nielsen (1976) and Nielsen et. al. (1973). Little correlation can be seen between the parameters.

Fractile diagrams of the zeroeth, first and second moments (normal distribution) are illustrated in figures 4-9 through 4-11. Little to no correlation can be seen between these parameters. The zeroeth moment corresponds to the mass recoved T_o. A plot of the zeroeth moment against the t_o calculated from CXTFIT is shown in figure 4-12. It can be seen that the zeroeth moment is larger than that determined from the 1-D ADE. This was believed to be because the one-dimensional advection-dispersion equation usually underpredicts the concentration of tracer on the tail of the breakthrough curve (see appendix A). The first moment can be converted into a velocity using equation 2-14. Figure 4-13 plots the velocity calculated from the first moment against the velocity fitted by the one-dimensional advection-dispersion equation. It is seen that neither model consistently predicts larger velocities than the other. Butters and Jury (1989) suggest that dispersivity for a short duration pulse can be derived from equation 2-15. It is known that the pulse duration for this experiment was relatively long, but dispersivities were still calculated for each

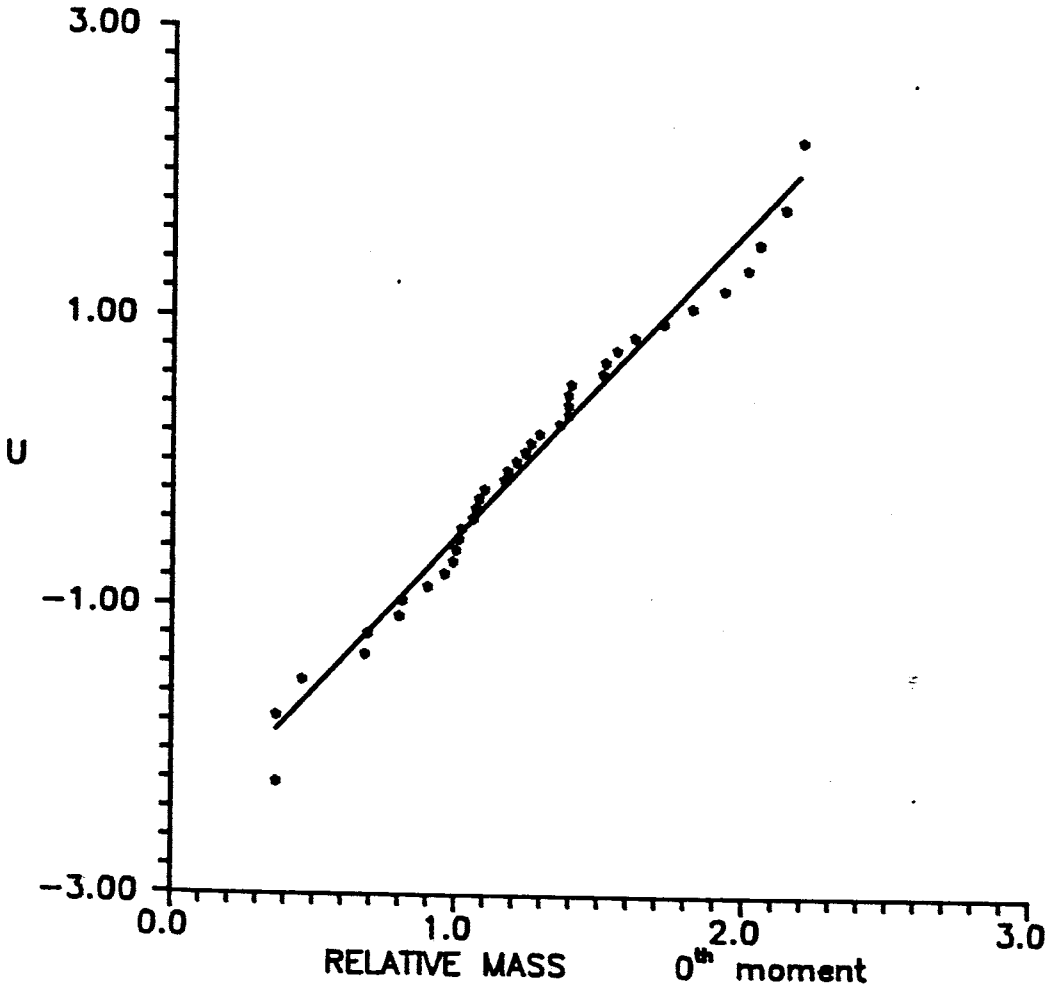

Figure 4-9. Fractile diagram of relative mass recovered from moment analysis.

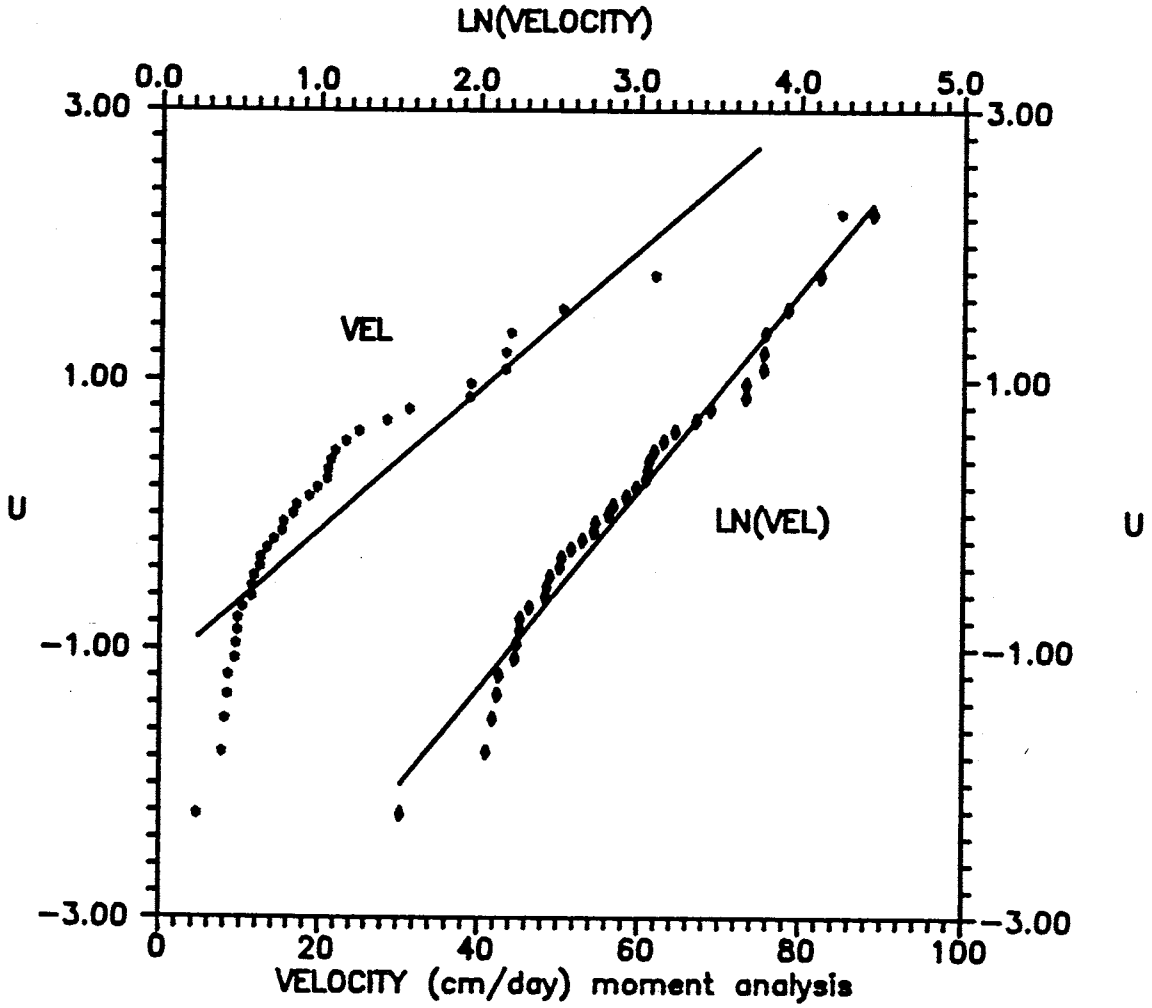

Figure 4-10. Fractile diagram of velocities calculated from first moments.

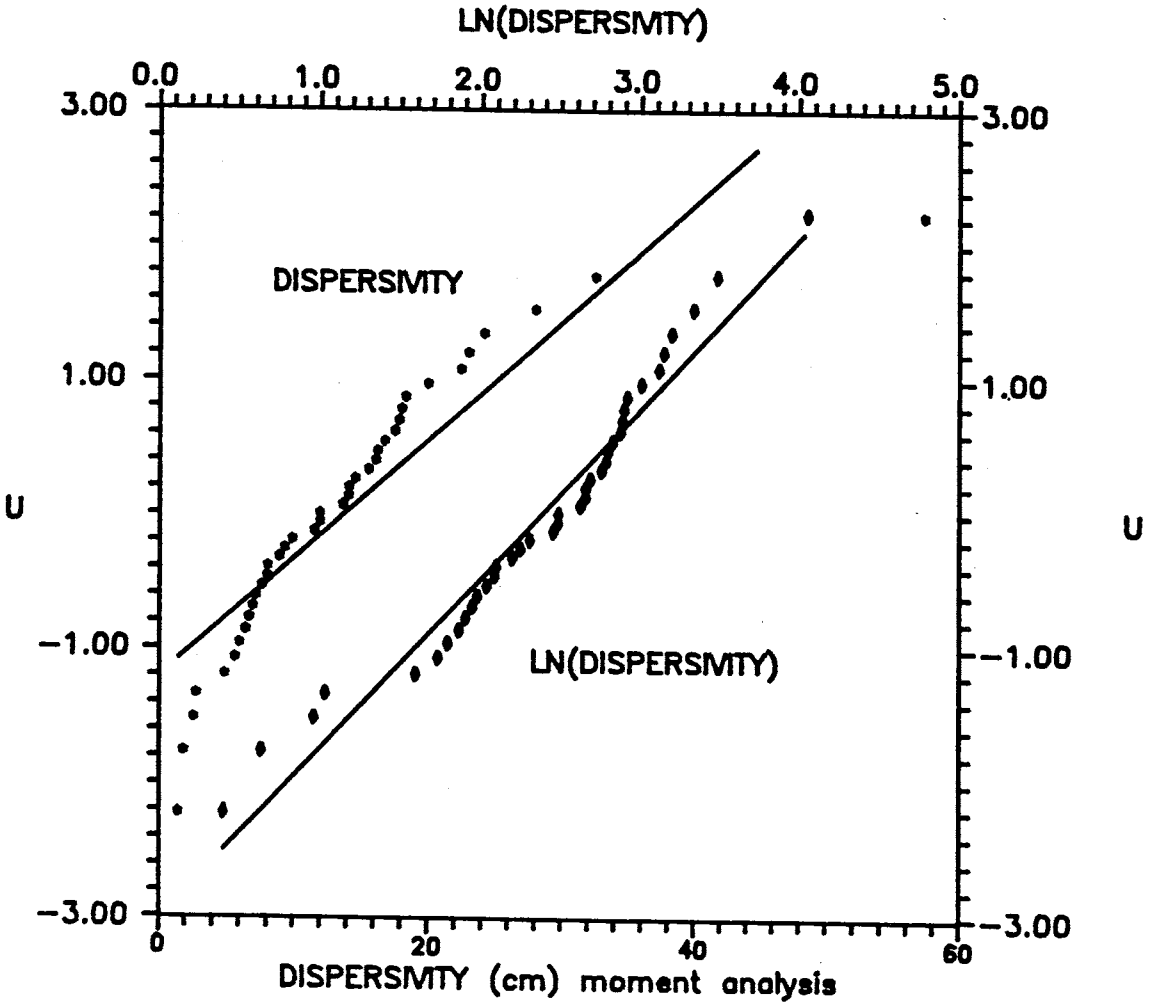

Figure 4-11. Fractile diagram of dispersivities calculated from first and second moments.

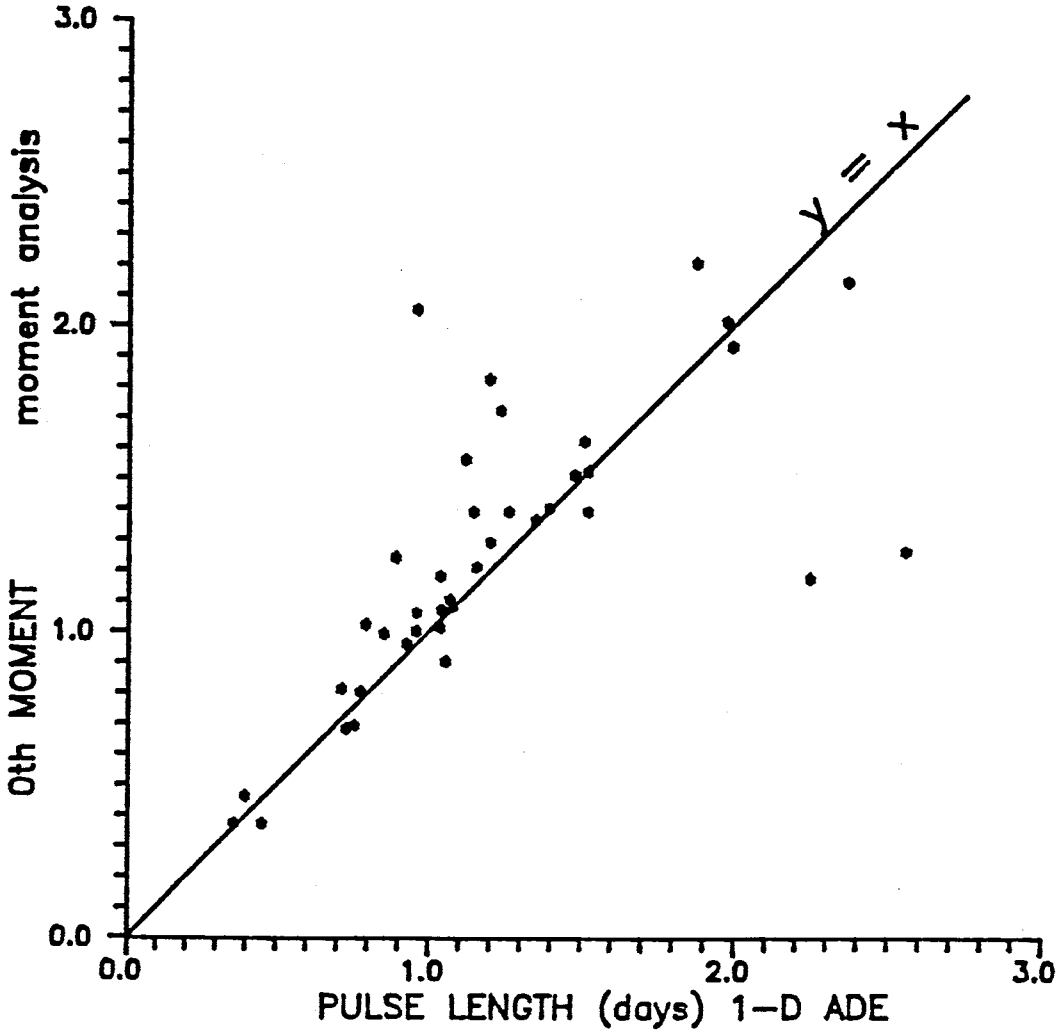

Figure 4-12. Comparison of pulse duration and mass recovered.

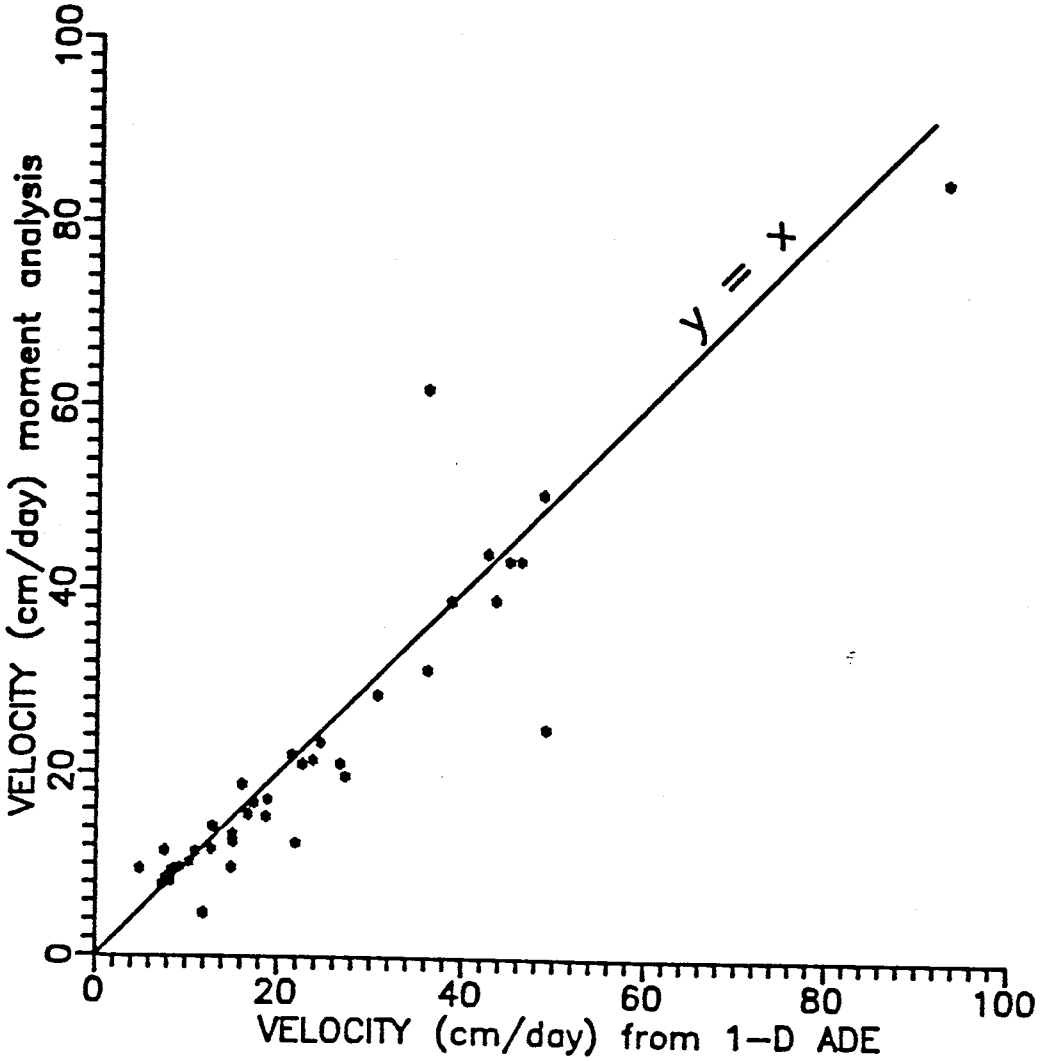

Figure 4-13. Comparison of velocities determined from 1-D ADE and from moment analysis.

sampler. Figure 4-14 plots the dispersivities calculated from moments versus those determined from the 1-D ADE. Neither seems to consistently predict higher dispersivities than the other.

VARIOGRAM ANALYSIS

In order to look at the correlation between BTC's of samplers at different locations but at approximately the same depth, variograms were taken looking at the parameters velocity and dispersivity. The parameters were taken from the least-squares analysis of the one-dimensional advection-dispersion equation. Variograms of the parameters at the 1-m depth and the 2.25-m depth (+/- .15 m) show little correlation between the samplers. This is believed to be because the samplers were emplaced in a grid which placed them at a distance apart greater than the correlation scale of the geology, either vertically or horizontally. Non-ergodic variograms tended to provide a better visual representation of the lack of correlation as it removes trends in the parameter that is being analyzed.

HORIZONTAL MOVEMENT OF TRACER

Some horizontal movement of the fluoro-organic tracers beneath the drip emitters was observed. The evidence for this

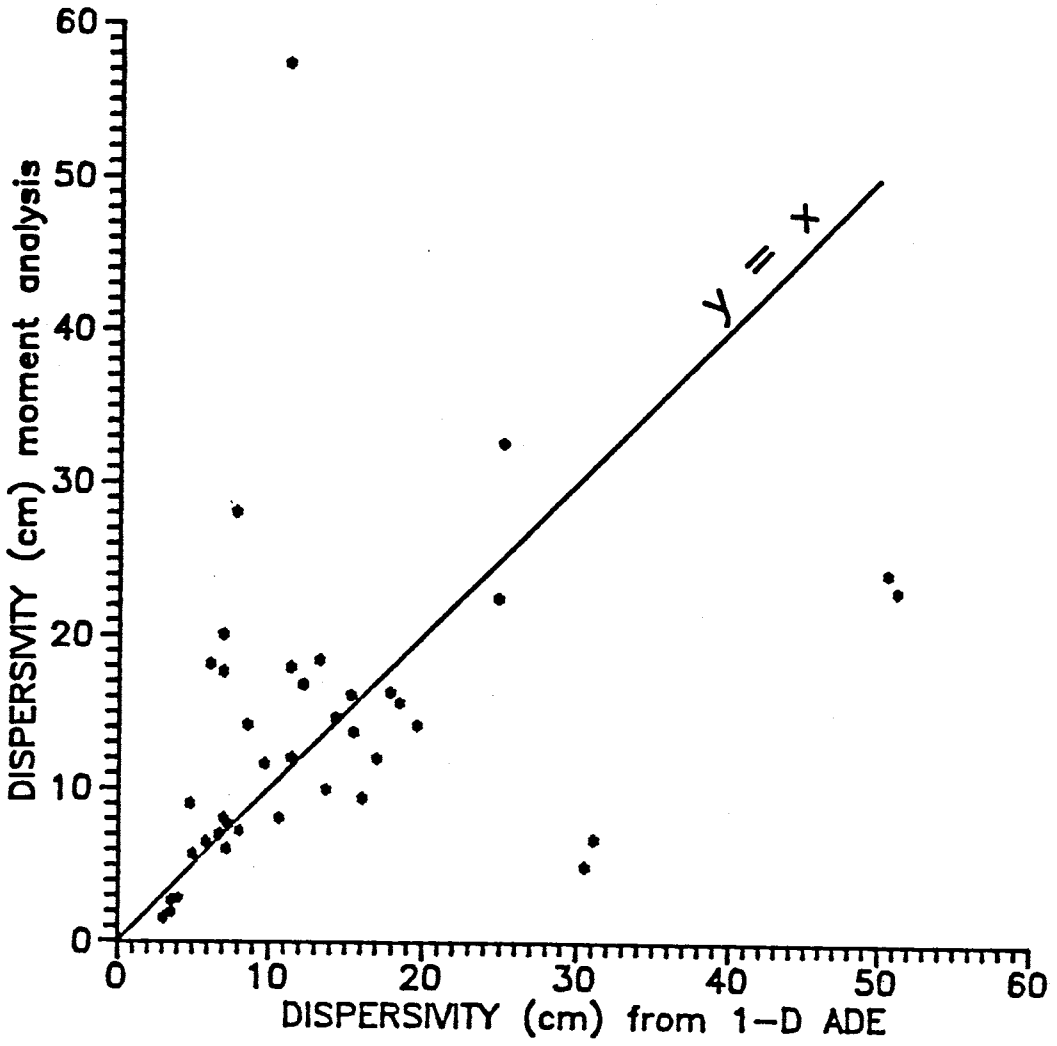

Figure 4-14. Comparison of dispersivities determined from 1-D ADE and from moment analysis.

was two different fluorobenzoate tracers showing up in samplers along with bromide. The addition of the relative concentrations of the organic tracers yielded a very close approximation to the relative bromide concentration, suggesting that the fluorobenzoate tracers were conserved. Samplers 6a, 17c, and 18c showed evidence of lateral spreading of solute. Figures 4-15 through 4-17 illustrate the breakthrough curves of the fluorobenzoate tracers, bromide and the addition of the two fluorobenzoate tracers. From the figures it is seen that the curve made from the addition of the two organic tracers approximately follows the bromide curve.

In all three cases, tracer moved northward, from a section to the south of the soil water sampler, to the sampler located in an adjacent northern section. Movement of tracer in the other direction was never observed, leading the author to believe that in general, there is a northward component to flow beneath the wetted region. Horizontal movement of tracer away from the wetted region was also observed. Breakthrough curves were made for outside samplers ENE-a, ENE-b, ENE-c and MEC. These BTC's suggest a significant eastward component to the flow away from the emitters and possibly suggest a slightly northward component to the flow. Figures 4-18 and 4-19 show the analyzed relative sampler concentrations vs. time.

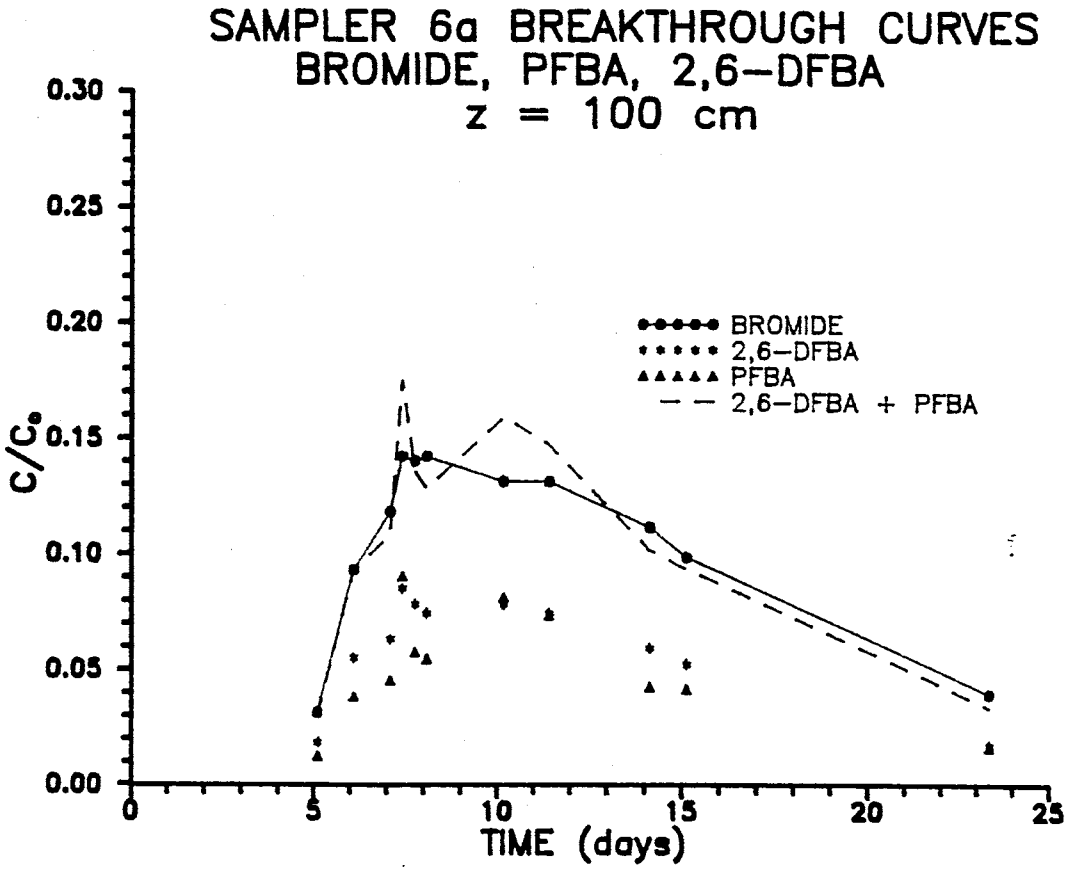

Figure 4-15. Sampler 6a breakthrough curve.

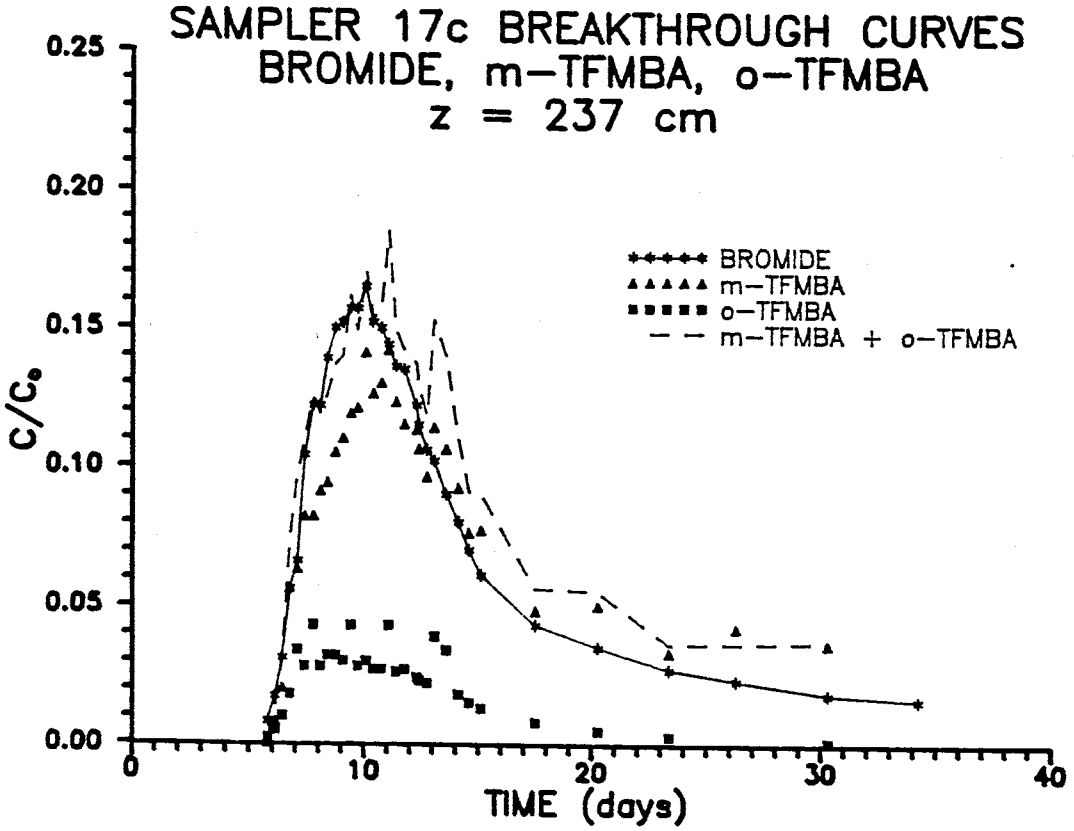

Figure 4-16. Sampler 17c breakthrough curve.

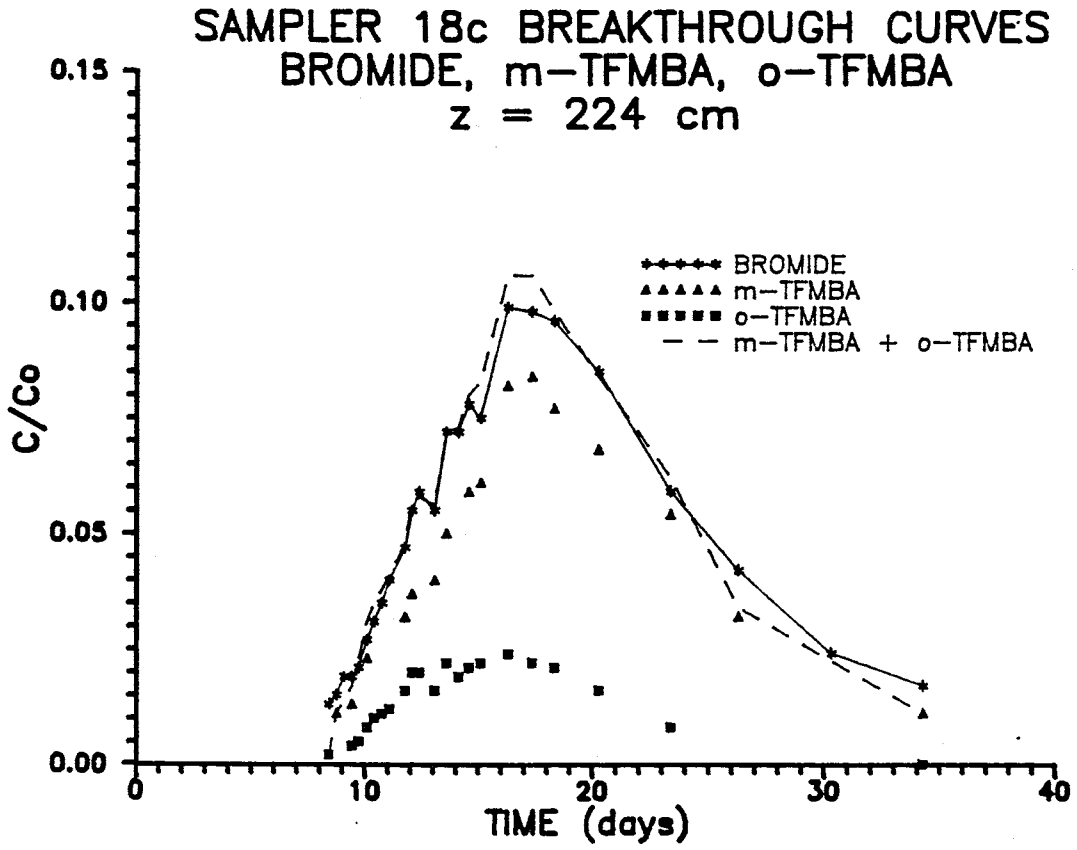

Figure 4-17. Sampler 18c breakthrough curve.

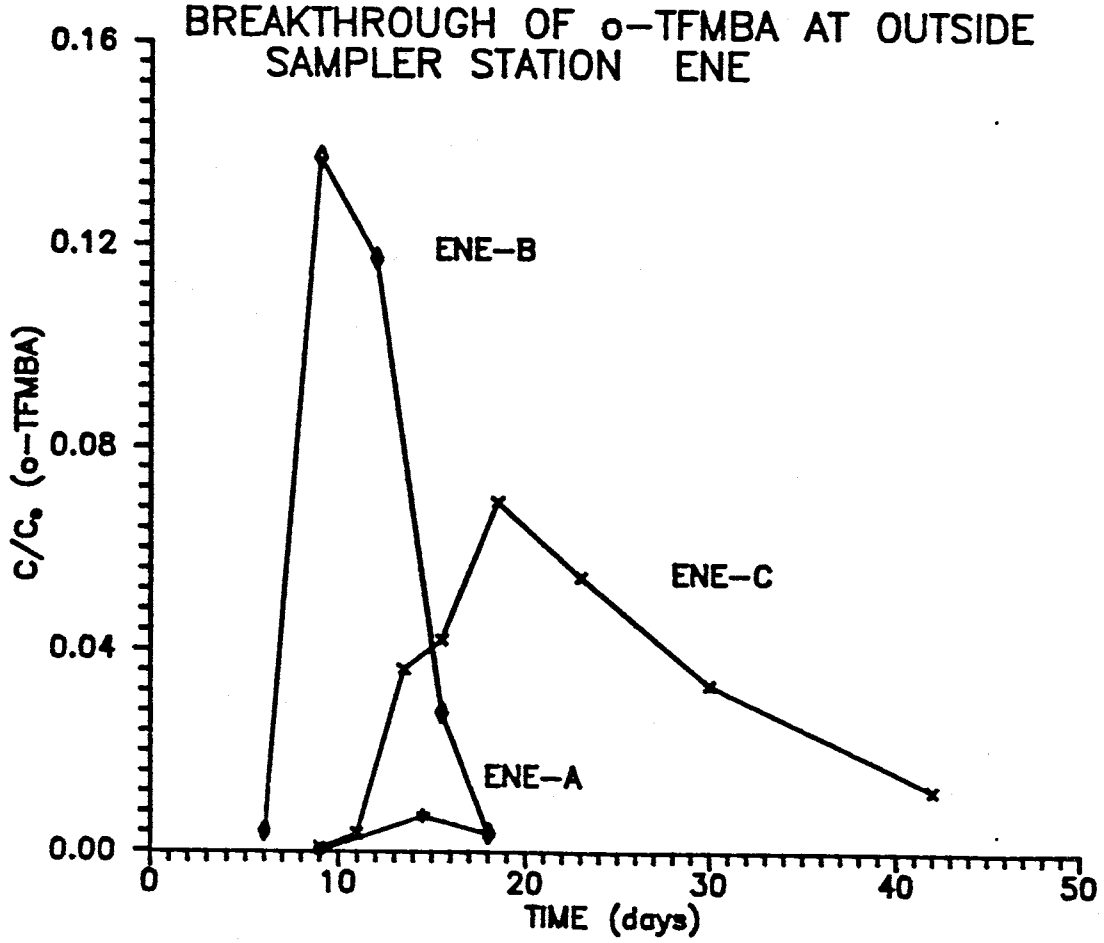

Figure 4-18. Concentration of tracers seen in samplers ENE-a, ENE-b, and ENE-c.

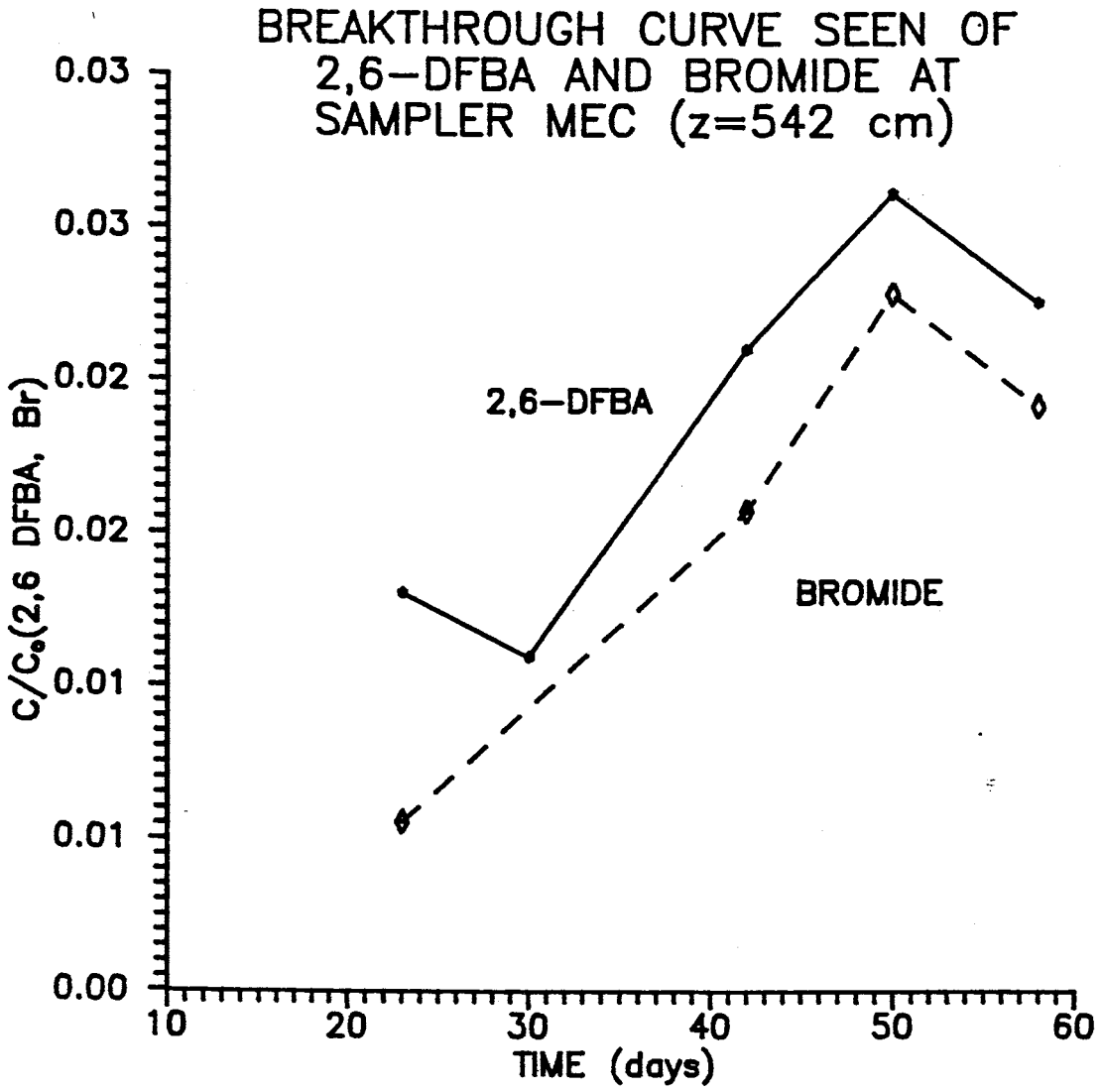

Figure 4-19. Concentration of tracer seen in sampler MEC.

METHODS OF AERIALLY AVERAGING CONCENTRATION

Three methods of aerially averaging concentration at a given depth were studied: (1) average resident concentration (ARC), (2) average flux weighted concentration (AFWC), and (3) concentration determined from averaging transport parameters from fitted breakthrough curves (ATPC). To the author's knowledge, it has not been convincingly proven which of the three methods apply in a heterogeneous system with three-dimensional fluid flow occurring. Two particular depths were chosen because there were considered sufficient samplers at approximately those depths to get a meaningful average. Seventeen samplers were chosen from approximately the one meter depth and sixteen samplers from a depth of 2.25 meters, plus or minus .15 meters.

Because water samples were taken at different times from the porous cup samplers and concentration data was not determined at all times, a method was needed to determine the concentration at each sampler at given times. The method used was to input the parameters determined from CXTFIT back into the one-dimensional advection-dispersion equation and thus calculate an idealized concentration for each sampler at various fixed times. These concentrations were then averaged using the three methods discussed in the theoretical section.

The ARC breakthrough curve for a particular depth was created by adding the concentrations of all the samplers at

that depth at particular times and then dividing this number by the number of samplers looked at (equation 2-24). This gives the average concentration breakthrough curve at a particular depth, but does not necessarily denote the mass passing through the plane at that depth, because it does not take into account that the water flux is not constant at every point in the plane. If the flux is a constant over the plane, then only variations in the moisture content should determine velocity variations.

The AFWC breakthrough curve for a particular depth was created in a similar manner, but variations in the water flux through the plane were used to weight the concentrations of particular samplers. The flux values were calculated by multiplying the fitted velocity calculated from the 1-D ADE by the average moisture content to that depth determined from neutron moisture measurements. Little variation was seen in the moisture content at a particular depth, so the average used was taken from all the neutron moisture measurements at the given depth. The flux values were multiplied by the concentrations seen in that sampler. This provided qC values at various times for all the soil solution samplers. The qC values for a given time were all added together and were then divided by the sum of the flux values (equation 2-25). This provided flux weighted concentrations at various times which were used to construct a AFWC BTC. The effect of weighting the concentration by the flux is to make the breakthrough

curve peak earlier, because samplers showing fast movement of tracer will necessarily have higher fluxes and will gain greater weight. This method is thought by the author to better represent the mass of tracer passing through a horizontal plane than that of the average resident concentration.

The concentrations from averaging transport parameters (ATPC) were calculated by first finding the average of the parameters v, D, and t_o for a given depth. These average values were then plugged into the 1-D ADE (equations 2-18 and 2-19) to provide breakthrough curves for the two depths. The ATPC BTC's gave a later breakthrough of tracer than the AFWC but earlier than the ATC. It also removed much of the tailing seen in the BTC's calculated by the other methods. Figure 4-20 shows the breakthrough curves calculated by all three methods for the 1-m depth and figure 4-21 illustrates the curves for the 2.25-m depth.

The hydrodynamic parameters v, D, α, and t_o were calculated from the curves generated by these averaging techniques using CXTFIT, with α calculated by dividing D by v. Table 4-3 lists these values. It is seen that using average resident concentrations predicts lower solute velocities, while the other two methods predict similar, higher velocities. From ARC data, there is a large increase in velocity with depth. The other averaging methods have velocity decreasing slightly with depth. Also, averaging

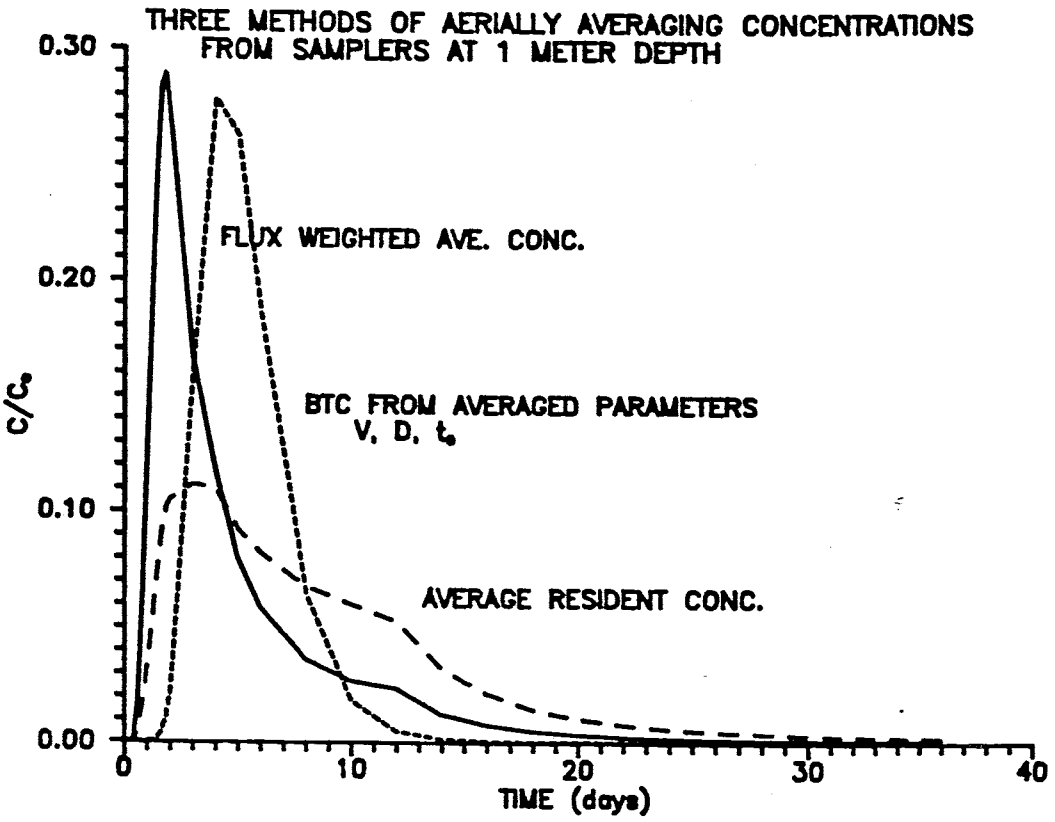

Figure 4-20. Breakthrough curves from three methods of aerially averaging concentration (ARC, AFWC, and ATPC) for samplers at one meter depth.

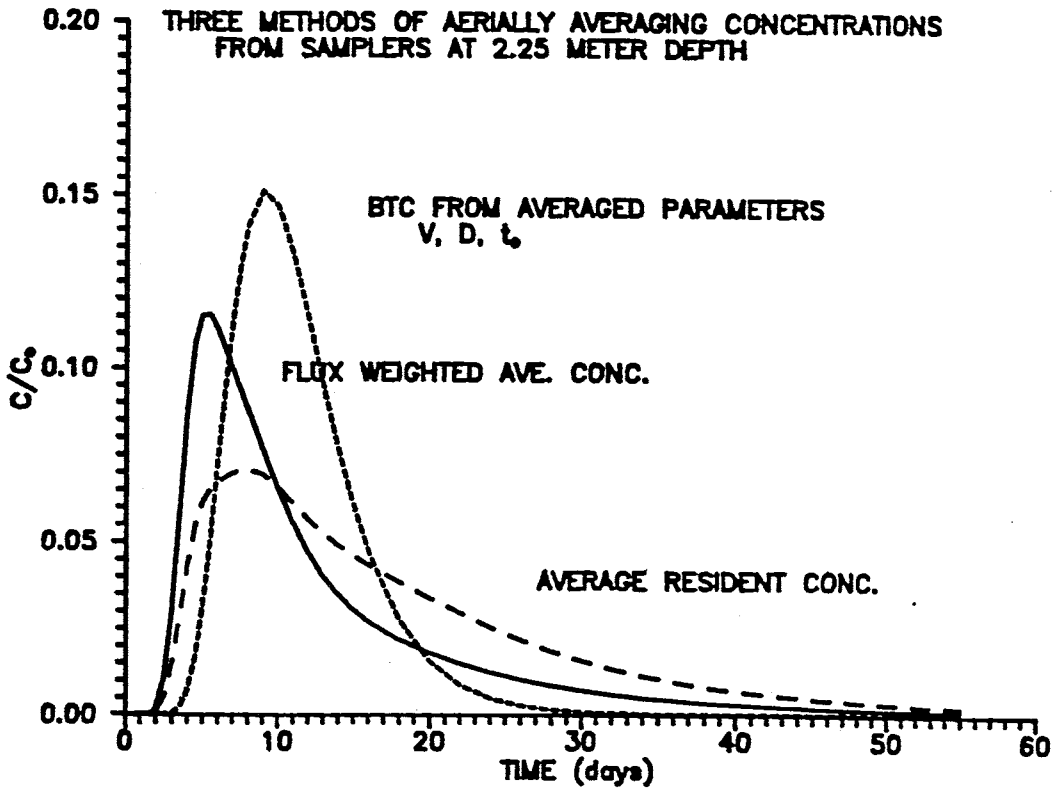

Figure 4-20. Breakthrough curves from three methods of aerially averaging concentration (ARC, AFWC, and ATPC) for samplers at 2.25 meter depth.

TABLE 4-3. Transport parameters v, D, α, and t_o of the curves generated by the three averaging methods mentioned (generated from CXTFIT.)

TYPE OF AVERAGE	Z(cm)	v(cm/day)	D(cm^2/day)	α(cm)	t_o
ARC	100	6.53	874	134	1.2
	225	11.30	1140	101	1.4
AFWC	100	28.18	1293	46	1.0
	225	24.35	1082	45	1.1
ATPC	100	23.17	191	8.3	1.2
	225	21.27	363	17	1.3

transport parameters (ATPC) gives much lower dispersion coefficients than the other methods. This leads to ATPC curves predicting the lowest dispersivity and ARC curves predicting the highest dispersivity. Several authors have suggested that dispersivity increases with depth. The dispersivities calculated from ARC and AFWC curves decreased with depth, while the ATPC curve has it increasing with depth.

Moment analysis was used on the three BTC's and velocity, dispersivity, and 0^{th} moment calculated. Dispersivity is calculated from equation 2-23. The parameters are listed in Table 4-4. The ARC method predicts lower solute velocities than the other two methods, but does not have velocity increasing with depth as drastically as from CXTFIT calculated velocities. Using moment analysis, the average flux weighted concentration curve is more dispersed than the other two. In contrast to ADE calculated dispersivities, moment analysis predicts increased dispersivity with depth using any of the averaging techniques.

It is interesting to note that the velocities calculated are all substantially less than the predicted solute velocity calculated from the water flux added to the site, 10^{-4} cm/sec, and moisture contents from the neutron probe data: θ_1 = .258 and $\theta_{2.25}$ = .226. q/θ or v thus becomes 33.5 cm/day at 1 meter and 38.2 cm/day at 2.25 meters. The lower velocities calculated from the three averaging methods are most likely due to lateral flow components.

TABLE 4-4. Transport parameters v_m, α_m, and T_o of the averaged breakthrough curves (m subscript denotes from moment analysis).

TYPE OF AVERAGE	Z(cm)	v_m(cm/day)	α_m(cm)	T_o
ARC	100	12.34	26.8	1.1
	225	13.85	46.7	1.3
AFWC	100	21.75	42.1	1.1
	225	19.28	61.2	1.2
ATPC	100	20.56	7.0	1.2
	225	20.85	15.5	1.3

TRANSFER FUNCTION MODEL

A transfer function model was applied to the data. Trial and error was used to determine the parameters from average resident concentration curves at the calibration depth using equation 2-28. Using a single calibration depth, such as one meter concentration data, one can supposedly calculate the BTC for any other depth. The parameters $C_o = 1.14$, $\mu = 1.85$, and $\sigma = .95$ optimized the transfer function curve to the ARC 1-m data. Figure 4-22 is a comparison of the curves determined from the transfer function model (calibrated against samplers at 1-m depth) and the curves of the average resident concentration. The parameters $C_o = 1.30$, $\mu = 2.55$, and $\sigma = .75$ fit the 2.25-m ARC data. Figure 4-23 is a similar graph depicting the transfer function curves calibrated at the 2.25-m depth. It was observed that the parameters from either calibration did not produce a good fit with the ARC curve of the uncalibrated depth. Due to the large degree of layering and heterogeneity, there was probably little correlation between flow paths to the two depths.

To predict the loading of tracer on the water table (approximately 20 m below drip lines), the parameters from two models were used. A tracer breakthrough curve was generated from transfer function theory with 2.25-m being the calibration depth. A second curve was generated using the one-dimensional advection dispersion equation, inputting

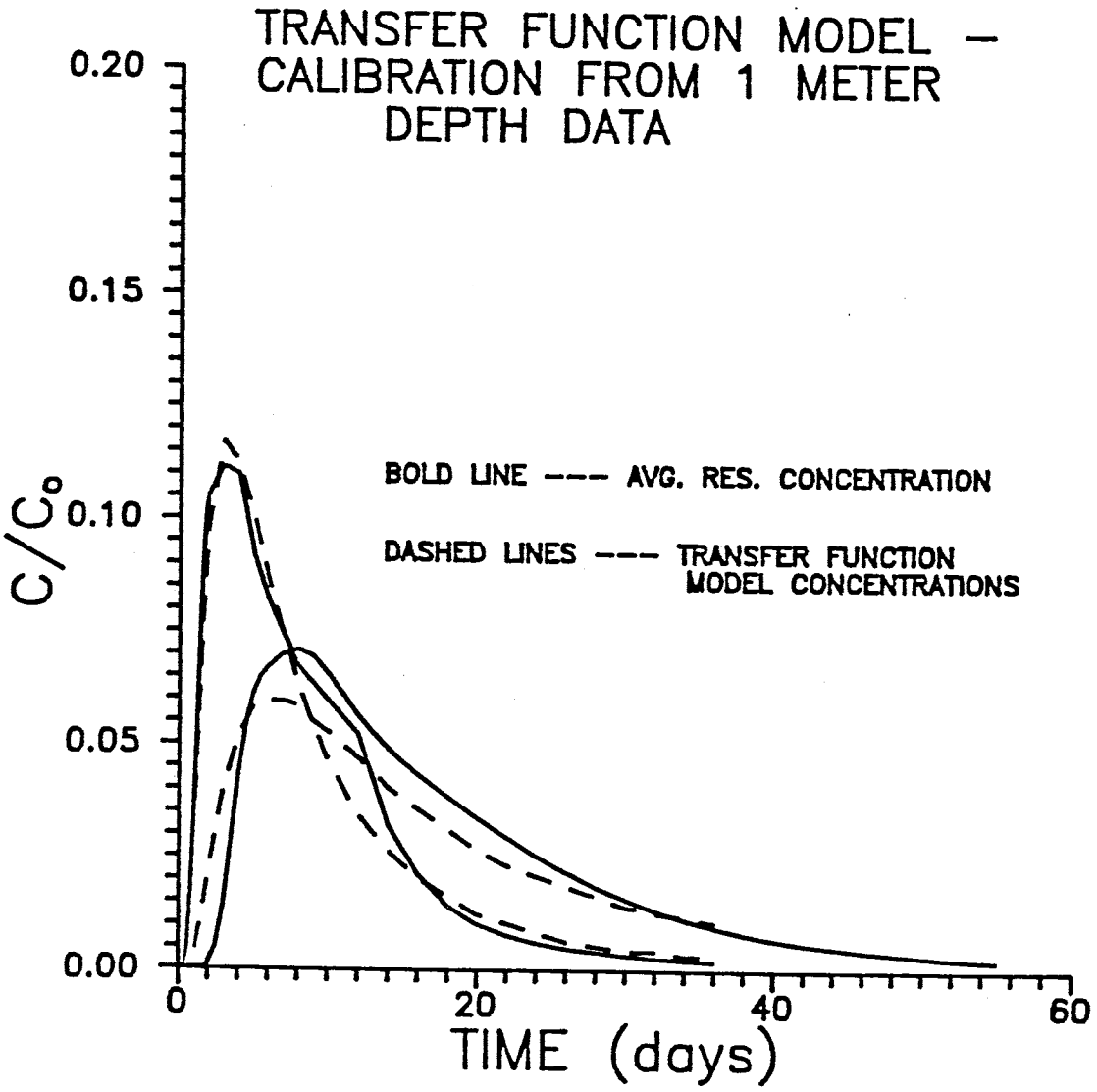

Figure 4-22. Comparison of ARC curves to curves generated from the transfer function calibrated at one meter.

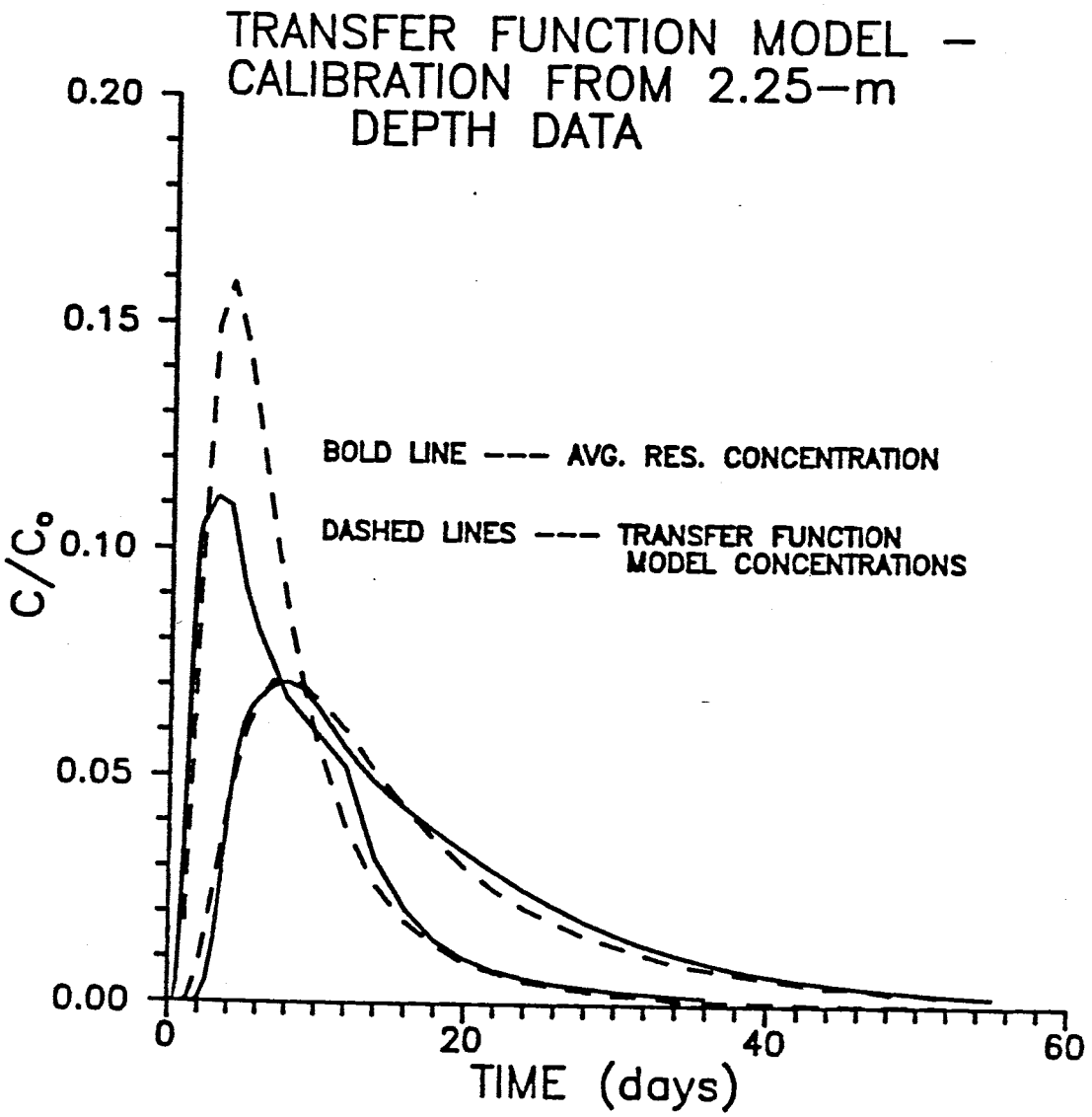

Figure 4-23. Comparison of ARC curves to curves generated from transfer function calibrated at 2.25 meters.

parameter values from the ARC curve at 2.25 meters. Compared to the 1-D ADE curve generated from CXTFIT, the transfer function model predicts much faster arrival of contaminants at the water table and a longer period of loading on the aquifer, but not as high a peak concentration (figure 4-24).

There are several problems inherent in applying the transfer function model to the actual data. The model does not allow for increasing or decreasing heterogeneity with depth. It also does not allow for tracer breakthrough at a particular depth until the tracer application at the surface is complete. This model is therefore best for looking at relatively homogeneous soil systems where the amount of time during which the tracer is added at the surface is very short compared to the travel time of the tracer to the depth of interest.

GENERAL DISCUSSION OF FITTING BREAKTHROUGH CURVES

There are problems fitting tracer breakthrough curves, where flow is three dimensional, with one dimensional models. The parameters that the one-dimensional ADE generates do well in creating good fitting curves to the data, but what actual significance do the parameters really have? The 1-D ADE gives the vertical velocity, neglecting any lateral components, gives the vertical spreading of the tracer pulse as the dispersion coefficient, and the mass under the curve as the

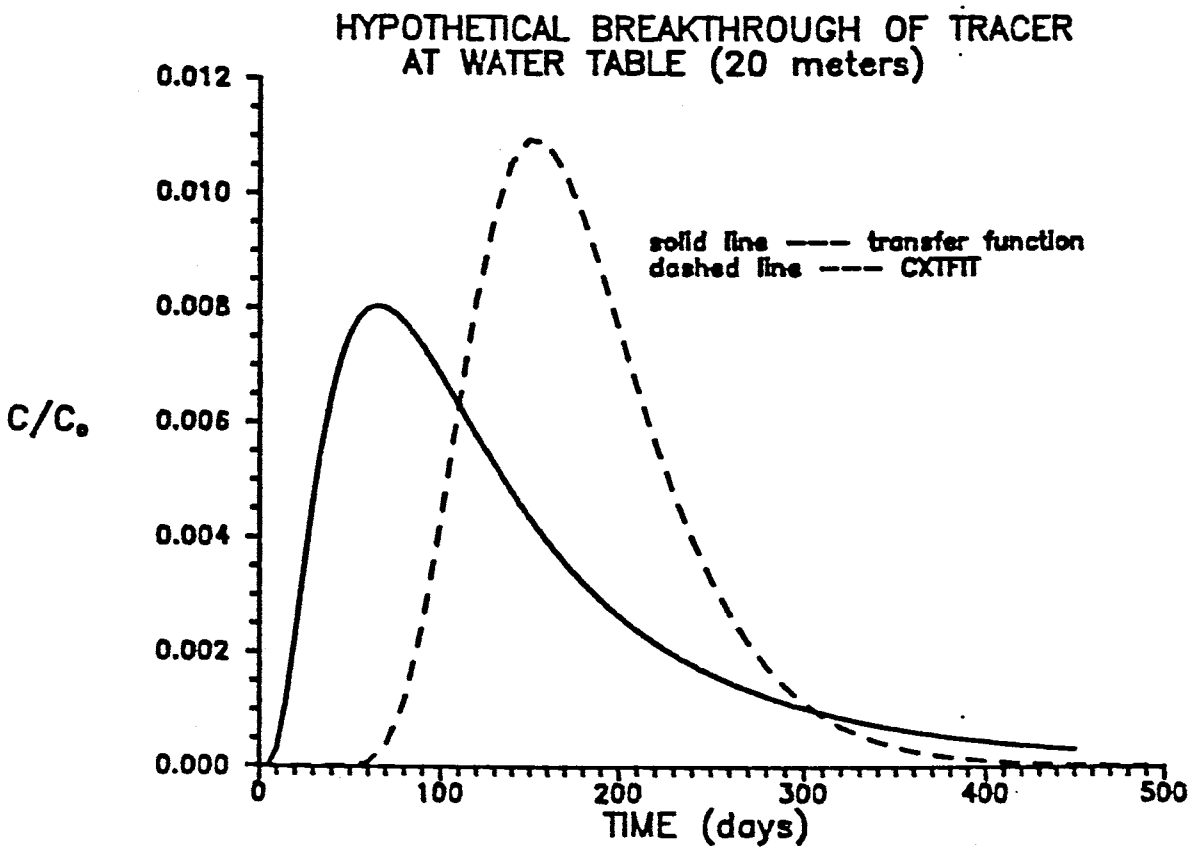

Figure 4-24. Comparison of predicted loading on water table of tracer by 1-D ADE and from transfer function (both calibrated to 2.25 meter depth).

pulse length. The time over which the pulse was applied is known to be one day, so that where the fitted pulse length is greater or less than one day, it implies convergent or divergent tracer flow respectively (figures 4-25 and 4-26).

Because this model determines pulse duration instead of the fraction of the tracer pulse recovered, the shape of the injection pulse is incorrect. Velocity is calculated from the center of the pulse input.

$$v = \frac{z}{T_1 - .5t_0} \qquad (4\text{-}1)$$

Moment analysis determines velocity from:

$$v = \frac{z}{T_1 - .5} \qquad (4\text{-}2)$$

as t_0 is known to be one day. Therefore, using CXTFIT, for pulse lengths greater than one day, faster velocities are calculated; for pulse lengths less than one day, slower velocities are calculated.

Several BTC's show what is apparently double peaks. This occurs because tracer flowing to a particular porous cup sampler can originate from several drip emitters, some tracer flowing to the cup via one flow path, other tracer flowing to the same cup from other routes. Some of these paths will be longer than others, some shorter. The BTC's showing two fluoro-organic tracers illustrate this phenomenon.

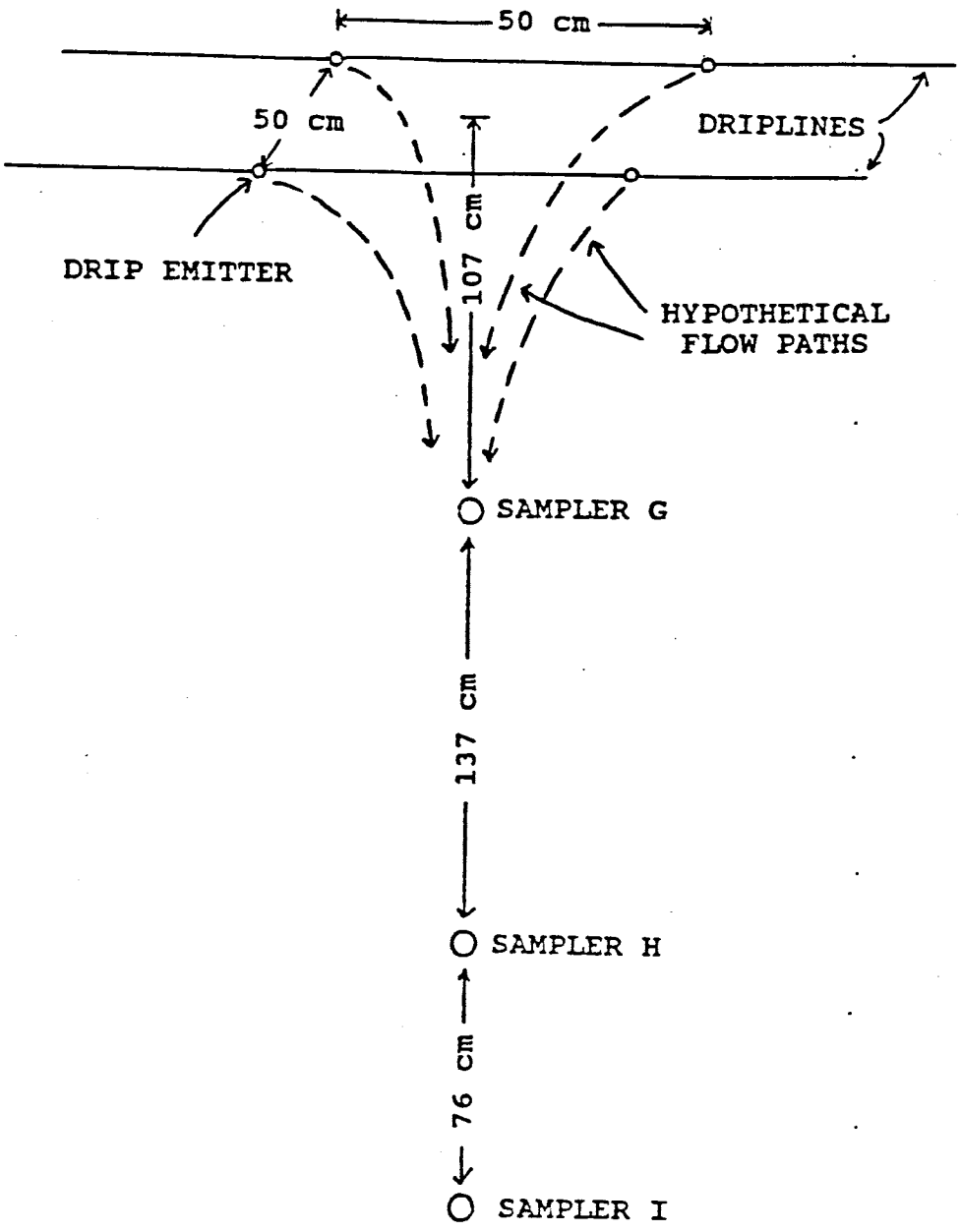

Figure 4-25. Illustration of convergent flow from multiple sources (from Flanigan, 1989).

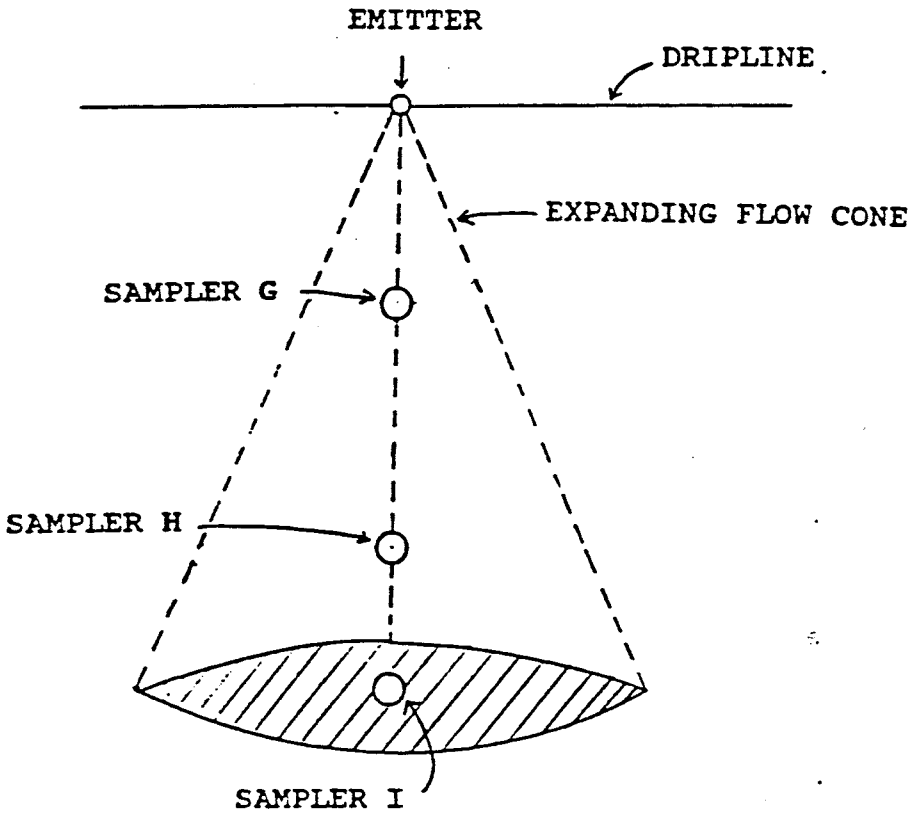

Figure 4-26. Illustration of divergent flow from a single source (from Flanigan, 1989).

A method was developed to look at these double peaks. The concentration data from early tracer breakthrough up to data belonging to the second peak (determined visually) was plugged into the CXTFIT program and parameters determined. These parameters were then used to determine what the concentrations should be for the various sampling times of the second peak if the second peak were nonexistent. These concentrations were subtracted from the concentrations of the second peak leaving a breakthrough curve of tracer moving through a different flow path minus the effects of the first breakthrough of tracer. The residual concentrations were then inputted into the CXTFIT program and parameters for the second flow path calculated. In actuality, there were probably many different separate flow paths to a particular sampler, but it seemed impossible to truly determine their number. Only the better fitting of BTC's with double peaks or pronounced tailing seemed to be accomplished by this method (figures 4-27 through 4-29).

POSSIBLE DESIGN PROBLEMS

There are some factors that were built into the design of the experiment that could possibly taint the data or invalidate some of the assumptions made about flow through this system. One problem was that flow through the emitters was uniform across the site. It is possible that some were

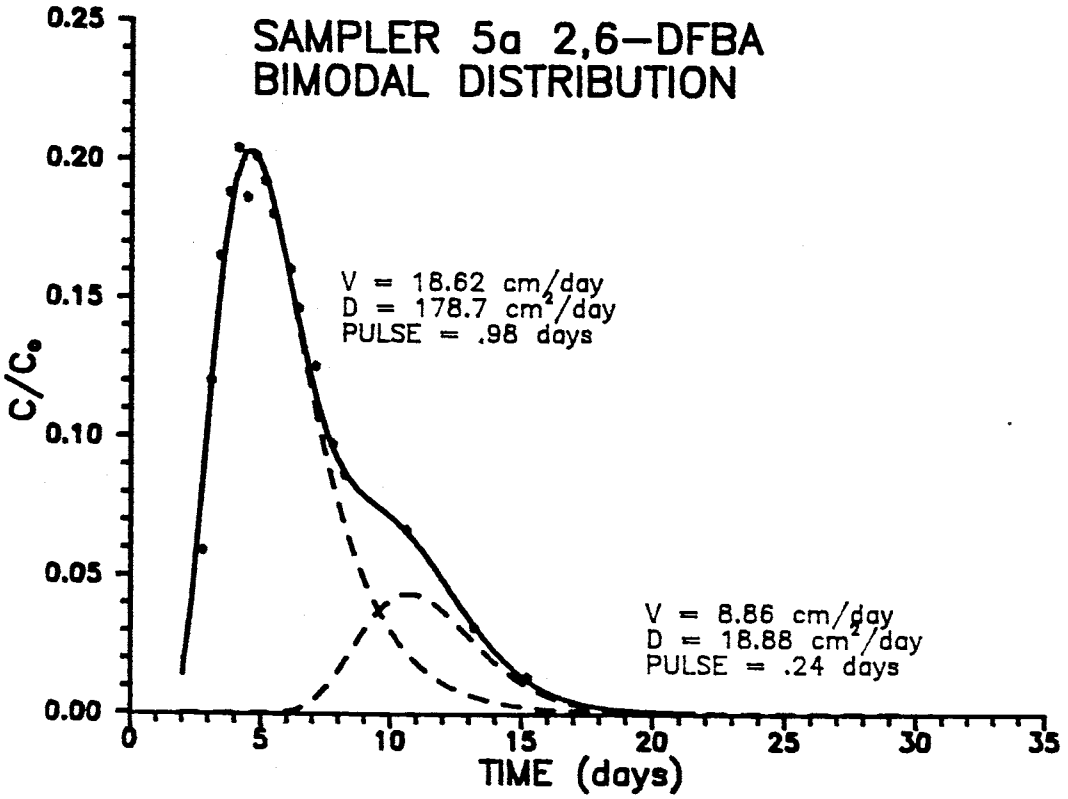

Figure 4-27. Sampler 5a breakthrough curve using peak addition. V, D and PULSE are parameters used to generate the dashed curves. Solid line is addition of dashed curves.

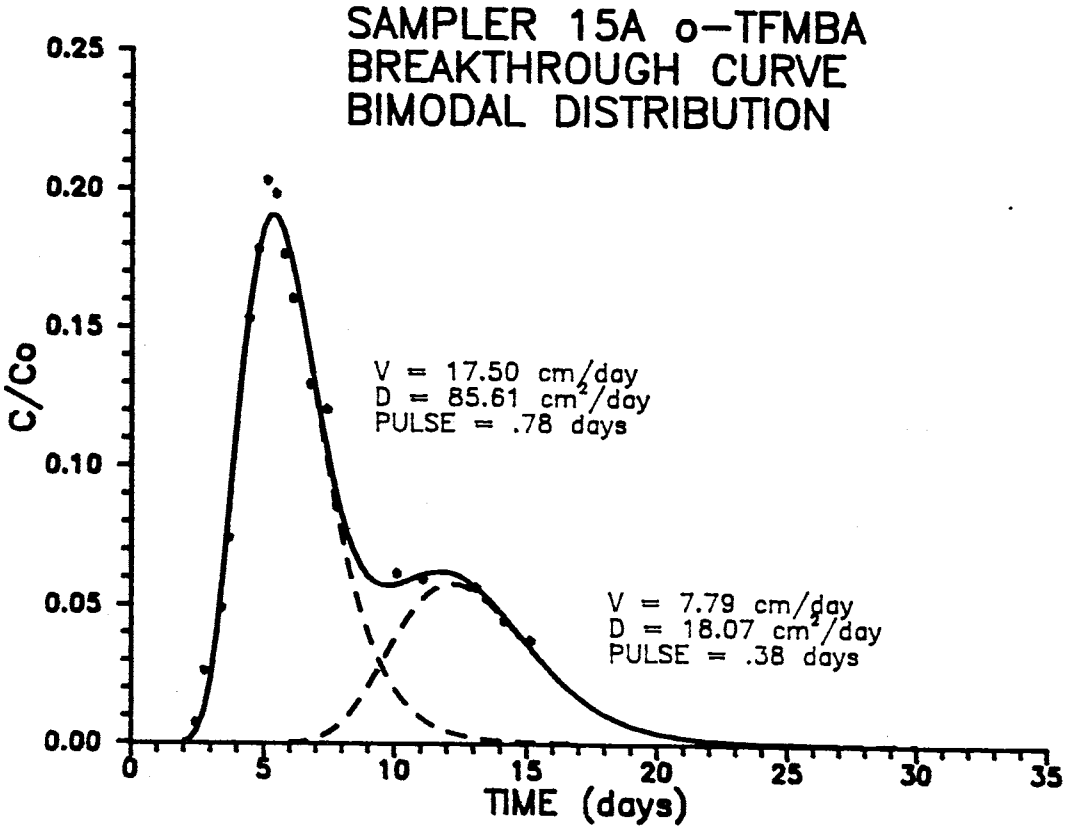

Figure 4-28. Sampler 15a breakthrough curve using peak addition. V, D and PULSE are parameters used to generate the dashed curves. Solid line is addition of dashed curves.

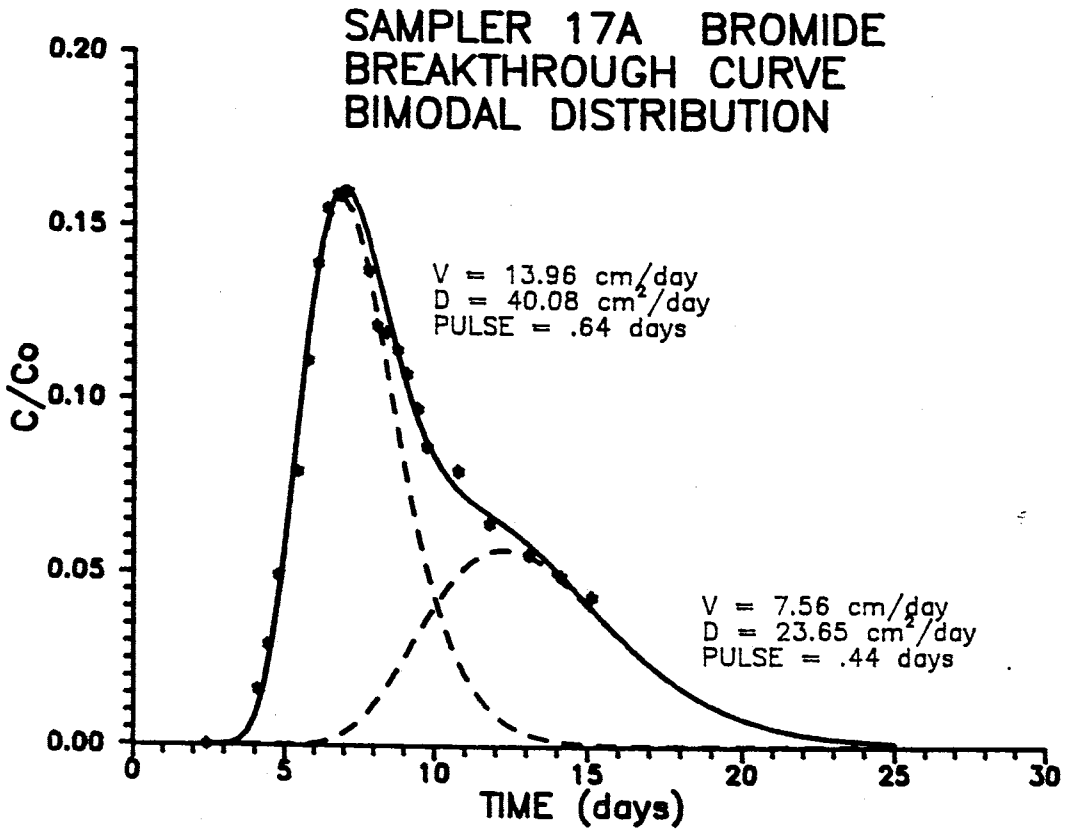

Figure 4-29. Sampler 17a breakthrough curve using peak addition. V, D and PULSE are parameters used to generate the dashed curves. Solid line is addition of dashed curves.

clogged, inhibiting flow out the emitter and creating more flow in other emitters in the same section.

Also, it is assumed that the flow through the soil is steady state. This is not completely correct. The water is applied to the soil in pulses, four every hour. The moisture content was not seen to noticably change between water applications, so the system was considered steady state. The slight transient nature of the water application might have little effect on moisture contents and suction values, but its effect on actual solute movement might be more noticable (i.e. possibly creating tailing).

Another possible design problem deals with the soil water sampler installation. It would have been ideal if the samplers could have been installed in holes approximately the same diameter as the sampler PVC tube, but this was not possible due to the soils found beneath the surface. Some of the backfill used to fill in the holes does not represent native material, so its hydraulic properties could be greatly different. Also, the silica flour and the bentonite seals could perturb flow paths to the porous cups, thus giving BTC's related more to sampler installation than to flow through the actual native material.

A comparison of fitted v, D, and t_o of the samplers installed previous to the first tracer test of Flanigan (1989) to the samplers installed later show that suction lysimeters installed earlier have much larger velocities on average than

samplers installed later. It is hypothesized that the installation of the earlier samplers was poor, or that the samplers had more established flow paths to them because of prior usage.

The pulling of soil water through the porous cup may have itself perturbed the flow field beneath the site. The different amounts of water pulled infers that some samplers are sampling a greater volume of soil around them than are others. The fact that samples were not taken continuously adds another transient to the system. Finally, stopping the sampling of some of the samplers before the breakthrough of tracer was complete leaves questions as to whether some late time phenomena was missed.

PRIOR AND CONTINUING WORK AT THE SITE

In a related report, Flanigan (1989) describes a bromide tracer test done at the New Mexico Tech site and column studies done on site material. Parsons (1988) provides details on the characterization of the hydraulic and geologic properties of the site, and applies a one-dimensional analytical model to observed moisture movement after water was initially applied. Mattson (1989) provides details on the experimental design and construction, and applies a two-dimensional analytical model to the observed moisture movement.

Current work involves extensive site characterization, including visual mapping of soil units seen from trenching, illustrations of dye movement, and various field and laboratory tests on the many soils at the site to determine unsaturated hydraulic parameters.

SUMMARY AND CONCLUSIONS

As concern for the environment grows, the safe usage and disposing of harmful chemicals becomes more and more urgent. To better attain these goals, it is necessary that a greater understanding of the processes by which solute is transported through the vadose zone is achieved.

A long term field study was undertaken west of New Mexico Tech from Jan. 1987 to Oct. 1989. The field site was comprised of a 30 meter by 30 meter area situated on an old arroyo channel, diked off to prevent runoff events. The soil profile consists of two distinct facies: an upper zone consisting of interbedded silts, sands, silty sands and clayey sands with intermittent cobble layers and a lower zone consisting mainly of ancestral Rio Grande fluvial fine sands with varying degrees of carbonate cementation.

The goals of the experiment were to investigate water and solute movement in stratified, heterogeneous soils and to determine the capability of existing analytical and numerical models to predict water and solute movement in the vadose zone.

This paper describes a solute transport field experiment carried out at the field site. Water was applied at the rate of 10^{-4} cm/sec to the center 10 meter by 10 meter area using agricultural drip lines. The experiment was designed to simulate solute movement from beneath a waste impoundment into the vadose zone.

Part of the experiment consisted of injecting a one day

pulse of five tracers into the water application system and monitoring their movement in both the vertical and horizontal directions. Bromide tracer was applied to the entire area, while a different fluoro-benzoate tracer was applied to each of four separate subregions of the water application area. Soil water samples were taken using soil water samplers installed at various locations and depths within and outside the tracer application area. Tracer concentrations were determined via High Performance Liquid Chromatography.

Solute transport parameters were determined from concentration verses time data for the many samplers using the non-linear least squares curve fitting model CXTFIT (Parker and van Genuchten, 1984) and using moment analysis. Three methods of aerially averaging concentration were also investigated. Finally, the transfer function of Jury (1982a) was applied to aerially averaged concentration data to determine if the model would predict tracer breakthrough curves at depths other than the calibration depth.

From these experiments, the following conclusions are drawn:

1. Water and tracer transport at the field site is controlled by anisotropy, heterogeneity, the orientation of the stratified layers, and differences in hydraulic properties between adjacent stratigraphic units. Significant lateral movement of tracer was observed. Beneath the tracer

application area, fluoro-benzoate tracer was detected as much as .75 meters north of its application area at a depth of one meter. Bromide and fluoro-benzoate tracer was observed as much as six meters outside the plot at a depth of 5.6 meters after approximately 23 days.

2. A wide distribution of transport parameters were observed. Seepage velocity, dispersion coefficient, and dispersivity were log-normally distributed across the site. The amount of tracer seen and the average volume of soil water sampled were normally distributed.

3. By weighting the concentration seen at a particular point by the assumed water flux passing that point and averaging over a horizontal area, a better representation of the total mass of solute passing through the plane at that depth was obtained. This method predicted much faster movement of tracer than by aerially averaging resident concentrations or by simply averaging the transport parameters.

4. The transfer function model did not adequately describe solute movement in the top 2.5 meters of soil. This was probably due to the large degree of heterogeneity at the site, lateral movement of solute, and the boundary condition at the point tracer was applied to the soil. The transfer function predicted much faster tracer loading on the water table than

the classical one-dimensional advection dispersion equation.

5. The data obtained from this experiment will be useful in validating multi-dimensional numerical models. The experiments that have been done at the site have resulted in a large data base of moisture and solute movement within the vadose zone, as well as a large collection of field and laboratory measured values of unsaturated hydrodynamic parameters. Most existing multi-dimensional solute transport codes have not been validated against actual field data. It is hoped that a greater understanding of tracer transport in this complicated system will lead to models better able to predict contaminant transport in other systems.

In hindsight, several improvements to the site design would be beneficial. The installation of soil water samplers before the water application system was laid down would have enabled the emplacement of interior samplers at greater depths. A shelter could be constructed to house the site, thereby removing the need for insulating hay and soil cover. The drip lines could then be placed on the surface, where they would be available for inspection and periodic replacement.

REFERENCES

Biggar, J.W., and D.R. Nielsen, 1976, Spatial variability of the leaching characteristics of a field soil, Water Resour. Res., 12: 78-84.

Bowman, R.S., 1984, Analysis of soil extracts for inorganic and organic tracer anions via high performance liquid chromatography, Journal of Chromatography, 285: 467-477.

Bowman, R.S., and R.C. Rice, 1986, Accelerated herbicide leaching resulting from preferential flow phenomena and its implications for ground water contamination. p. 413-425. In Proceedings of the conference on southwestern ground water issues, Phoenix, AZ. October 20-22, 1986. National Water Well Association, Dublin, OH.

Bresler, E., and G. Dagan, 1981, Convective and pore scale dispersive solute transport in unsaturated heterogeneous field, Water Resour. Res., 17: 1683-1693.

Butters, G.L., W.A. Jury, and F.F. Ernst, 1989a, Field scale transport of bromide in an unsaturated soil: 1. Experimental methodology and results, Water Resour. Res., 25: 1575-1581.

Butters, G.L., and W.A. Jury, 1989b, Field scale transport of bromide in an unsaturated soil: 2. Dispersion modeling, Water Resour. Res., 25: 1583-1589.

Crosby, J.W., D.L. Johnstone, C.H. Drake, and R.C. Fenton, 1968, Migration of pollutants in a glacial outwash environment, Water Resour. Res., 4: 1095-1114.

Crosby, J.W., D.L. Johnstone, and R.L. Fenton, 1971, Migration of pollutants in a glacial outwash environment 2., Water Resour. Res., 7: 204-208.

Dagan, G., and E. Bresler, 1979, Solute dispersion in unsaturated heterogeneous soil at field scale: I. Theory, Soil Sci. Soc. Am. J., 43, 461-467.

Flanigan, K.G., 1989, Field simulation of waster impoundment seepage in the vadose zone: Non-reactive solute transport through a stratified, unsaturated field soil, Unpublished M.S. Independent study paper, New Mexico Institute of Mining and Technology, Socorro, NM.

Gelhar, L.W., and C. Axness, 1983, Three-dimensional stochastic analysis of macrodispersion in aquifers, Water Resour. Res., 19: 161-190.

Gibbens, J.F., 1989, An evaluation of several fluorinated benzoic acids for use as soil and groundwater tracers, M.S. Thesis, New Mexico Institute of Mining and Technology, Socorro, NM: 116 pages.

Jury, W.A., 1982, Simulation of solute transport using a transfer function model, Water Resour. Res., 18: 363-368.

Jury, W.A., L.H. Stolzy, and P. Shouse, 1982, A field test of the transfer function model for predicting solute transport, Water Resour. Res., 18: 369-375.

Jury, W.A., and G. Sposito, 1985, Field calibration and validation of solute transport models for the unsaturated zone, Soil Sci. Soc. Am. J., 49: 1331-1341.

Kreft, A. and A. Zuber, 1978, On the physical meaning of the dispersion coefficient and its solution for different initial boundary conditions, Chem. Eng. Sci., 33: 1471-1480.

Mantoglou, A., and L.W. Gelhar, 1987, Stochastic modeling of large scale transient unsaturated flow systems, Water Resour. Res., 23: 37-46.

Mattson, E.D., 1989, Field simulation of waste impoundment seepage in the vadose zone: Experimental design and two-dimensional modeling, Unpublished M.S. Independent study paper, New Mexico Institute of Mining and Technology, Socorro, NM.

Mualem, Y.A., 1984, Soil anisotropy of unsaturated soils, Soil Sci. Soc. Am. J., 48: 505-509.

Neumann, S.P., and L.A. Davis, 1983, **UNSAT2**, U.S. Nuclear Regulatory Comission Technical Report NUREG-CR-3390.

Nielsen, D.R., J.W. Biggar, and K.T. Erh, 1973, Spatial variability of field measured soil-water properties, Hilgardia, 42: 215-259.

Palmquist, W.N. and A.I. Johnson, 1962, Vadose zone flow in layered and non-layered materials, USGS Professional Paper 450 -C: C142-143.

Parker, J.C., and M. Th. van Genuchten, 1984, Determining transport parameters from laboratory and field tracer experiments, Bull. 84-3, Va. Agric. Exp. Sta., Blacksburg: 96 pages.

Parsons, A.M., 1988, Field simulation of waste impoundment seepage in the vadose zone: Site characterization and one-dimensional analytical modeling, M.S. thesis, New Mexico Inst. Mining and Tech., Socorro, NM.

Stephens, D.B., and S. Heerman, 1988, Dependence of anisotropy on saturation in a stratified sand, Water Resour. Res., 24: 770-778.

Tang, D.H., F.W. Schwartz, and L. Smith, 1982, Stochastic modeling of mass transport in a random velocity field, Water Resour. Res., 18: 231-244.

van Genuchten, M. Th. and W.J. Alves, 1982, Analytical solutions of the one-dimensional convective-dispersive solute transport equation, U.S. Dept. of Agriculture, Tech. Bull. No. 1661: 151 pages.

Warrick, A.W., J.W. Biggar, and D.R. Nielsen, 1971, Simultaneous solute and water transfer for an unsaturated soil, Water Resour. Res., 7: 1216-1225.

Yeh, J.T.C., L.W. Gelhar, and A.L. Gutjahr, 1985, Stochastic analysis of unsaturated flow in heterogeneous soils 2. Statistically anisotropic media with variable α, Water Resour. Res., 21: 457-464.

Yeh, G.T., 1987, **FEMWATER**. Oak Ridge National Laboratory Technical Report ORNL-5567.

APPENDIX A

Tracer breakthrough curves from CXTFIT analysis (Parker and van Genuchten, 1984) used to determine transport parameters listed in Table 4-1. Plots are of relative concentration of tracer (C/C_o) versus time.

V = seepage velocity
D = dispersion coefficient
t_o = duration of pulse addition
Z = depth of sampler

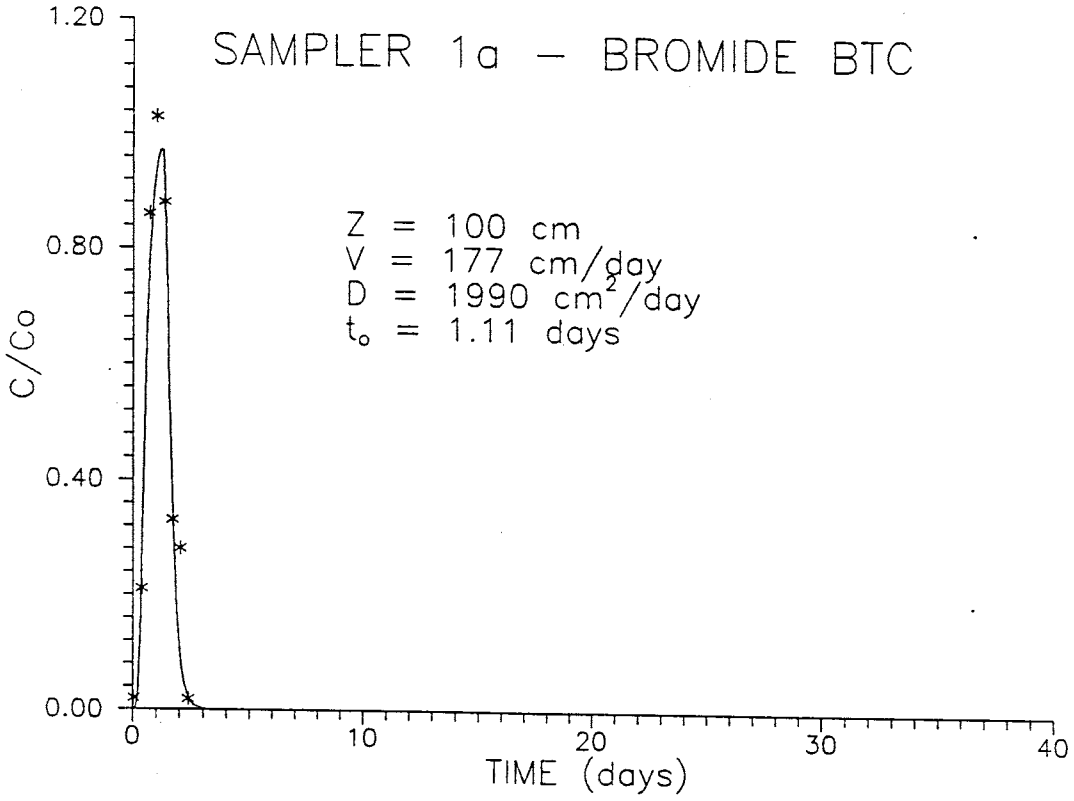
SAMPLER 1a – BROMIDE BTC
Z = 100 cm
V = 177 cm/day
D = 1990 cm²/day
t₀ = 1.11 days
C/Co
1.20
0.80
0.40
0.00
0
10
20
30
40
TIME (days)

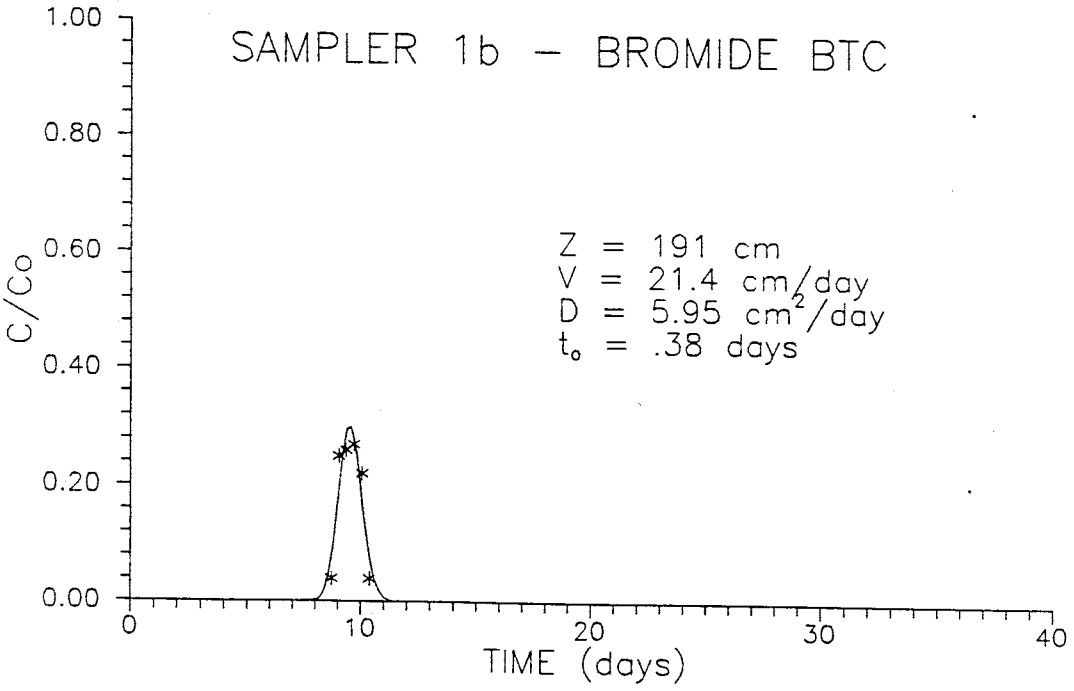
SAMPLER 1b – BROMIDE BTC
Z = 191 cm
V = 21.4 cm/day
D = 5.95 cm²/day
t₀ = .38 days
C/Co
1.00
0.80
0.60
0.40
0.20
0.00
0
10
20
30
40
TIME (days)

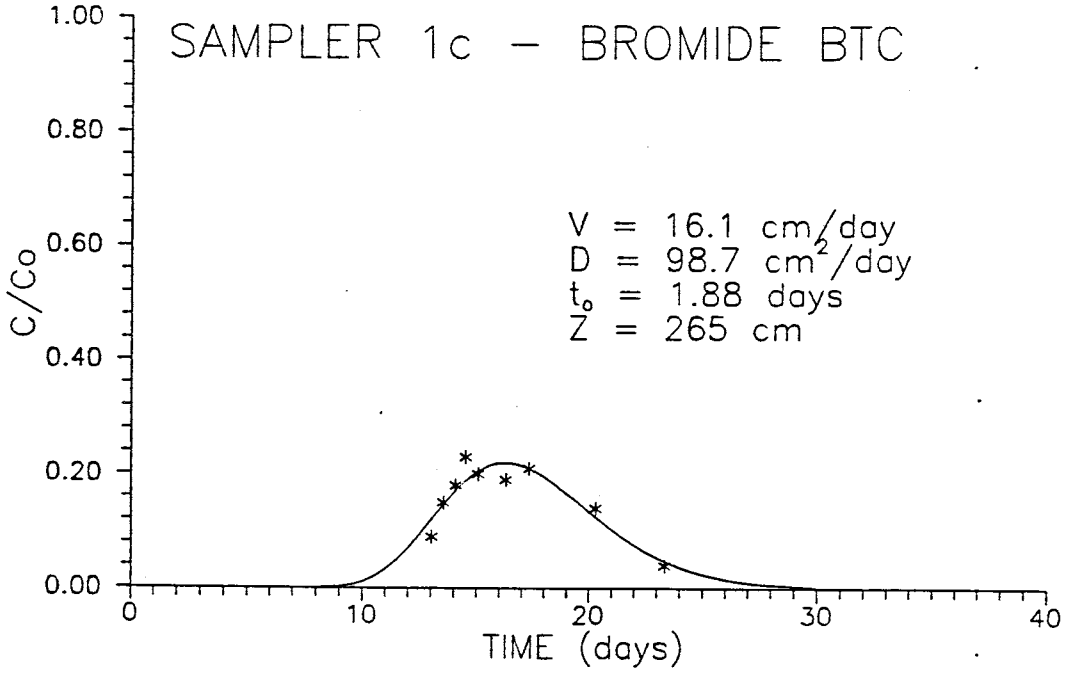
SAMPLER 1c – BROMIDE BTC
V = 16.1 cm/day
D = 98.7 cm²/day
t₀ = 1.88 days
Z = 265 cm
C/Co
1.00
0.80
0.60
0.40
0.20
0.00
0
10
20
30
40
TIME (days)

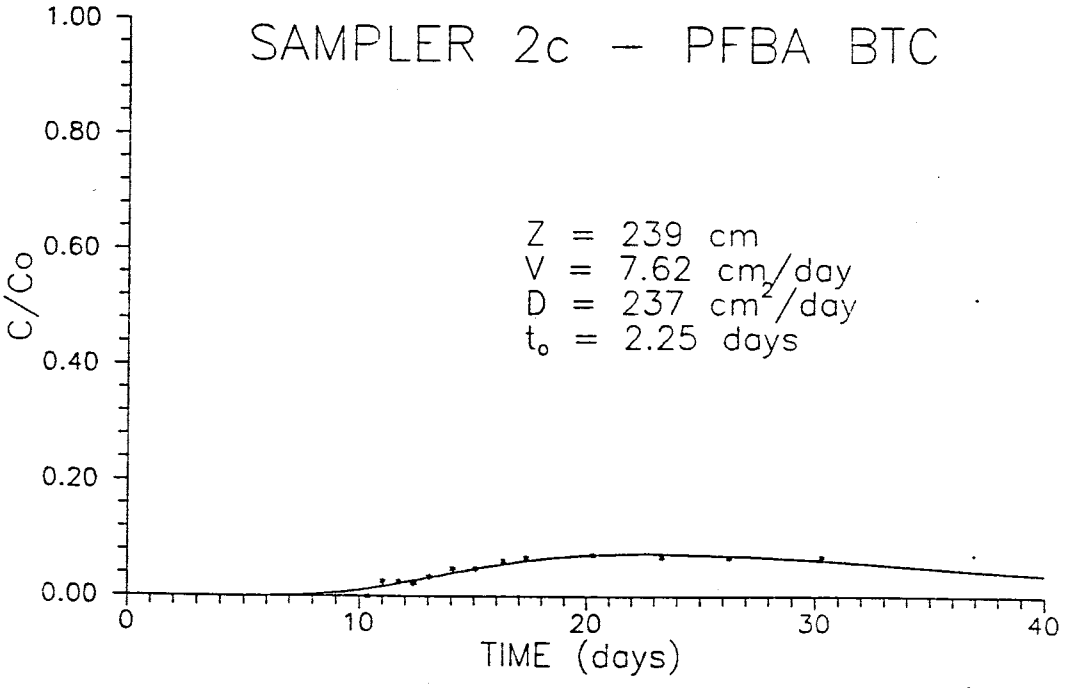
SAMPLER 2c – PFBA BTC
Z = 239 cm
V = 7.62 cm/day
D = 237 cm²/day
t₀ = 2.25 days
C/Co
1.00
0.80
0.60
0.40
0.20
0.00
0
10
20
30
40
TIME (days)

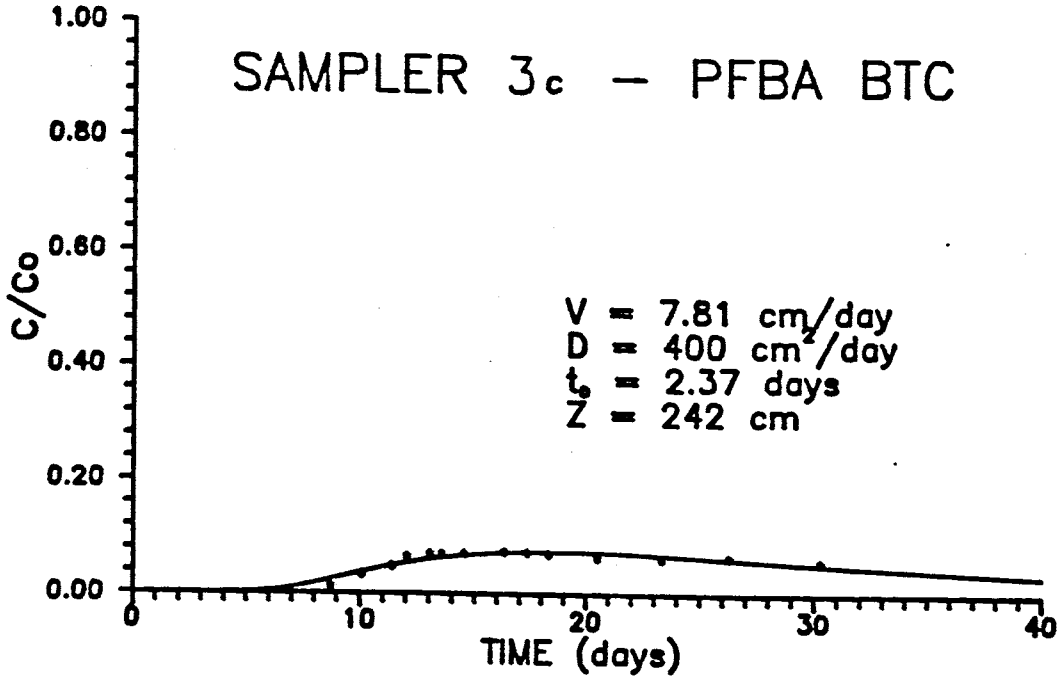
SAMPLER 3c – PFBA BTC
V = 7.81 cm/day
D = 400 cm²/day
t₀ = 2.37 days
Z = 242 cm
C/Co
1.00
0.80
0.60
0.40
0.20
0.00
0
10
20
30
40
TIME (days)

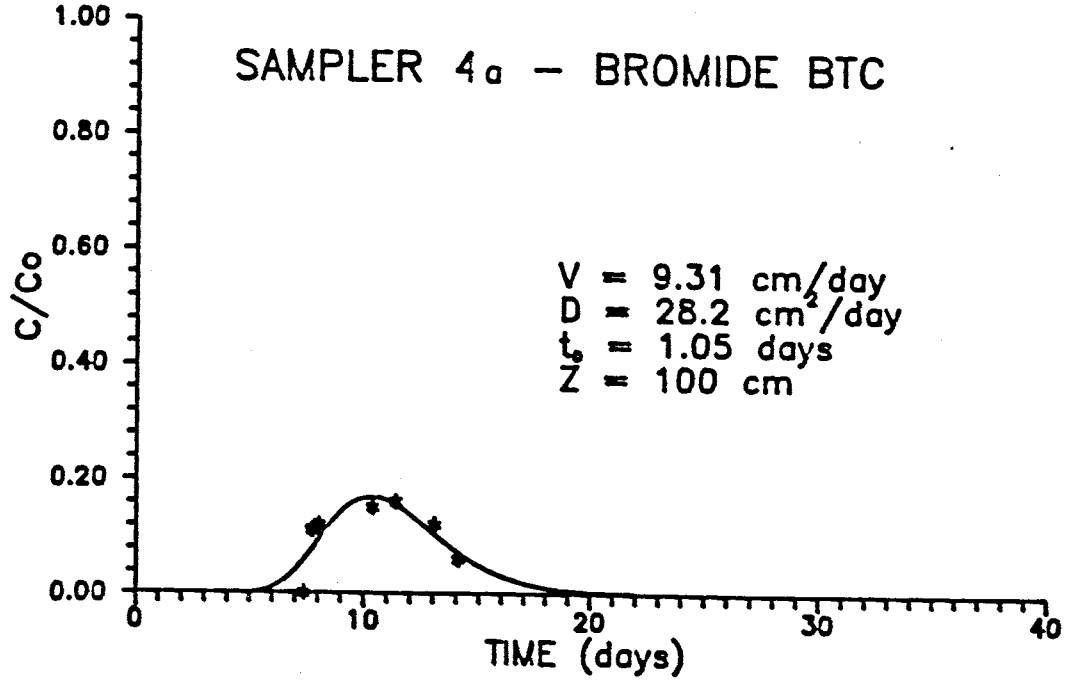
SAMPLER 4a – BROMIDE BTC
V = 9.31 cm/day
D = 28.2 cm²/day
t₀ = 1.05 days
Z = 100 cm
C/Co
1.00
0.80
0.60
0.40
0.20
0.00
0
10
20
30
40
TIME (days)

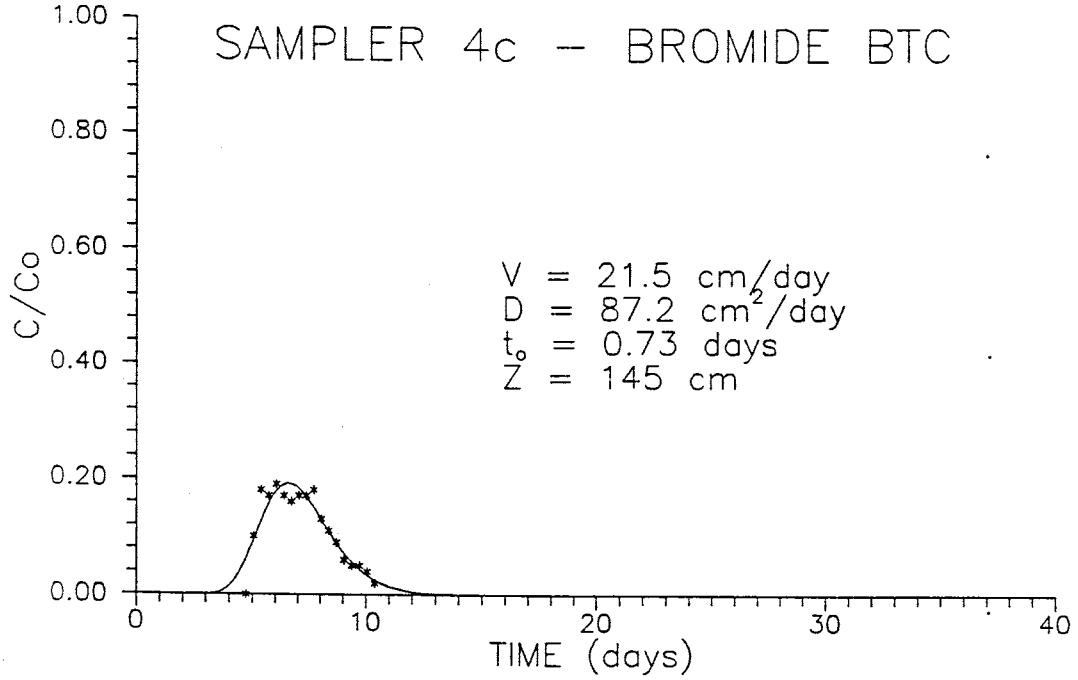
SAMPLER 4c – BROMIDE BTC
V = 21.5 cm/day
D = 87.2 cm²/day
t₀ = 0.73 days
Z = 145 cm
C/Co
1.00
0.80
0.60
0.40
0.20
0.00
0
10
20
30
40
TIME (days)

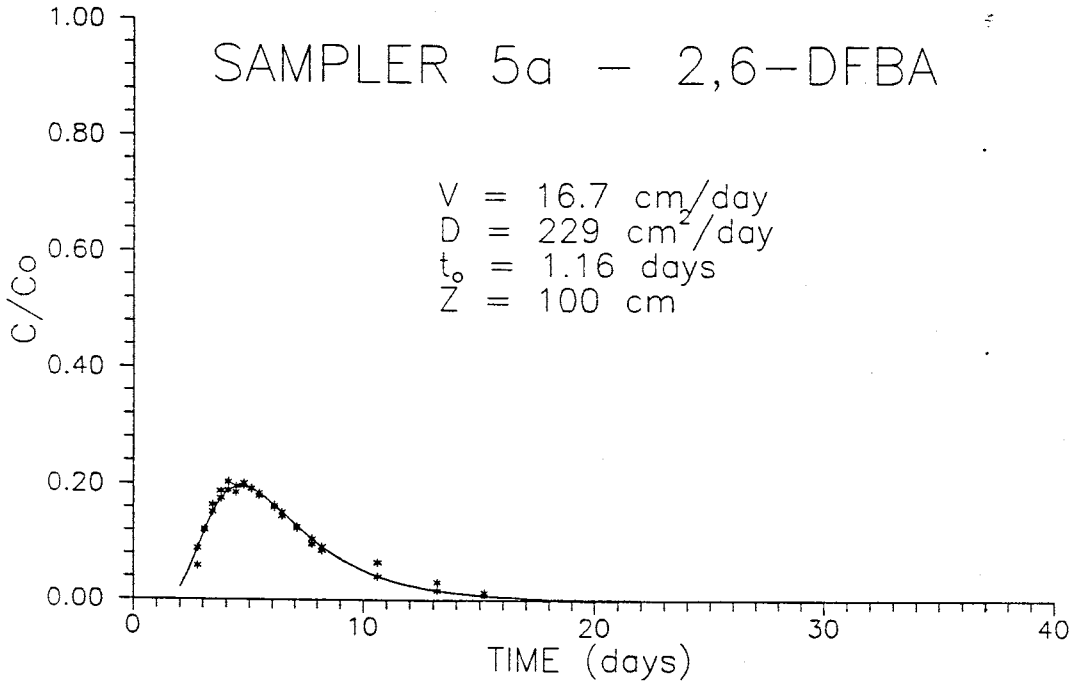
SAMPLER 5a – 2,6–DFBA
V = 16.7 cm/day
D = 229 cm²/day
t₀ = 1.16 days
Z = 100 cm
C/Co
1.00
0.80
0.60
0.40
0.20
0.00
0
10
20
30
40
TIME (days)

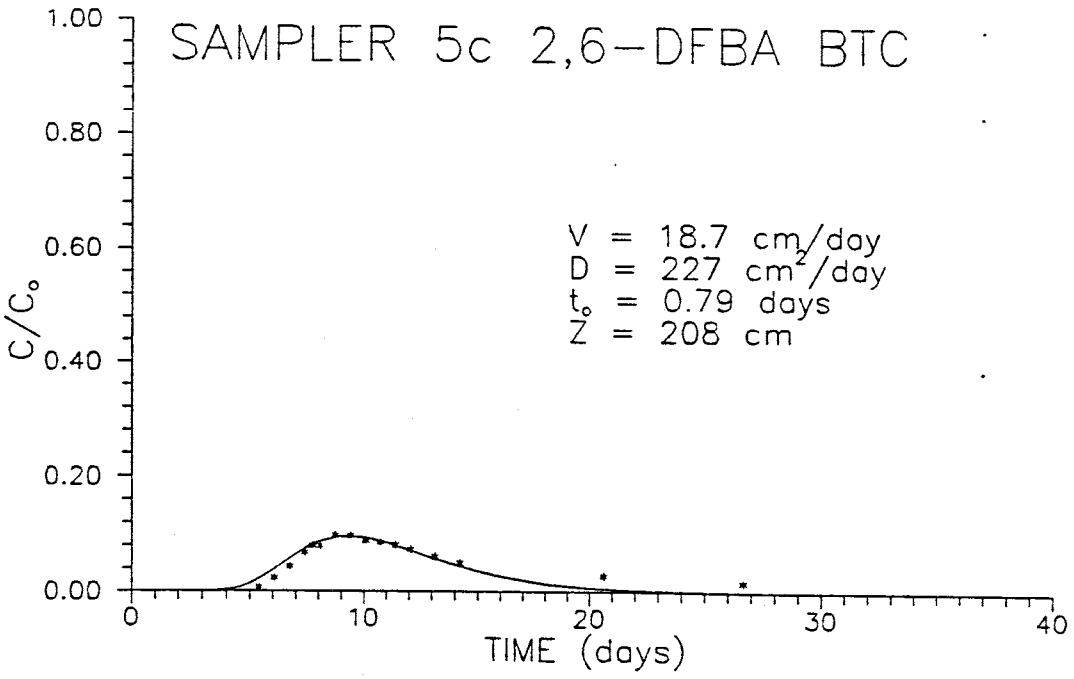
SAMPLER 5c 2,6-DFBA BTC
V = 18.7 cm/day
D = 227 cm²/day
t₀ = 0.79 days
Z = 208 cm
C/C₀
TIME (days)
1.00
0.80
0.60
0.40
0.20
0.00
0
10
20
30
40

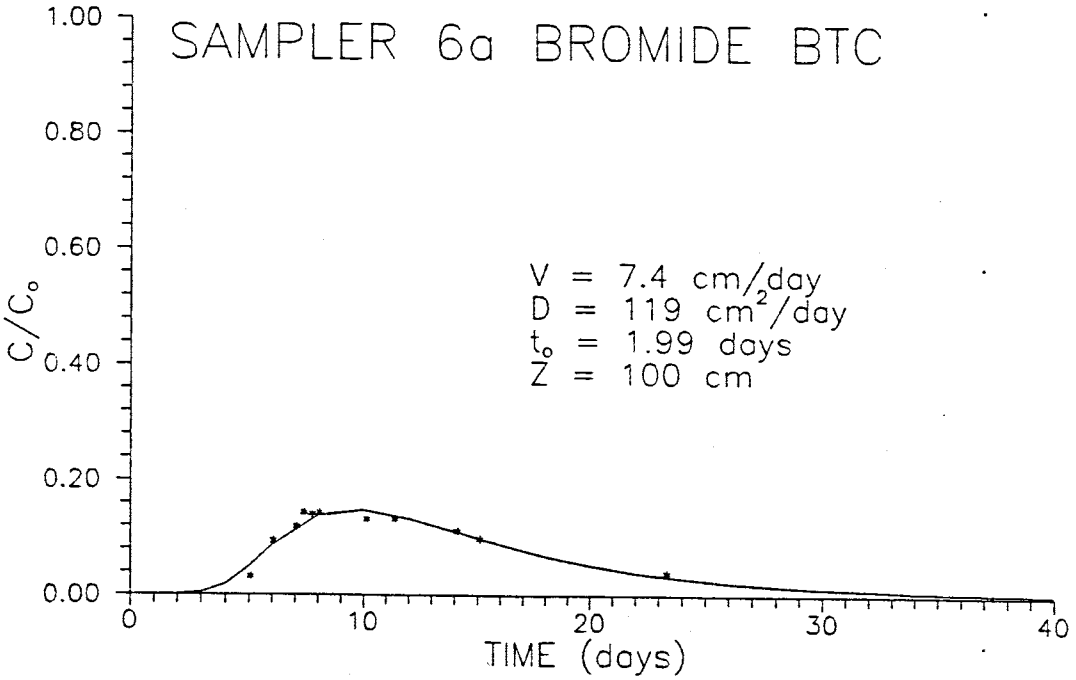
SAMPLER 6a BROMIDE BTC
V = 7.4 cm/day
D = 119 cm²/day
t₀ = 1.99 days
Z = 100 cm
C/C₀
TIME (days)
1.00
0.80
0.60
0.40
0.20
0.00
0
10
20
30
40

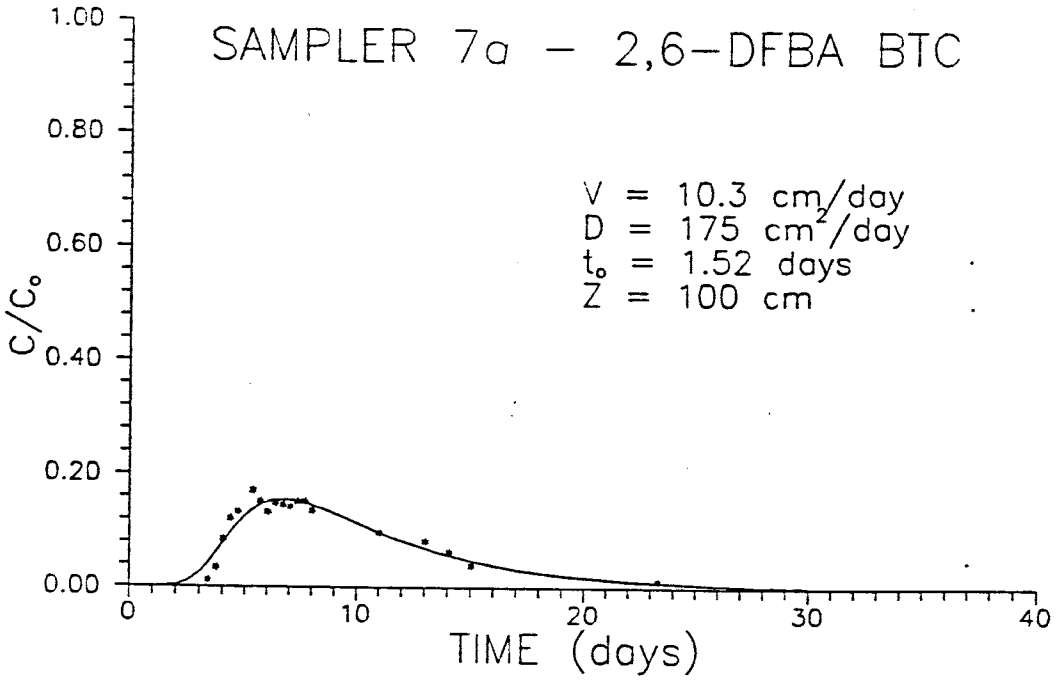
SAMPLER 7a – 2,6–DFBA BTC
V = 10.3 cm/day
D = 175 cm²/day
t₀ = 1.52 days
Z = 100 cm
C/C₀
1.00
0.80
0.60
0.40
0.20
0.00
0
10
20
30
40
TIME (days)

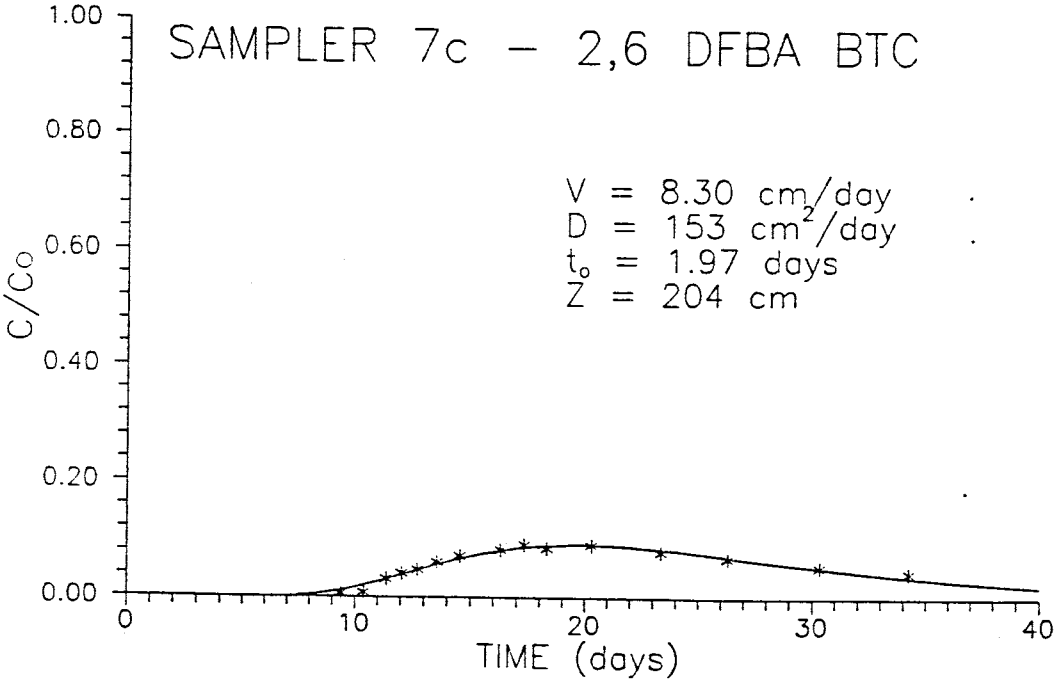
SAMPLER 7c – 2,6 DFBA BTC
V = 8.30 cm/day
D = 153 cm²/day
t₀ = 1.97 days
Z = 204 cm
C/C₀
1.00
0.80
0.60
0.40
0.20
0.00
0
10
20
30
40
TIME (days)

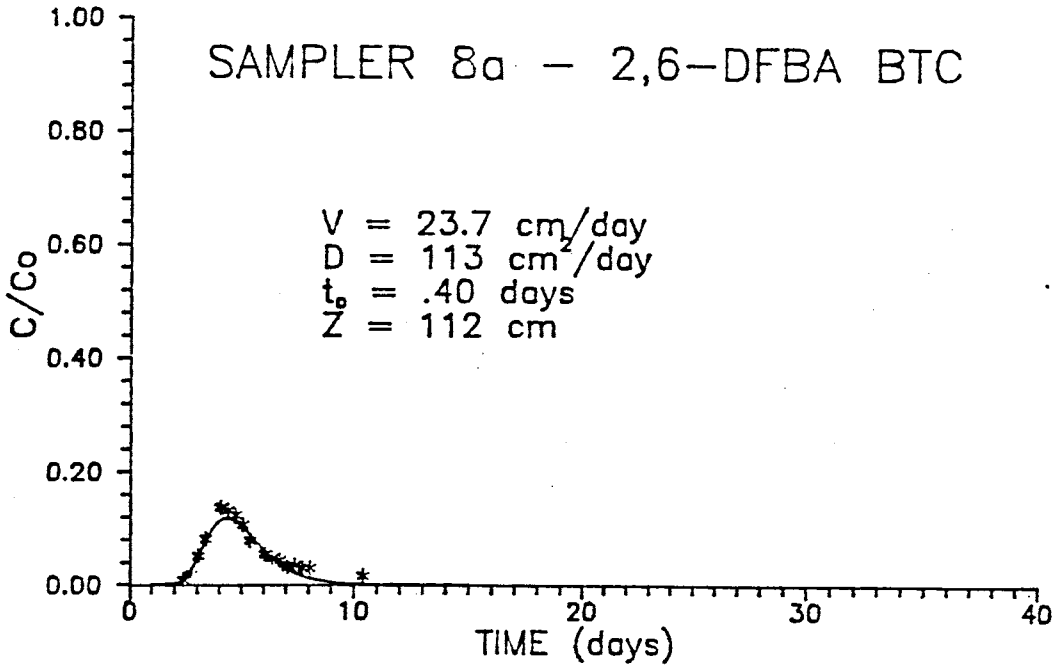
SAMPLER 8a – 2,6–DFBA BTC
V = 23.7 cm/day
D = 113 cm²/day
t₀ = .40 days
Z = 112 cm
C/Co
1.00
0.80
0.60
0.40
0.20
0.00
0
10
20
30
40
TIME (days)

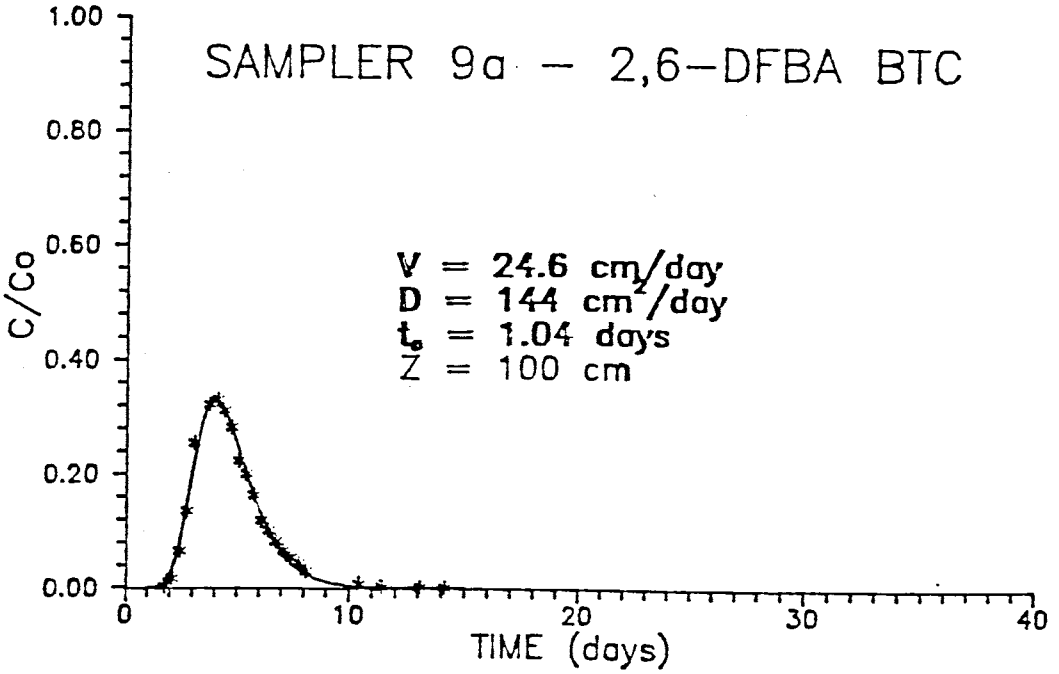
SAMPLER 9a – 2,6–DFBA BTC
V = 24.6 cm/day
D = 144 cm²/day
t₀ = 1.04 days
Z = 100 cm
C/Co
1.00
0.80
0.60
0.40
0.20
0.00
0
10
20
30
40
TIME (days)

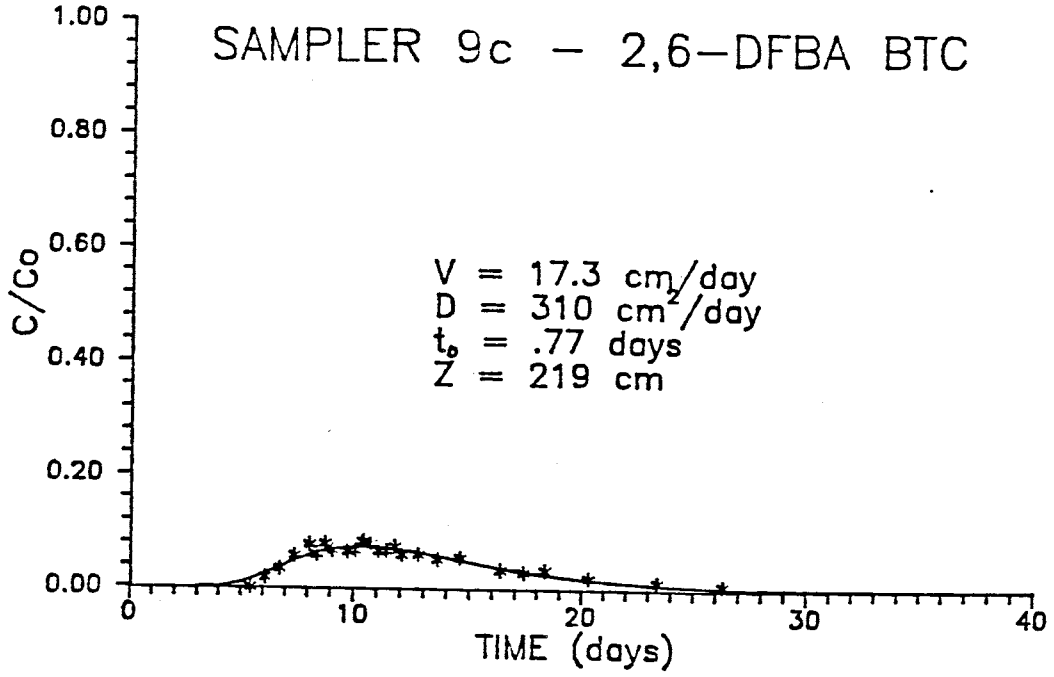
SAMPLER 9c – 2,6–DFBA BTC
V = 17.3 cm/day
D = 310 cm²/day
t_o = .77 days
Z = 219 cm
C/Co
1.00
0.80
0.60
0.40
0.20
0.00
0
10
20
30
40
TIME (days)

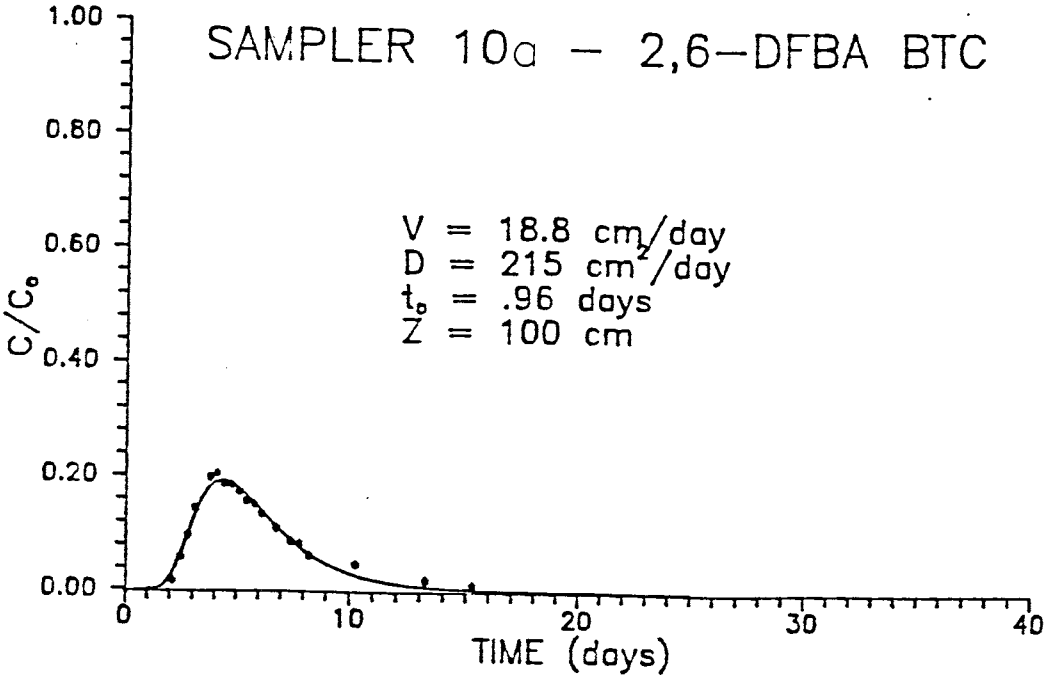
SAMPLER 10a – 2,6–DFBA BTC
V = 18.8 cm/day
D = 215 cm²/day
t_o = .96 days
Z = 100 cm
C/Co
1.00
0.80
0.60
0.40
0.20
0.00
0
10
20
30
40
TIME (days)

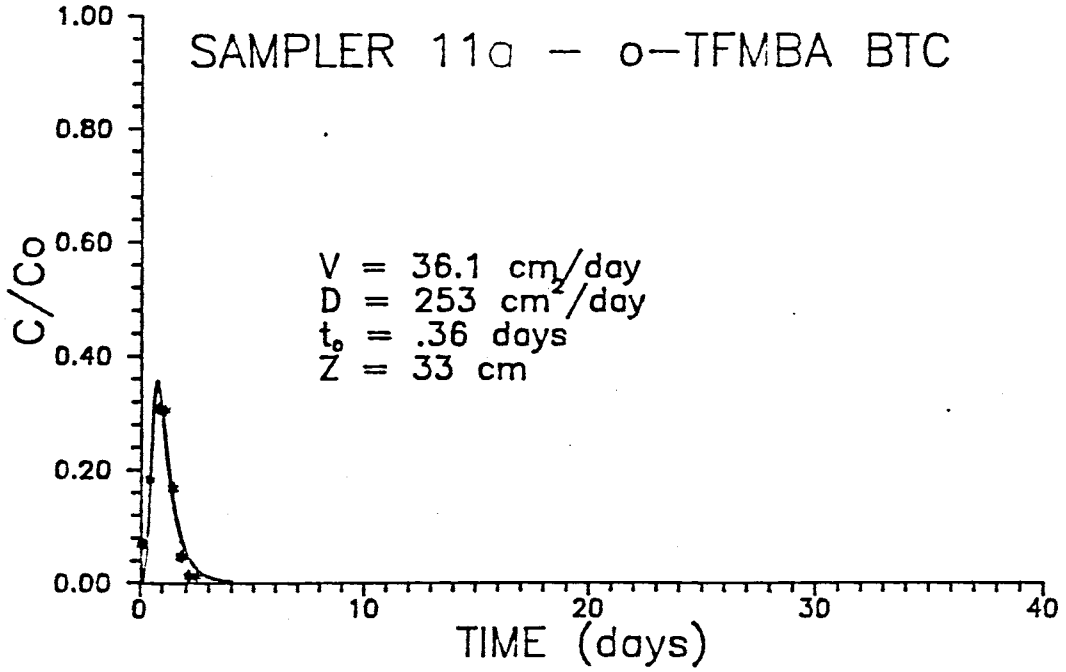
SAMPLER 11a – o–TFMBA BTC
V = 36.1 cm/day
D = 253 cm²/day
t₀ = .36 days
Z = 33 cm
C/Co
1.00
0.80
0.60
0.40
0.20
0.00
0
10
20
30
40
TIME (days)

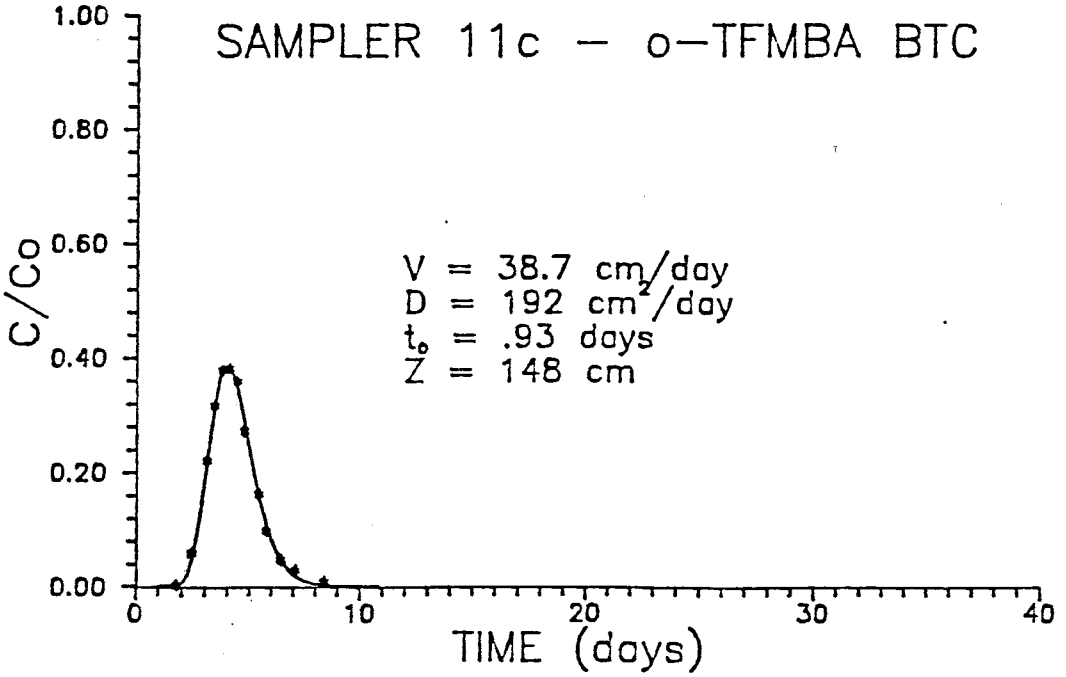
SAMPLER 11c – o–TFMBA BTC
V = 38.7 cm/day
D = 192 cm²/day
t₀ = .93 days
Z = 148 cm
C/Co
1.00
0.80
0.60
0.40
0.20
0.00
0
10
20
30
40
TIME (days)

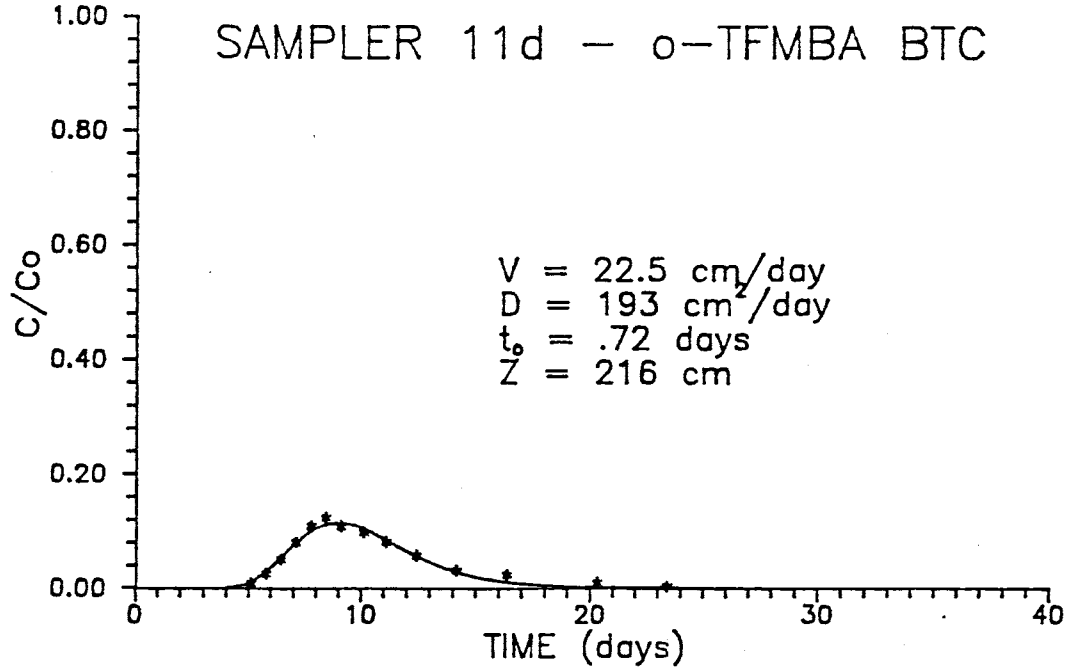
SAMPLER 11d – o–TFMBA BTC
V = 22.5 cm/day
D = 193 cm²/day
t₀ = .72 days
Z = 216 cm
C/Co
TIME (days)
1.00
0.80
0.60
0.40
0.20
0.00
0
10
20
30
40

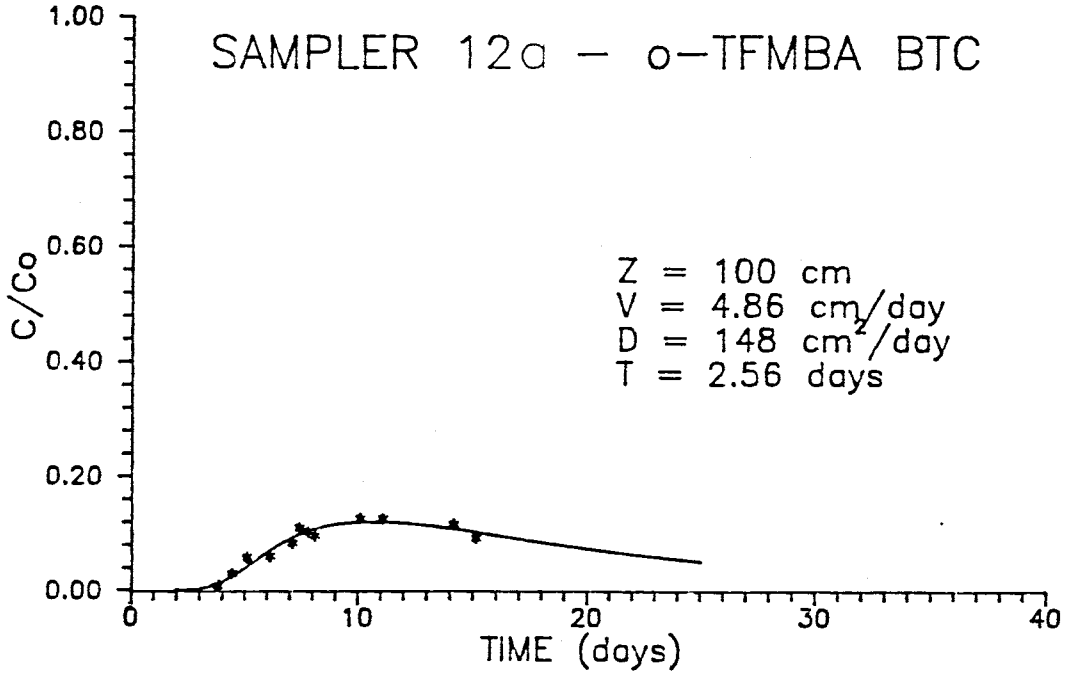
SAMPLER 12a – o–TFMBA BTC
Z = 100 cm
V = 4.86 cm/day
D = 148 cm²/day
T = 2.56 days
C/Co
TIME (days)
1.00
0.80
0.60
0.40
0.20
0.00
0
10
20
30
40

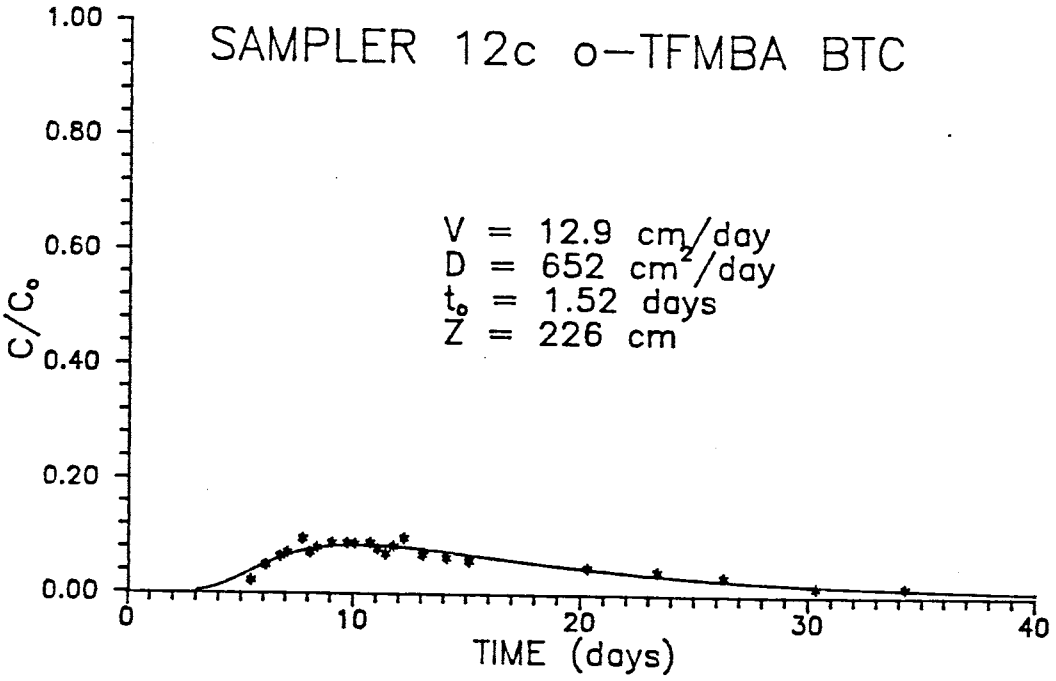
SAMPLER 12c o-TFMBA BTC
V = 12.9 cm/day
D = 652 cm²/day
t_o = 1.52 days
Z = 226 cm
C/C$_o$
1.00
0.80
0.60
0.40
0.20
0.00
0
10
20
30
40
TIME (days)

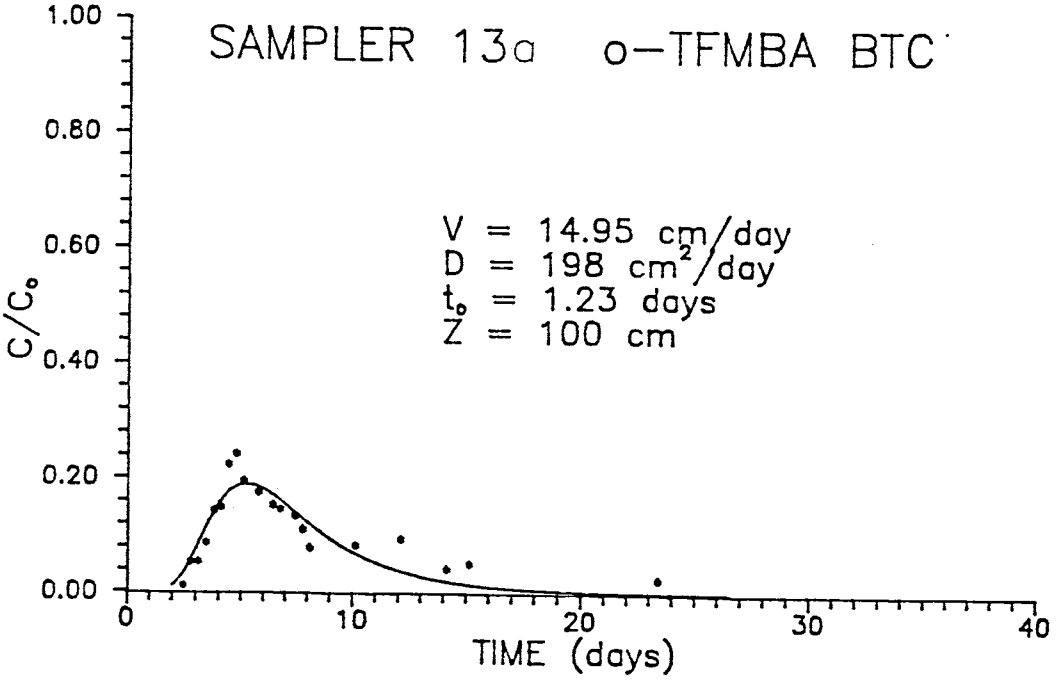
SAMPLER 13a o-TFMBA BTC
V = 14.95 cm/day
D = 198 cm²/day
t_o = 1.23 days
Z = 100 cm
C/C$_o$
1.00
0.80
0.60
0.40
0.20
0.00
0
10
20
30
40
TIME (days)

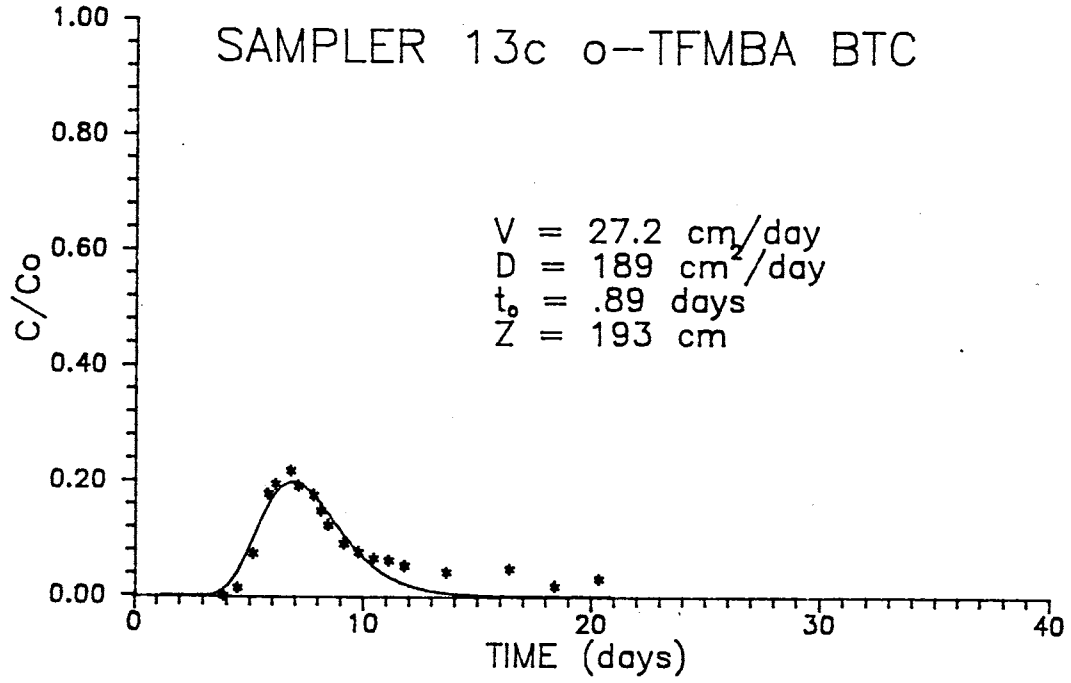
SAMPLER 13c o-TFMBA BTC
V = 27.2 cm/day
D = 189 cm²/day
t₀ = .89 days
Z = 193 cm
C/Co
TIME (days)
1.00
0.80
0.60
0.40
0.20
0.00
0
10
20
30
40

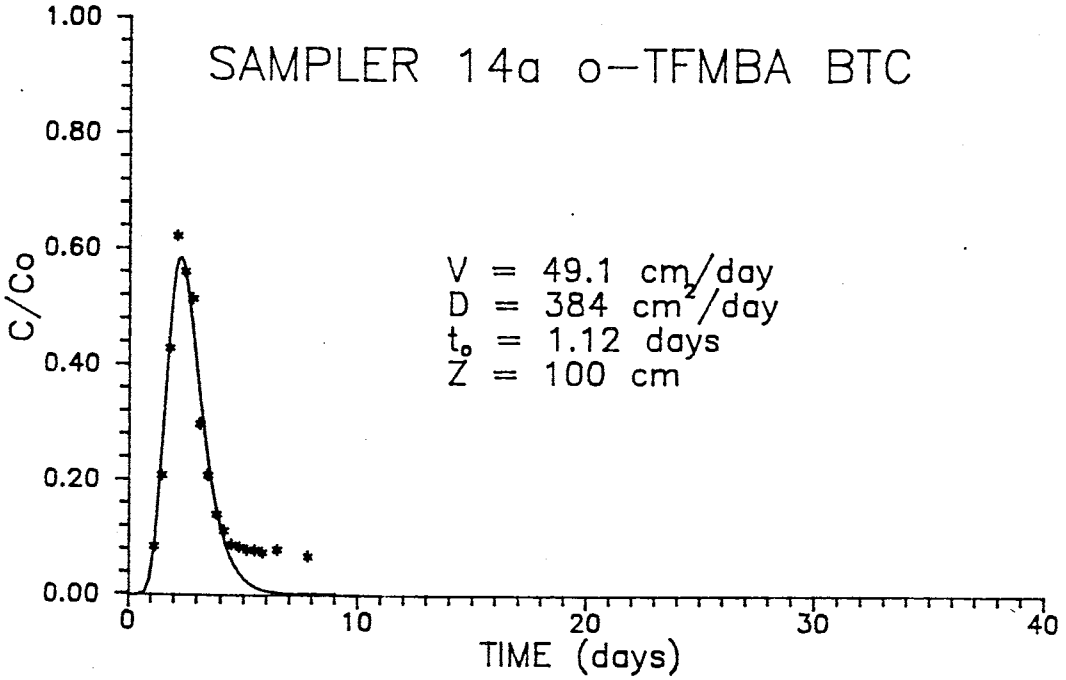
SAMPLER 14a o-TFMBA BTC
V = 49.1 cm/day
D = 384 cm²/day
t₀ = 1.12 days
Z = 100 cm
C/Co
TIME (days)
1.00
0.80
0.60
0.40
0.20
0.00
0
10
20
30
40

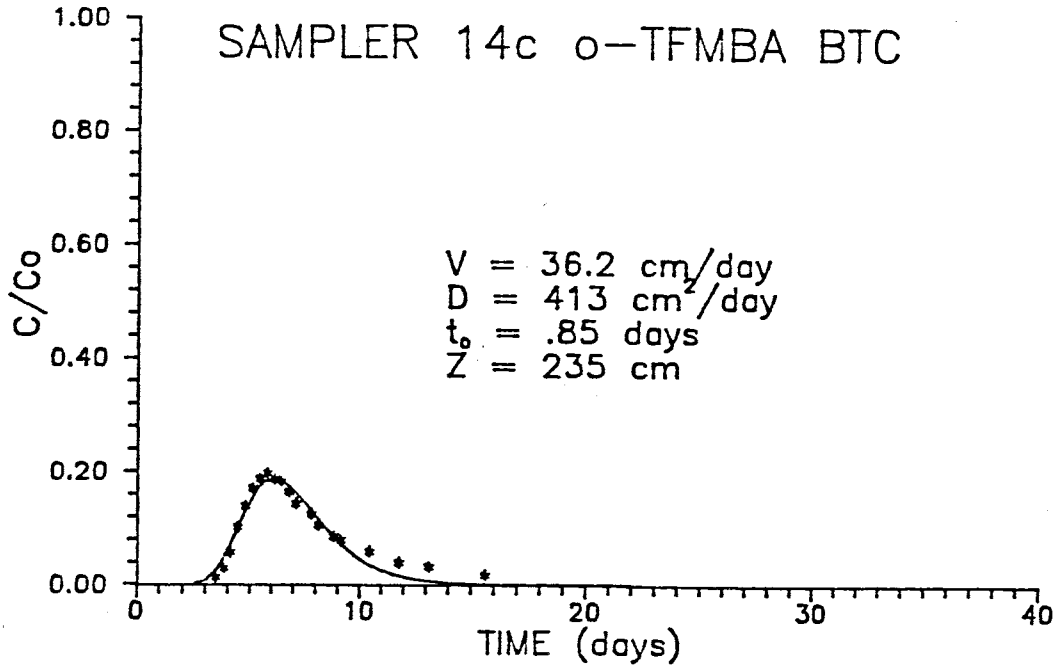
SAMPLER 14c o-TFMBA BTC
V = 36.2 cm/day
D = 413 cm²/day
t₀ = .85 days
Z = 235 cm
C/Co
1.00
0.80
0.60
0.40
0.20
0.00
0
10
20
30
40
TIME (days)

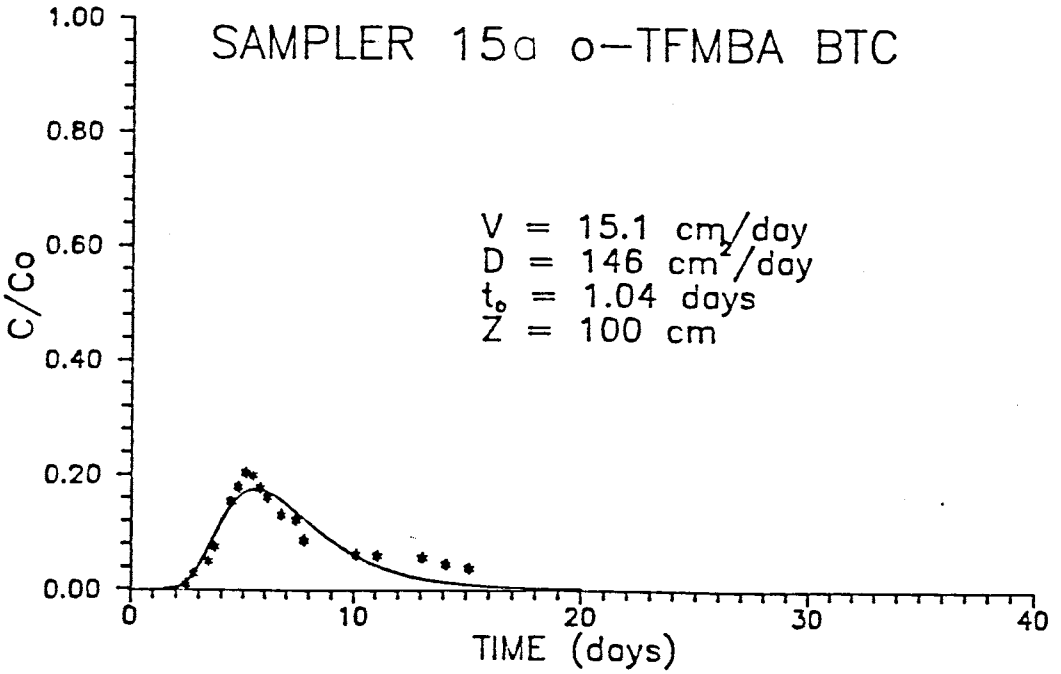
SAMPLER 15a o-TFMBA BTC
V = 15.1 cm/day
D = 146 cm²/day
t₀ = 1.04 days
Z = 100 cm
C/Co
1.00
0.80
0.60
0.40
0.20
0.00
0
10
20
30
40
TIME (days)

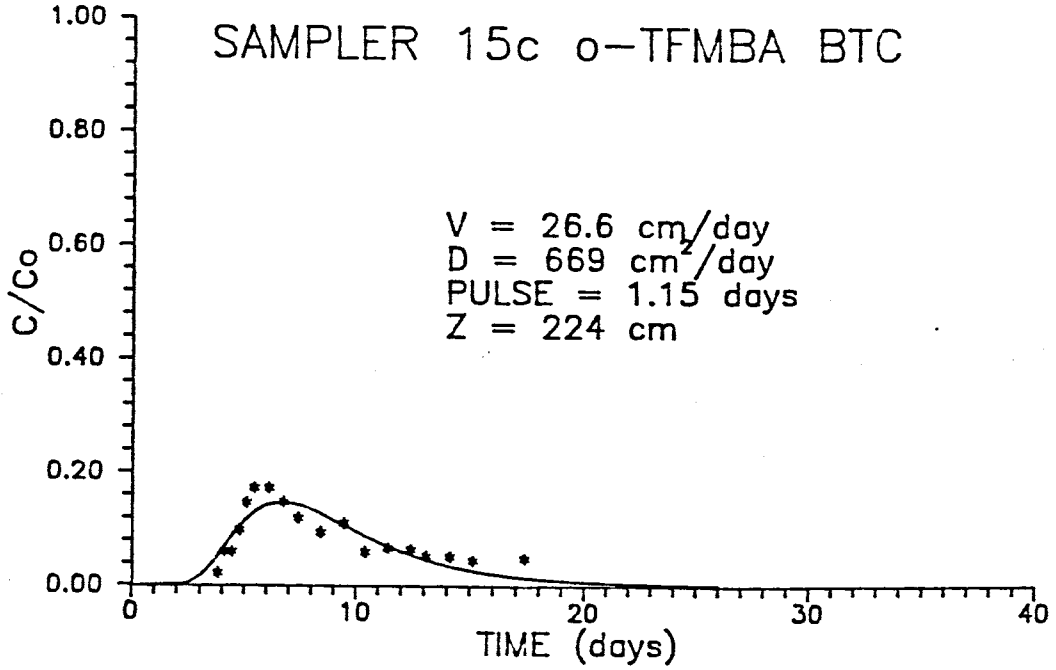
SAMPLER 15c o-TFMBA BTC
V = 26.6 cm/day
D = 669 cm²/day
PULSE = 1.15 days
Z = 224 cm
C/Co
TIME (days)
1.00
0.80
0.60
0.40
0.20
0.00
0
10
20
30
40

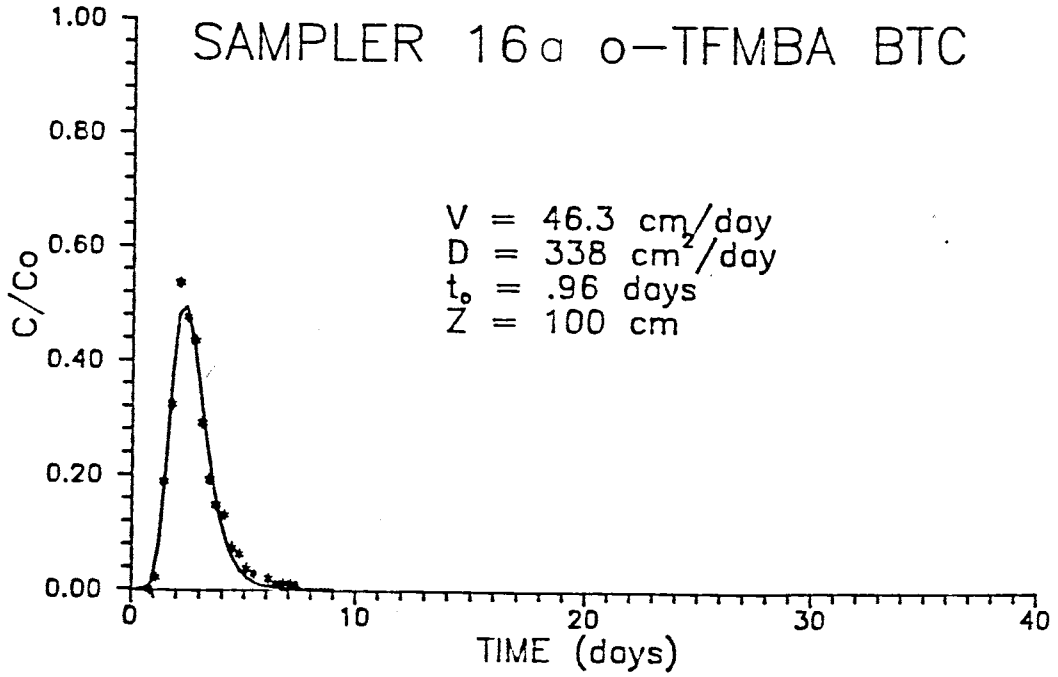
SAMPLER 16a o-TFMBA BTC
V = 46.3 cm/day
D = 338 cm²/day
t₀ = .96 days
Z = 100 cm
C/Co
TIME (days)
1.00
0.80
0.60
0.40
0.20
0.00
0
10
20
30
40

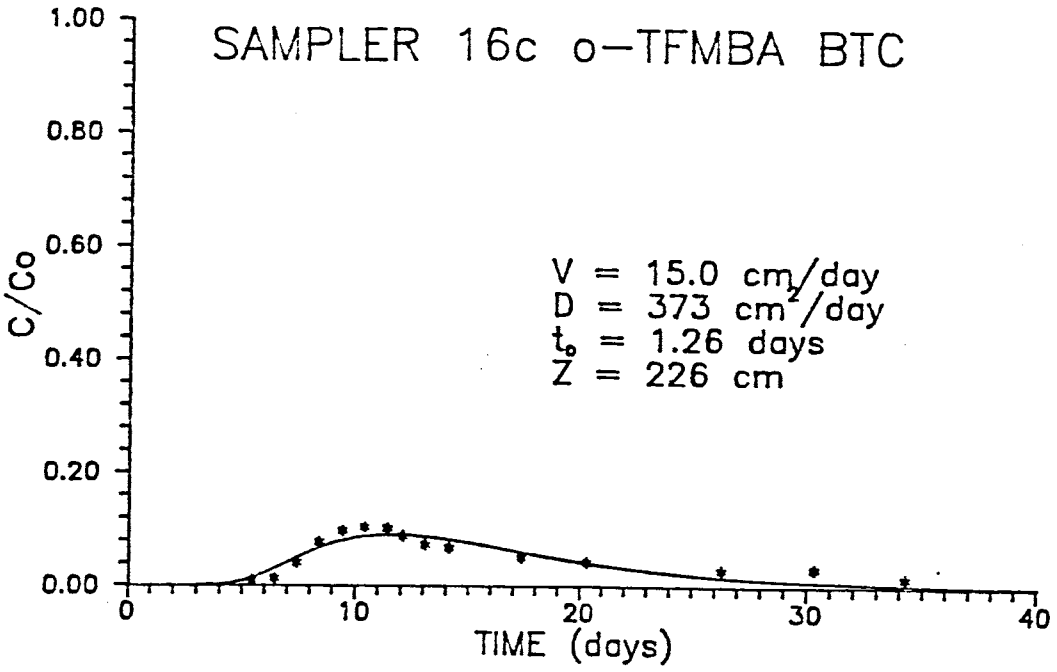
SAMPLER 16c o-TFMBA BTC
V = 15.0 cm/day
D = 373 cm²/day
t_o = 1.26 days
Z = 226 cm
C/Co
1.00
0.80
0.60
0.40
0.20
0.00
0
10
20
30
40
TIME (days)

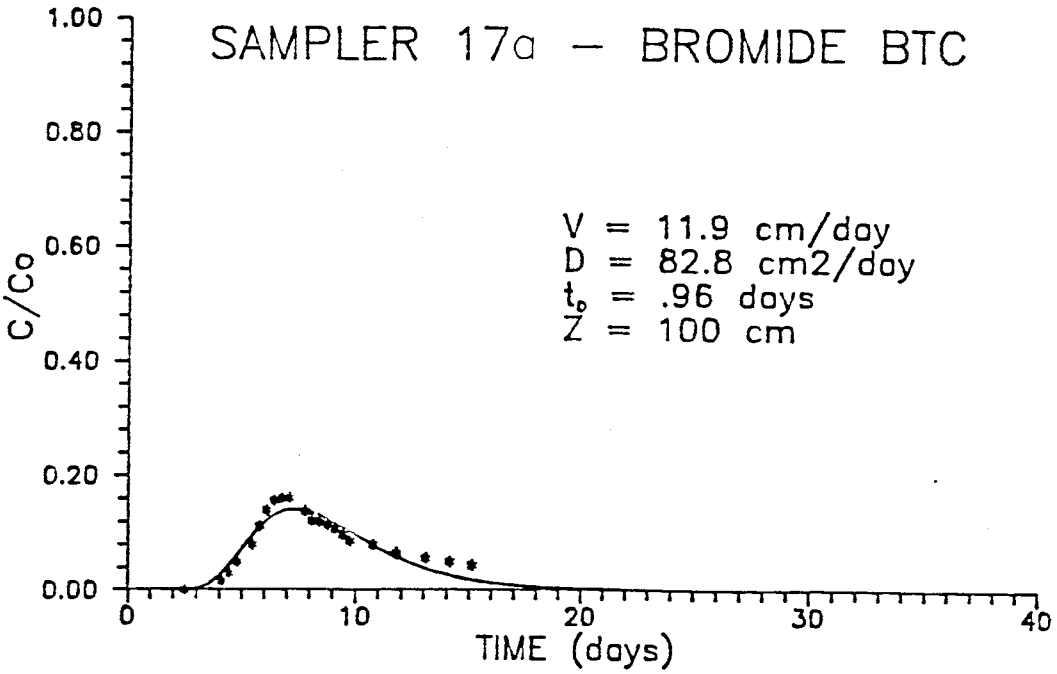
SAMPLER 17a - BROMIDE BTC
V = 11.9 cm/day
D = 82.8 cm2/day
t_o = .96 days
Z = 100 cm
C/Co
1.00
0.80
0.60
0.40
0.20
0.00
0
10
20
30
40
TIME (days)

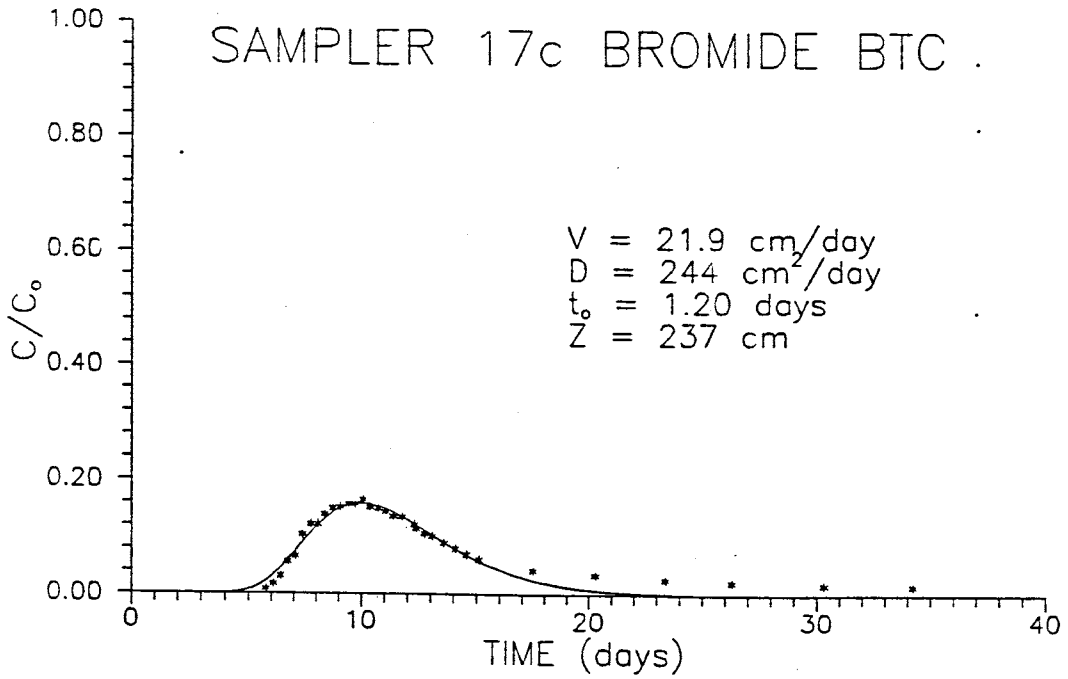
SAMPLER 17c BROMIDE BTC
V = 21.9 cm/day
D = 244 cm²/day
t₀ = 1.20 days
Z = 237 cm
C/C₀
1.00
0.80
0.60
0.40
0.20
0.00
0
10
20
30
40
TIME (days)

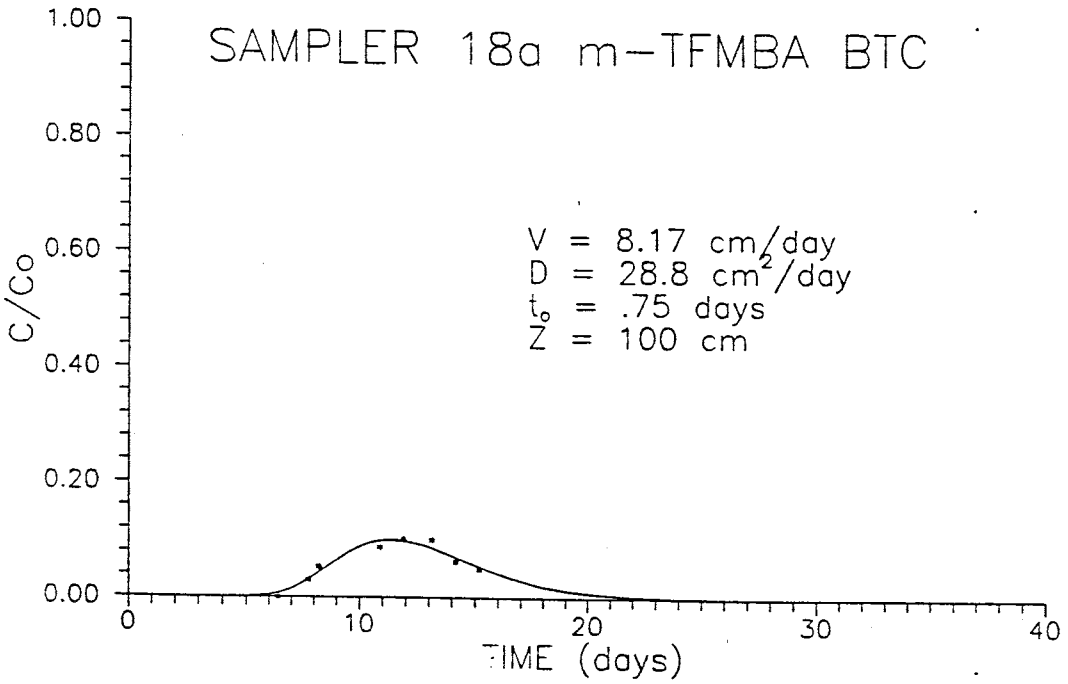
SAMPLER 18a m-TFMBA BTC
V = 8.17 cm/day
D = 28.8 cm²/day
t₀ = .75 days
Z = 100 cm
C/Co
1.00
0.80
0.60
0.40
0.20
0.00
0
10
20
30
40
TIME (days)

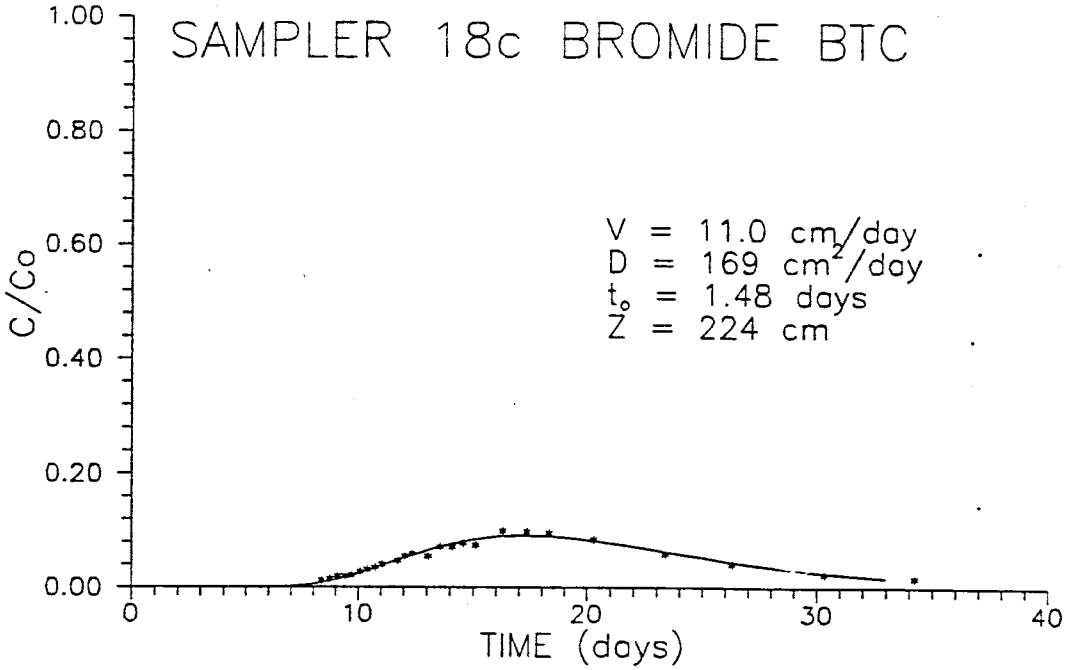
SAMPLER 18c BROMIDE BTC
V = 11.0 cm/day
D = 169 cm²/day
t₀ = 1.48 days
Z = 224 cm
C/Co
TIME (days)
1.00
0.80
0.60
0.40
0.20
0.00
0
10
20
30
40

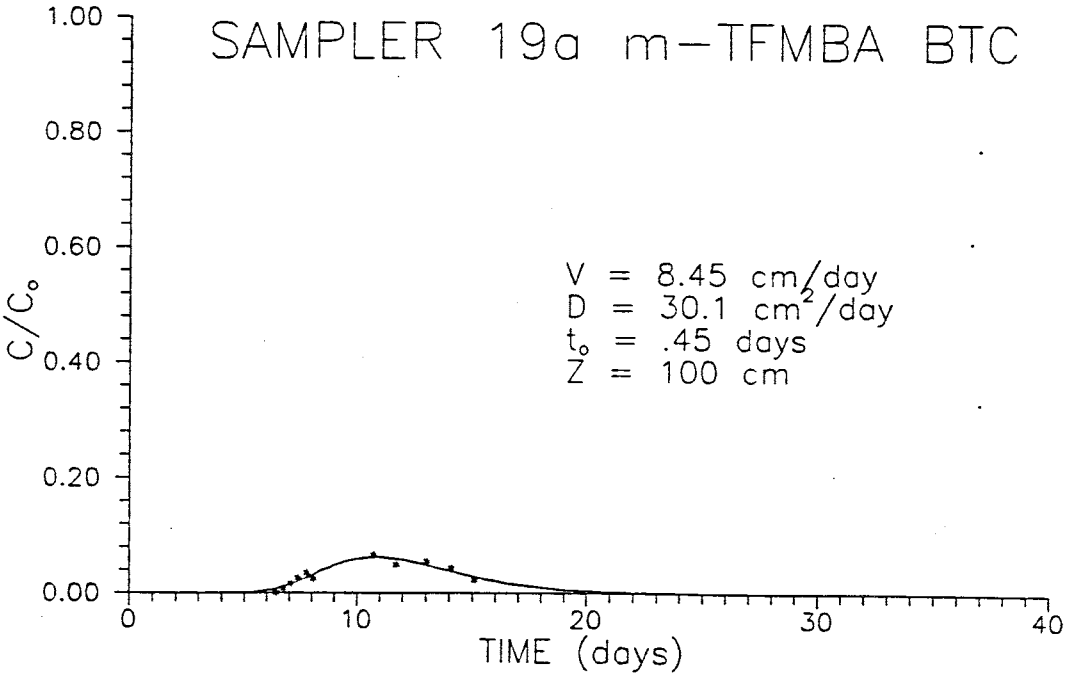
SAMPLER 19a m-TFMBA BTC
V = 8.45 cm/day
D = 30.1 cm²/day
t₀ = .45 days
Z = 100 cm
C/C₀
TIME (days)
1.00
0.80
0.60
0.40
0.20
0.00
0
10
20
30
40

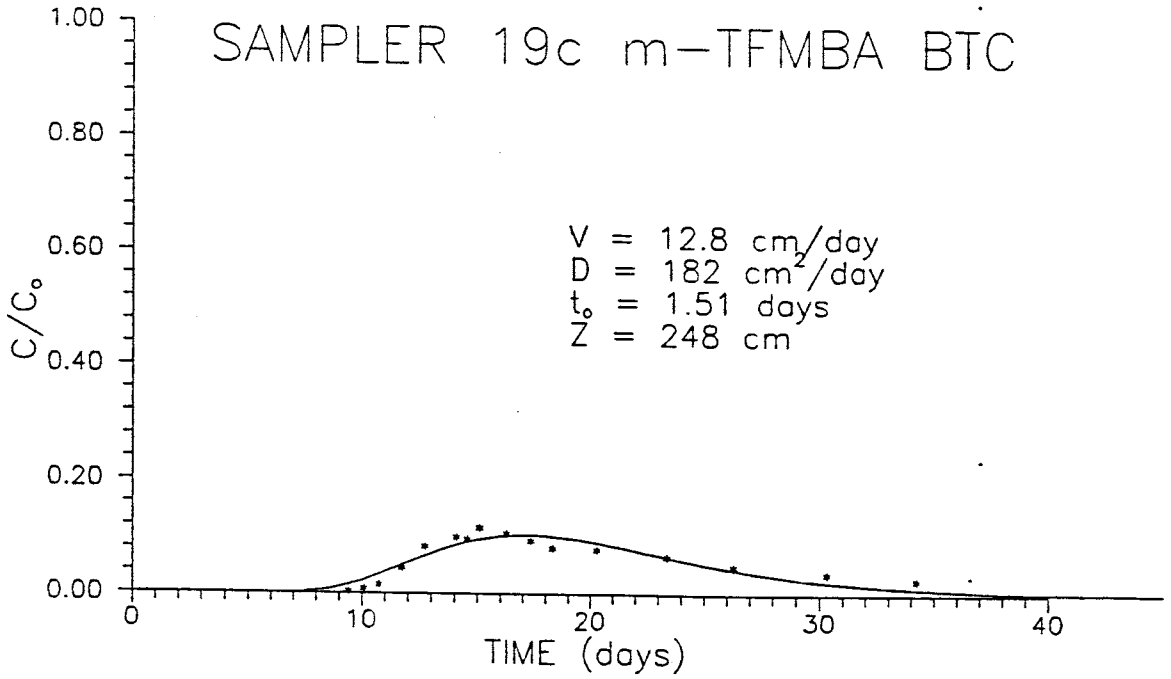
SAMPLER 19c m-TFMBA BTC
V = 12.8 cm/day
D = 182 cm²/day
t₀ = 1.51 days
Z = 248 cm
C/C₀
TIME (days)
1.00
0.80
0.60
0.40
0.20
0.00
0
10
20
30
40

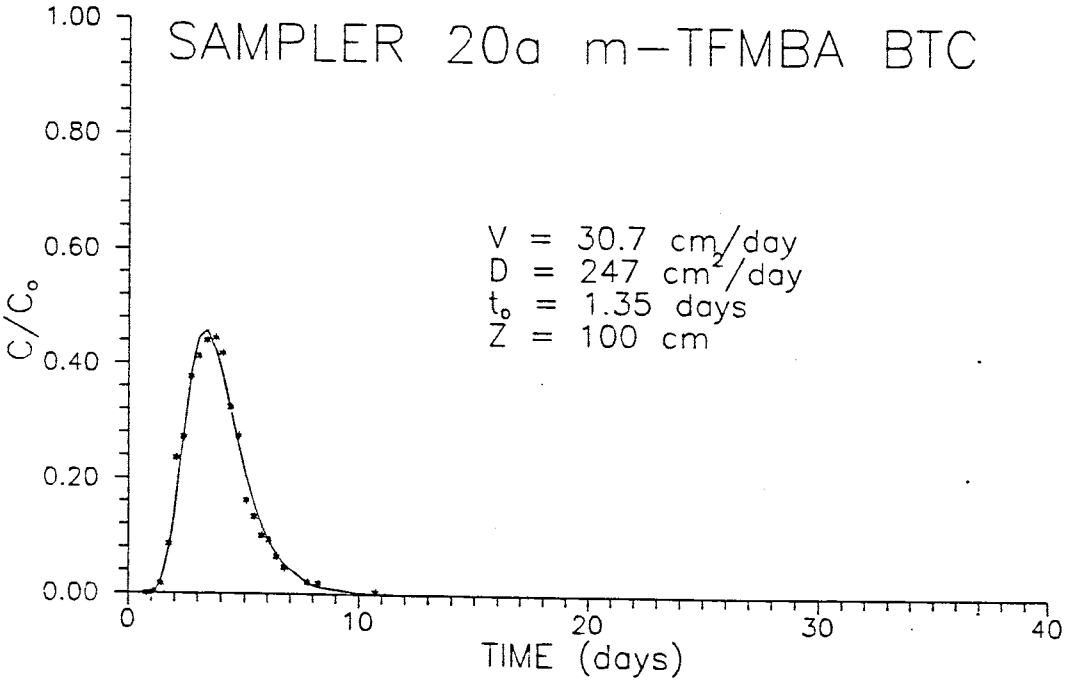
SAMPLER 20a m-TFMBA BTC
V = 30.7 cm/day
D = 247 cm²/day
t₀ = 1.35 days
Z = 100 cm
C/C₀
TIME (days)
1.00
0.80
0.60
0.40
0.20
0.00
0
10
20
30
40

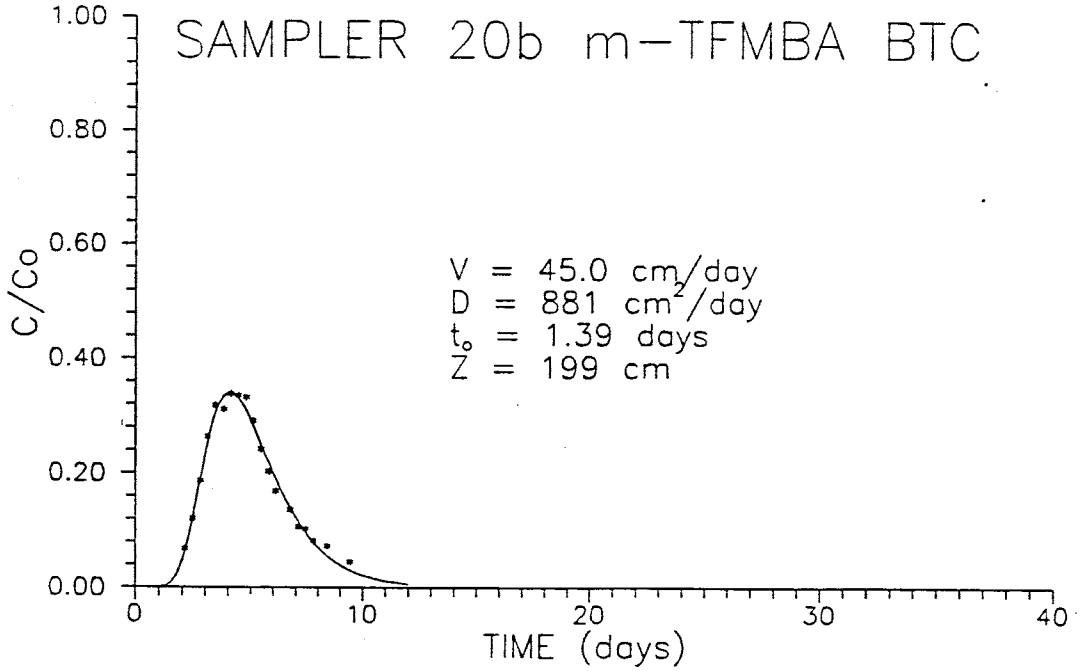
SAMPLER 20b m-TFMBA BTC
V = 45.0 cm/day
D = 881 cm²/day
t₀ = 1.39 days
Z = 199 cm
C/Co
TIME (days)
1.00
0.80
0.60
0.40
0.20
0.00
0
10
20
30
40

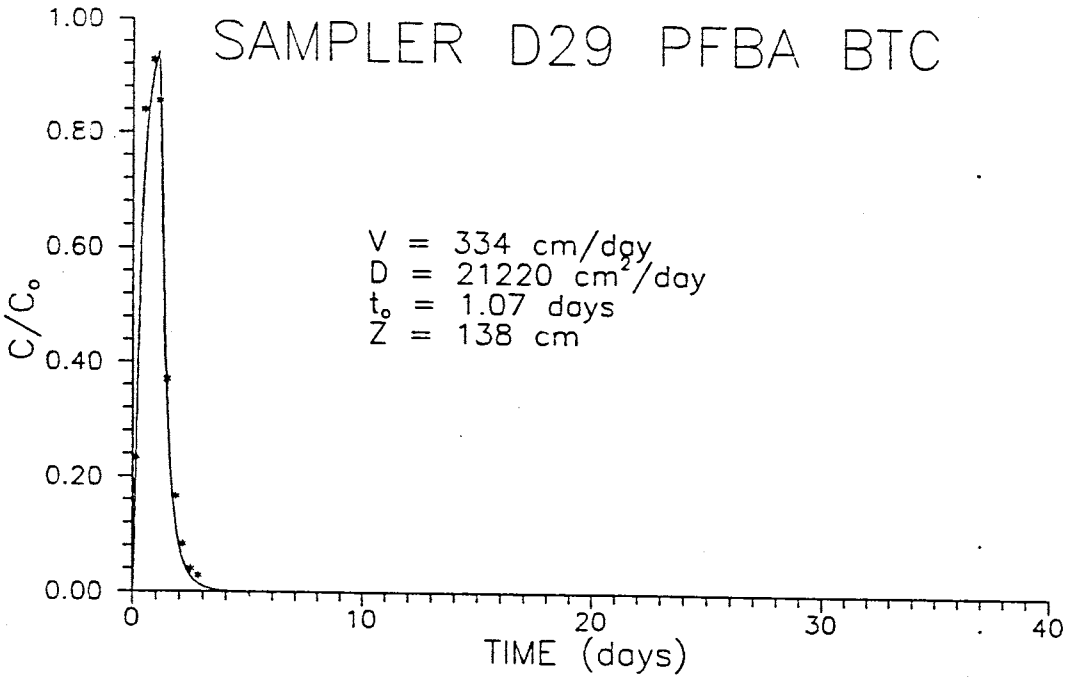
SAMPLER D29 PFBA BTC
V = 334 cm/day
D = 21220 cm²/day
t₀ = 1.07 days
Z = 138 cm
C/C₀
1.00
0.80
0.60
0.40
0.20
0.00
0
10
20
30
40
TIME (days)

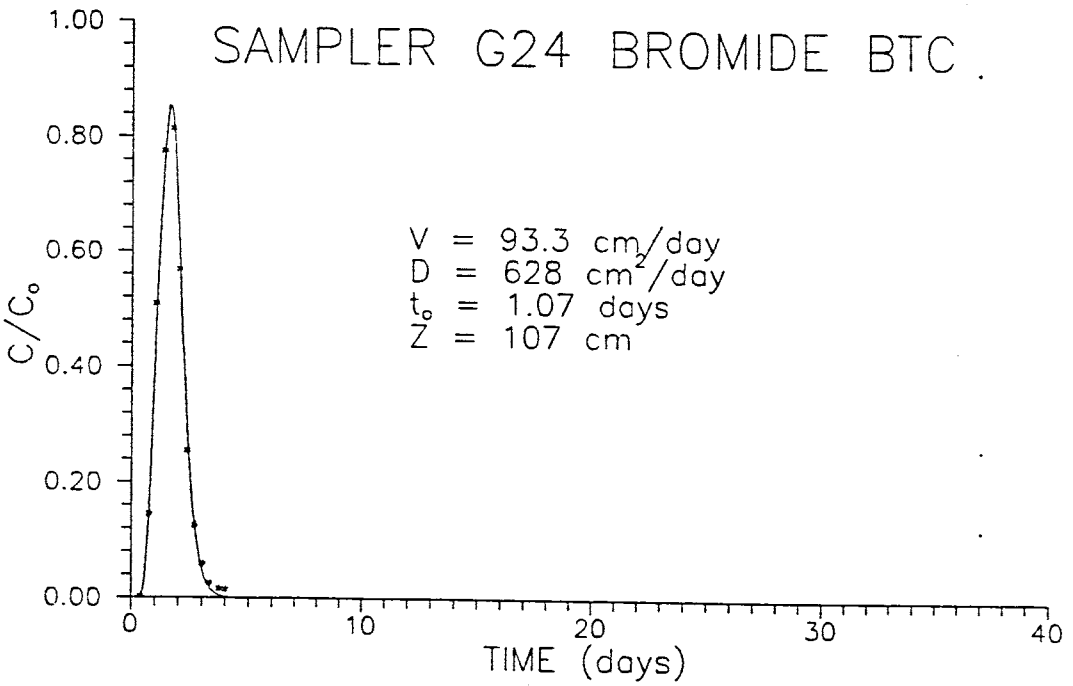
SAMPLER G24 BROMIDE BTC
V = 93.3 cm/day
D = 628 cm²/day
t₀ = 1.07 days
Z = 107 cm
C/C₀
1.00
0.80
0.60
0.40
0.20
0.00
0
10
20
30
40
TIME (days)

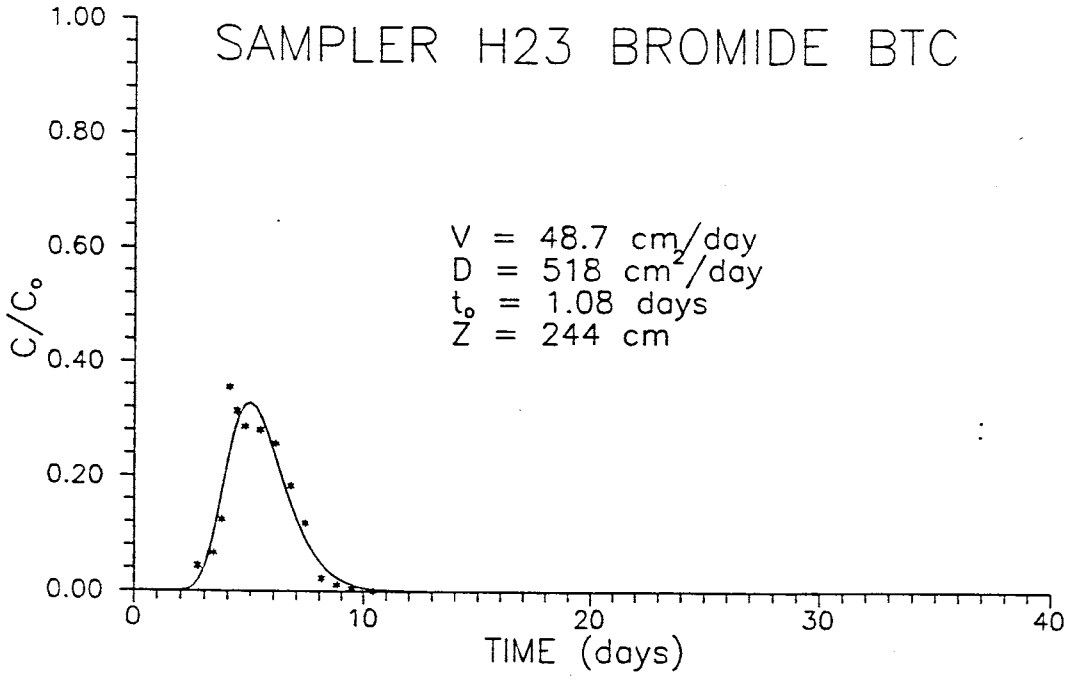
SAMPLER H23 BROMIDE BTC
V = 48.7 cm/day
D = 518 cm²/day
t₀ = 1.08 days
Z = 244 cm
C/C₀
TIME (days)
1.00
0.80
0.60
0.40
0.20
0.00
0
10
20
30
40

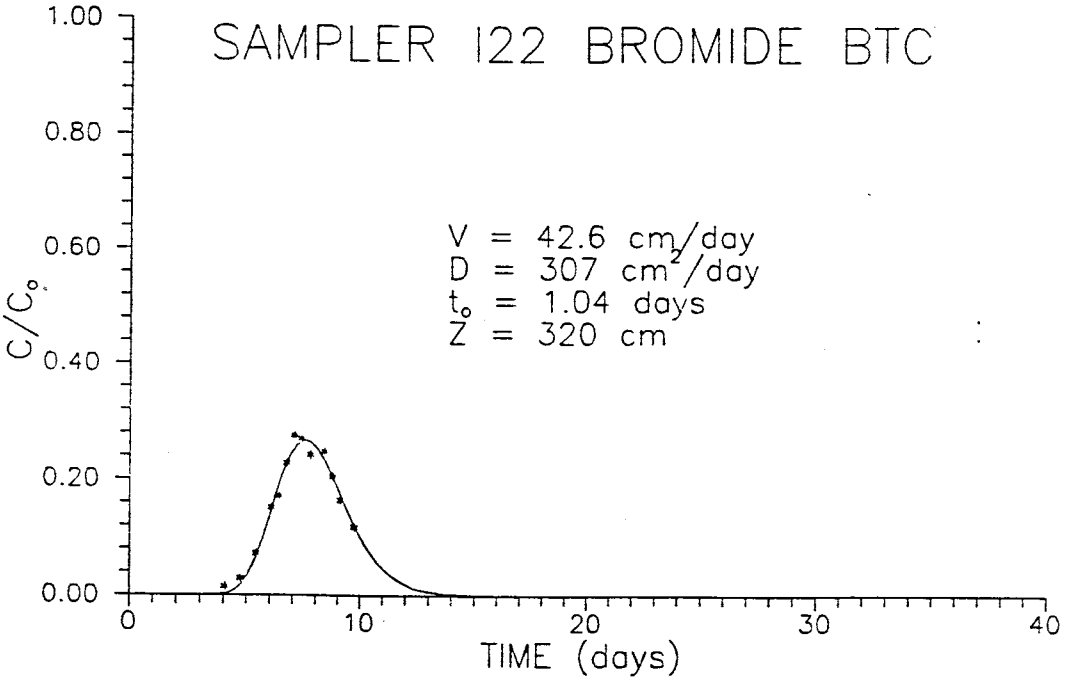
SAMPLER I22 BROMIDE BTC
V = 42.6 cm/day
D = 307 cm²/day
t₀ = 1.04 days
Z = 320 cm
C/C₀
TIME (days)
1.00
0.80
0.60
0.40
0.20
0.00
0
10
20
30
40

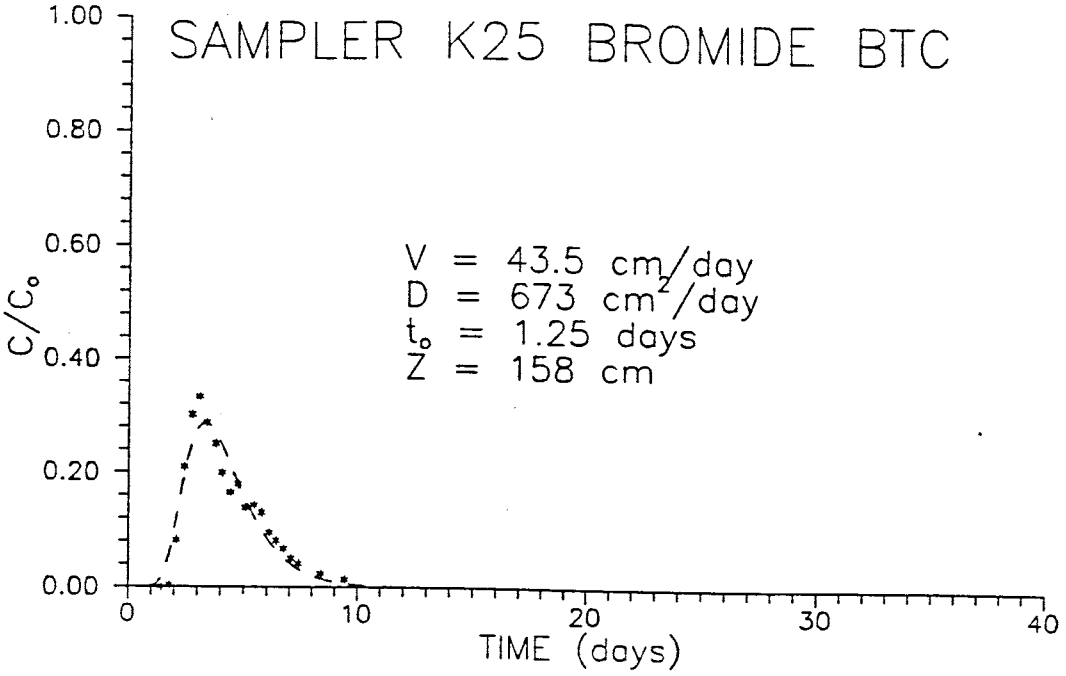
SAMPLER K25 BROMIDE BTC
V = 43.5 cm/day
D = 673 cm²/day
t₀ = 1.25 days
Z = 158 cm
C/C₀
1.00
0.80
0.60
0.40
0.20
0.00
0
10
20
30
40
TIME (days)

APPENDIX B

Time soil water samples were taken and the concentration of tracer observed. Time is in days and concentrations are calculated relative to the average concentration seen in the drip lines during tracer addition.

N = high concentration of nitrate, bromide concentration not determined

? = tracer concentration uncertain due to interference

DNA = data not available

AVERAGE C_o CONCENTRATIONS IN DRIPLINES FOR TRACERS APPLIED

	TRACER	CONCENTRATION (PPM)	TRACER	CONCENTRATION (PPM)
SECTION A	PFBA	31.3	Br^-	123.8
SECTION B	2,6-DFBA	36.9	Br^-	146.9
SECTION C	*o*-TFMBA	34.4	Br^-	137.0
SECTION D	*m*-TFMBA	30.9	Br^-	122.7

PPM = parts per million

Br^- = ionic bromide

Sampler 1a			: Sampler 1b		
	Concentration			Concentration	
Time	Bromide	PFBA	: Time	Bromide	PFBA
0.000	0.000	DNA	: 8.375	0.000	DNA
0.042	0.020	DNA	: 8.729	0.040	DNA
0.383	0.210	DNA	: 9.059	0.250	DNA
0.715	0.860	DNA	: 9.375	0.260	DNA
1.047	1.030	DNA	: 9.716	0.270	DNA
1.378	0.880	DNA	: 10.064	0.220	DNA
1.714	0.330	DNA	: 10.387	0.040	DNA
2.048	0.280	DNA	: 10.716	0.000	DNA
2.385	0.019	DNA	:		
2.714	0.000	DNA	:		

Sampler 1c			:	Sampler 2c		
	Concentration				Concentration	
Time	Bromide	PFBA	:	Time	Bromide	PFBA
13.052	0.090	DNA	:	10.390	N	0.000
13.556	0.150	DNA	:	11.051	N	0.026
14.099	0.180	DNA	:	11.731	N	0.025
14.549	0.230	DNA	:	12.386	N	0.023
15.093	0.200	DNA	:	13.058	N	0.034
16.317	0.190	DNA	:	14.103	N	0.048
17.350	0.210	DNA	:	15.096	N	0.048
20.282	0.140	DNA	:	16.317	N	0.062
23.340	0.040	DNA	:	17.350	N	0.067
24.563	0.000	DNA	:	20.285	N	0.072
			:	23.344	N	0.068
			:	26.283	N	0.067
			:	30.309	N	0.068

Sampler 3c			: Sampler 4a		
	Concentration			Concentration	
Time	Bromide	PFBA	: Time	Bromide	PFBA
8.300	0.000	0.000	:		
8.733	N	0.013	: 7.388	0.000	DNA
10.067	0.050	0.033	: 7.733	0.110	DNA
11.387	0.068	0.053	: 8.053	0.120	DNA
12.055	0.076	0.064	: 10.391	0.150	DNA
13.056	0.086	0.076	: 11.389	0.160	DNA
13.559	N	0.069	: 13.059	0.120	DNA
14.551	0.085	0.078	: 14.106	0.060	DNA
16.317	N	0.073	:		
17.350	0.082	0.080	:		
18.313	0.073	0.070	:		
20.509	0.069	0.071	:		
23.342	0.063	0.062	:		
26.283	0.056	0.065	:		
30.309	0.064	0.057	:		

Sampler 4c			:	Sampler 5a		
	Concentration		:		Concentration	
Time	Bromide	PFBA	:	Time	Bromide	2,6
4.728	0.000	DNA	:	2.773	N	0.059
5.060	0.100	DNA	:	3.092	N	0.120
5.394	0.180	DNA	:	3.426	N	0.165
5.728	0.170	DNA	:	3.775	N	0.188
6.060	0.190	DNA	:	4.094	N	0.204
6.392	0.170	DNA	:	4.427	N	0.186
6.721	0.160	DNA	:	4.765	N	0.201
7.060	0.170	DNA	:	5.097	N	0.192
7.389	0.170	DNA	:	5.431	N	0.180
7.733	0.180	DNA	:	6.099	N	0.160
8.054	0.130	DNA	:	6.427	N	0.146
8.389	0.110	DNA	:	7.097	N	0.125
8.737	0.090	DNA	:	7.772	N	0.097
9.065	0.060	DNA	:	8.215	N	0.086
9.389	0.050	DNA	:	10.634	N	0.066
9.722	0.050	DNA	:	13.178	N	0.031
10.073	0.040	DNA	:	15.215	N	0.013
10.392	0.020	DNA	:			

Sampler 5c

Time	Concentration Bromide*	2,6	PFBA
5.431	0.023	0.007	?
6.099	0.049	0.024	?
6.758	0.073	0.044	?
7.424	0.102	0.068	?
7.772	0.117	0.080	?
8.091	0.119	0.080	?
8.772	0.132	0.098	?
9.418	0.128	0.097	?
10.107	0.12	0.088	?
10.758	0.112	0.086	?
11.426	0.104	0.081	?
12.090	0.094	0.074	?
13.178	0.08	0.061	?
14.226	0.066	0.050	?
20.626	0.043	0.028	?
26.651	0.029	0.017	?

Sampler 6a

Time	Concentration Bromide	2,6	PFBA
5.094	0.031	0.018	0.012
6.097	0.093	0.055	0.038
7.096	0.118	0.063	0.045
7.422	0.142	0.085	0.09
7.769	0.140	0.078	0.057
8.088	0.142	0.074	0.054
10.179	0.131	0.078	0.081
11.424	0.131	0.074	0.073
14.141	0.111	0.059	0.042
15.131	0.098	0.052	0.041
23.340	0.039	0.017	0.016
28.766	0.000	0.000	0.000

Sampler 7a			Sampler 7c		
	Concentration			Concentration	
Time	Bromide	2,6	Time	Bromide	2,6
3.398	0.011	0.012	9.389	N	0.006
3.750	0.025	0.035	10.397	N	0.008
4.067	0.083	0.085	11.397	N	0.032
4.402	0.12	0.122	12.063	N	0.042
4.740	0.125	0.134	12.740	N	0.048
5.403	0.173	0.171	13.573	N	0.061
5.742	0.158	0.153	14.567	N	0.072
6.073	0.141	0.134	16.319	N	0.083
6.401	0.156	0.149	17.354	N	0.092
6.730	0.153	0.146	18.326	N	0.086
7.071	0.156	0.143	20.288	N	0.091
7.394	0.159	0.152	23.356	N	0.079
7.747	0.164	0.153	26.285	N	0.069
8.063	0.152	0.136	30.313	N	0.054
11.060	0.119	0.098	34.243	N	0.044
13.066	0.105	0.083			
14.114	N	0.064			
15.106	N	0.039			
23.357	N	0.013			
27.482	N	0.000			

Sampler 8a			Sampler 9a		
	Concentration			Concentration	
Time	Bromide	2,6	Time	Bromide	2,6
2.060	N	0.000	1.399	N	0.000
2.403	N	0.007	1.745	N	0.002
2.727	N	0.017	2.078	N	0.016
3.057	N	0.050	2.411	N	0.064
3.391	N	0.080	2.734	N	0.134
4.060	N	0.136	3.064	N	0.254
4.392	N	0.131	3.747	N	0.321
4.730	N	0.122	4.106	N	0.328
5.062	N	0.105	4.398	N	0.311
5.396	N	0.077	4.737	N	0.280
6.063	N	0.053	5.067	N	0.222
6.393	N	0.047	5.401	N	0.199
6.723	N	0.043	5.739	N	0.161
7.063	N	0.031	6.071	N	0.118
7.390	N	0.034	6.399	N	0.100
7.735	N	0.029	6.728	N	0.081
8.057	N	0.029	7.067	N	0.065
10.392	N	0.016	7.392	N	0.053
13.266	N	0.000	7.744	N	0.043
			8.061	N	0.029
			10.395	N	0.007
			11.397	N	0.003
			13.065	N	0.002
			14.113	N	0.001
			15.292	N	0.000

Sampler 9c			Sampler 10a		
	Concentration			Concentration	
Time	Bromide	2,6	Time	Bromide	2,6
5.402	N	0.000	2.093	N	0.016
6.072	N	0.017	2.448	N	0.058
6.728	N	0.033	2.773	N	0.096
7.393	N	0.056	3.101	N	0.143
8.064	N	0.076	3.785	N	0.197
8.391	N	0.059	4.099	N	0.204
8.743	N	0.078	4.436	N	0.186
9.071	N	0.066	4.774	N	0.184
9.726	N	0.064	5.103	N	0.172
10.076	N	0.066	5.440	N	0.156
10.396	N	0.082	5.776	N	0.150
10.729	N	0.078	6.107	N	0.133
11.058	N	0.065	6.764	N	0.109
11.397	N	0.065	7.426	N	0.085
11.738	N	0.073	7.783	N	0.082
12.060	N	0.059	8.222	N	0.061
12.738	N	0.059	10.242	N	0.046
13.570	N	0.051	13.216	N	0.019
14.565	N	0.054	15.263	N	0.010
16.319	N	0.033	17.537	N	0.000
17.354	N	0.029			
18.326	N	0.033			
20.288	N	0.019			
23.356	N	0.013			
26.285	N	0.008			
30.971	N	0.000			

Sampler 11a			Sampler 11c		
	Concentration			Concentration	
Time	Bromide	o-TFMBA	Time	Bromide	o-TFMBA
0.083	N	0.069	1.764	N	0.002
0.422	N	0.182	2.427	N	0.058
0.788	N	0.307	3.077	N	0.220
1.083	N	0.304	3.406	N	0.316
1.413	N	0.166	3.769	N	0.378
1.764	N	0.045	4.074	N	0.382
2.089	N	0.011	4.411	N	0.359
2.427	N	0.010	4.751	N	0.272
5.187	N	0.000	5.417	N	0.161
			5.753	N	0.097
			6.410	N	0.047
			7.078	N	0.028
			8.400	N	0.008
			8.929	N	0.000

Sampler 11d

Time	Concentration Bromide	o-TFMBA
5.078	N	0.007
5.753	N	0.024
6.410	N	0.049
7.078	N	0.079
7.760	N	0.108
8.400	N	0.123
9.080	N	0.107
10.090	N	0.097
11.068	N	0.080
12.398	N	0.056
14.119	N	0.030
16.326	N	0.023
20.292	N	0.009
23.367	N	0.003
24.692	N	0.000

Sampler 12a			Sampler 12c		
	Concentration			Concentration	
Time	Bromide	o-TFMBA	Time	Bromide	o-TFMBA
3.756	N	0.008	5.413	N	0.021
4.406	N	0.030	6.078	N	0.048
5.072	N	0.058	6.735	N	0.063
6.081	N	0.060	7.076	N	0.070
7.075	N	0.083	7.754	N	0.094
7.397	N	0.110	8.067	N	0.070
7.753	N	0.103	8.397	N	0.079
8.066	N	0.096	9.076	N	0.087
10.087	N	0.126	9.728	N	0.087
11.063	N	0.125	10.086	N	0.086
14.116	N	0.115	10.733	N	0.088
15.108	N	0.091	11.065	N	0.077
18.869	N	0.000	11.399	N	0.069
			11.743	N	0.082
			12.222	N	0.096
			13.067	N	0.067
			14.115	N	0.062
			15.108	N	0.057
			20.292	N	0.046
			23.363	N	0.040
			26.288	N	0.032
			30.316	N	0.014
			34.250	N	0.015

Sampler 13a			Sampler 13c		
	Concentration			Concentration	
Time	Bromide	o-TFMBA	Time	Bromide	o-TFMBA
2.431	0.016	0.011	3.777	0.000	0.000
2.754	0.052	0.052	4.414	0.018	0.014
3.079	0.041	0.053	5.081	0.086	0.074
3.408	0.108	0.086	5.756	0.199	0.178
3.775	0.164	0.142	6.087	0.195	0.195
4.076	0.163	0.148	6.742	0.219	0.218
4.413	0.227	0.223	7.081	0.209	0.191
4.754	0.261	0.241	7.765	0.187	0.175
5.080	0.214	0.193	8.075	0.166	0.148
5.756	0.189	0.173	8.401	0.141	0.123
6.411	0.166	0.151	9.083	0.106	0.091
6.741	0.161	0.144	9.733	0.092	0.076
7.403	0.126	0.133	10.403	0.069	0.065
7.765	0.119	0.109	11.07	0.061	0.062
8.074	0.092	0.077	11.751	0.048	0.053
10.092	0.09	0.082	13.586	?	0.042
12.073	0.089	0.093	16.333	?	0.048
14.120	0.046	0.041	18.344	?	0.018
15.117	0.034	0.051	20.292	?	0.031
23.369	?	0.025			
31.304	?	0.000			

Sampler 14a			Sampler 14c		
	Concentration			Concentration	
Time	Bromide	o-TFMBA	Time	Bromide	o-TFMBA
1.112	0.047	0.083	3.435	?	0.012
1.441	0.198	0.207	3.797	0.028	0.028
1.790	0.421	0.427	4.103	0.056	0.056
2.115	0.634	0.621	4.441	0.102	0.100
2.453	0.582	0.559	4.779	0.142	0.137
2.777	0.525	0.512	5.107	0.176	0.169
3.094	0.325	0.295	5.447	0.196	0.186
3.436	0.237	0.206	5.781	0.207	0.195
3.795	0.156	0.139	6.113	0.200	0.185
4.102	0.106	0.110	6.438	0.193	0.182
4.439	0.097	0.086	6.768	0.176	0.162
4.778	0.079	0.082	7.108	0.157	0.141
5.106	0.071	0.077	7.789	0.137	0.123
5.446	0.073	0.077	8.101	0.117	0.104
5.780	0.072	0.073	8.779	0.099	0.084
6.438	0.089	0.078	9.108	0.090	0.077
7.788	0.116	0.066	10.431	0.068	0.057
15.213	0.000	0.000	11.776	0.048	0.038
			13.099	0.039	0.031
			15.606	0.024	0.017
			18.650	0.000	0.000

Sampler 15a			Sampler 15c		
	Concentration			Concentration	
Time	Bromide	o-TFMBA	Time	Bromide	o-TFMBA
			3.411	0.011	?
2.435	0.010	0.007	3.780	0.026	0.021
2.757	?	0.026	4.078	0.048	0.059
3.410	0.040	0.049	4.420	0.065	0.059
3.696	0.071	0.074	4.758	0.104	0.097
4.420	0.159	0.153	5.083	0.137	0.145
4.757	0.177	0.178	5.423	0.168	0.171
5.082	0.191	0.203	6.090	0.172	0.171
5.421	0.185	0.198	6.744	0.146	0.146
5.760	0.166	0.176	7.406	0.134	0.118
6.089	0.163	0.160	8.402	0.103	0.093
6.744	0.135	0.129	9.434	0.104	0.110
7.403	0.121	0.120	10.403	0.068	0.059
7.770	0.091	0.085	11.403	0.058	0.066
10.094	0.067	0.061	12.399	0.057	0.063
11.072	0.055	0.059	13.074	?	0.052
13.072	0.054	0.056	14.121	?	0.051
14.122	?	0.044	15.119	?	0.044
15.119	?	0.037	17.361	0.040	0.048
20.389	?	0.000			

Sampler 16a

Time	Concentration Bromide	o-TFMBA
0.770	N	0.000
1.097	N	0.020
1.423	N	0.188
1.779	N	0.323
2.094	N	0.535
2.438	N	0.475
2.760	N	0.433
3.085	N	0.290
3.413	N	0.191
3.699	N	0.148
4.078	N	0.130
4.422	N	0.073
4.760	N	0.062
5.085	N	0.036
5.424	N	0.028
6.092	N	0.019
6.417	N	0.011
6.747	N	0.011
7.086	N	0.010
7.406	N	0.007

Sampler 16c			Sampler 17a		
	Concentration			Concentration	
Time	Bromide	o-TFMBA	Time	Bromide	m-TFMBA
5.425	N	0.008	2.449	0.000	0.000
6.417	N	0.012	4.088	0.016	0.004
7.407	N	0.040	4.432	0.029	0.013
8.403	N	0.076	4.773	0.049	0.028
9.437	N	0.096	5.435	0.079	0.070
10.404	N	0.103	5.776	0.111	0.078
11.404	N	0.101	6.101	0.139	0.121
12.073	N	0.087	6.425	0.155	0.143
13.076	N	0.072	6.756	0.159	0.140
14.122	N	0.067	7.096	0.160	0.142
17.365	N	0.050	7.788	0.137	0.130
20.295	N	0.042	8.088	0.121	0.115
26.292	N	0.029	8.407	0.119	0.133
30.319	N	0.032	8.763	0.114	0.083
34.247	N	0.016	9.090	0.107	0.119
			9.442	0.097	0.076
			9.744	0.086	0.066
			10.758	0.079	0.078
			11.774	0.064	0.051
			13.083	0.055	0.044
			14.128	0.049	0.055
			15.126	0.043	0.037
			23.384	0.039	0.050
			45.222	?	0.018

Sampler 17c

Time	Concentration Bromide	o-TFMBA	m-TFMBA
5.777	0.008	0.002	?
6.103	0.017	0.005	0.008
6.425	0.031	0.010	0.020
6.757	0.056	0.018	0.016
7.097	0.066	0.034	0.031
7.412	0.104	0.028	0.082
7.789	0.122	0.043	0.082
8.089	0.122	0.028	0.091
8.408	0.139	0.032	0.094
8.763	0.150	0.032	0.105
9.091	0.152	0.030	0.110
9.444	0.157	0.043	0.133
9.745	0.157	0.028	0.121
10.101	0.165	0.030	0.141
10.408	0.152	0.027	0.126
10.758	0.150	0.027	0.130
11.078	0.144	0.043	0.142
11.408	0.136	0.026	0.123
11.774	0.135	0.027	0.115
12.310	0.122	0.024	0.113
12.405	0.115	0.023	0.106
12.766	0.106	0.022	0.096
13.083	0.102	0.039	0.114
13.604	0.090	0.034	0.106
14.127	0.080	0.018	0.092
14.597	0.070	0.015	0.076
15.126	0.061	0.013	0.077
17.517	0.043	0.008	0.048
20.282	0.035	0.005	0.050
23.385	0.027	0.003	0.033
26.285	0.023	?	0.042
30.309	0.018	0.001	0.036
34.243	0.016	0.011	?

Sampler 18a

	Concentration	
Time	Bromide	m-TFMBA
6.421	0.000	0.000
7.781	0.030	0.030
8.251	0.053	0.043
10.919	0.087	0.070
11.931	0.102	0.116
13.164	0.100	0.099
14.208	0.091	0.062
15.208	0.081	0.050

Sampler 18c

Time	Concentration Bromide	o-TFMBA	m-TFMBA
8.406	0.013	0.002	?
8.759	0.015	?	0.011
9.088	0.019	?	?
9.440	0.019	0.004	0.013
9.740	0.021	0.005	?
10.097	0.027	0.008	0.023
10.406	0.031	0.010	0.036
10.752	0.035	0.011	0.038
11.076	0.040	0.012	?
11.765	0.047	0.016	0.032
12.074	0.055	0.020	0.037
12.403	0.059	0.020	?
13.080	0.055	0.016	0.036
13.599	0.072	0.022	0.050
14.124	0.072	0.019	0.057
14.591	0.078	0.021	0.059
15.124	0.075	0.022	0.061
16.317	0.099	0.024	0.082
17.368	0.098	0.022	0.084
18.347	0.096	0.021	0.077
20.292	0.085	0.016	0.068
23.380	0.059	0.008	0.054
26.292	0.042	?	0.032
30.319	0.024	0.000	0.054
34.250	0.017	0.000	0.011

Sampler 19a			Sampler 19c		
	Concentration			Concentration	
Time	Bromide	m-TFMBA	Time	Bromide	m-TFMBA
6.424	N	0.000	9.441	N	0.004
6.756	N	0.007	10.099	N	0.008
7.094	N	0.016	10.755	N	0.015
7.410	N	0.026	11.770	N	0.045
7.785	N	0.035	12.763	N	0.083
8.086	N	0.025	14.126	N	0.099
10.755	N	0.066	14.594	N	0.096
11.769	N	0.049	15.124	N	0.117
13.082	N	0.054	16.292	N	0.106
14.126	N	0.043	17.375	N	0.094
15.125	N	0.022	18.347	N	0.081
			20.292	N	0.079
			23.383	N	0.066
			26.292	N	0.050
			30.319	N	0.037
			34.250	N	0.026

Sampler 20a

	Concentration	
Time	Bromide	m-TFMBA
0.803	0.001	0.000
1.099	0.007	0.003
1.423	0.022	0.017
1.784	0.099	0.086
2.097	0.208	0.236
2.440	0.293	0.272
2.763	0.387	0.377
3.085	0.427	0.413
3.416	0.516	0.440
3.786	0.515	0.445
4.081	0.402	0.418
4.424	0.361	0.324
4.764	0.269	0.275
5.088	0.178	0.162
5.427	0.150	0.134
5.765	0.115	0.101
6.094	0.102	0.094
6.418	0.072	0.065
6.749	0.055	0.046
7.778	0.025	0.021
8.249	0.022	0.019
10.749	0.010	0.004

Sampler 20b

Time	Concentration Bromide	m-TFMBA
2.129	0.066	0.068
2.472	0.138	0.121
2.796	0.196	0.187
3.121	0.272	0.263
3.448	0.332	0.318
3.819	0.335	0.311
4.114	0.355	0.339
4.456	0.346	0.336
4.797	0.324	0.332
5.120	0.296	0.291
5.459	0.239	0.242
5.798	0.215	0.203
6.126	0.180	0.169
6.780	0.149	0.137
7.122	0.113	0.107
7.440	0.099	0.103
7.810	0.090	0.082
8.435	0.068	0.073
9.469	0.064	0.045

Sampler D29			Sampler K25		
	Concentration			Concentration	
Time	Bromide	PFBA	Time	Bromide	2,6
0.167	0.238	0.234	1.440	0.000	0.000
0.502	0.786	0.838	1.810	0.009	0.004
0.890	0.917	0.926	2.114	0.095	0.082
1.151	0.877	0.854	2.458	0.240	0.209
1.476	0.396	0.370	2.784	0.357	0.301
1.849	0.194	0.166	3.103	0.424	0.333
2.147	0.098	0.083	3.428	0.375	0.287
2.492	0.052	0.040	3.815	0.345	0.254
2.822	0.033	0.028	4.094	0.280	0.199
			4.441	0.226	0.165
			4.781	0.237	0.179
			5.102	0.186	0.138
			5.442	0.186	0.143
			5.785	0.170	0.130
			6.115	0.126	0.095
			6.431	0.108	0.081
			6.764	0.091	0.067
			7.101	0.071	0.050
			7.415	0.057	0.041
			8.413	0.035	0.024
			9.451	0.025	0.014

Sampler g24			Sampler h23		
	Concentration			Concentration	
Time	Bromide	o-TFMBA	Time	Bromide	o-TFMBA
0.408	0.002	0.000	2.730	0.044	0.018
0.790	0.145	0.167	3.380	0.067	0.069
1.062	0.508	0.524	3.760	0.125	0.123
1.388	0.775	0.777	4.080	0.356	0.354
1.755	0.814	0.782	4.430	0.314	0.280
2.060	0.568	0.520	4.770	0.287	0.264
2.402	0.255	0.225	5.430	0.281	0.247
2.731	0.125	0.113	6.100	0.258	0.172
3.049	0.059	0.056	6.750	0.184	0.105
3.375	0.026	0.024	7.400	0.119	0.059
3.760	0.016	0.014	8.120	0.023	0.038
4.042	0.014	0.013	8.800	0.011	0.030
			9.490	0.005	0.013

Sampler I22

Time	Concentration Bromide	o-TFMBA
4.080	0.015	0.004
4.770	0.029	0.027
5.430	0.072	0.070
6.100	0.151	0.147
6.420	0.171	0.167
6.750	0.228	0.220
7.090	0.259	0.252
7.400	0.267	0.258
7.780	0.259	0.252
8.400	0.248	0.241
8.800	0.205	0.197
9.130	0.164	0.151
9.770	0.118	0.106

Sampler MEC

Time	Concentration Bromide	2,6
23	0.013	0.006
30	0.011	0.006
42	0.021	0.016
50	0.026	0.023
58	0.023	0.019

Sampler ENE-a

Time	Concentration Bromide	o-TFMBA
9.0	0.000	?
14.5	0.007	?
18.0	0.003	?

Sampler ENE-b			Sampler ENE-c		
	Concentration			Concentration	
Time	Bromide	o-TFMBA	Time	Bromide	o-TFMBA
6.0	0.004	?	9.0	0.001	?
9.0	0.137	0.135	11.0	0.004	?
12.0	0.117	0.134	13.5	0.036	0.038
15.5	0.027	0.029	15.5	0.042	0.040
18.0	0.003	?	18.5	0.069	0.072
			23.0	0.054	0.057
			30.0	0.033	0.041
			42.0	0.012	?